U.S. Department
of Commerce

Volume 122
Number 4
October 2024

Fishery Bulletin

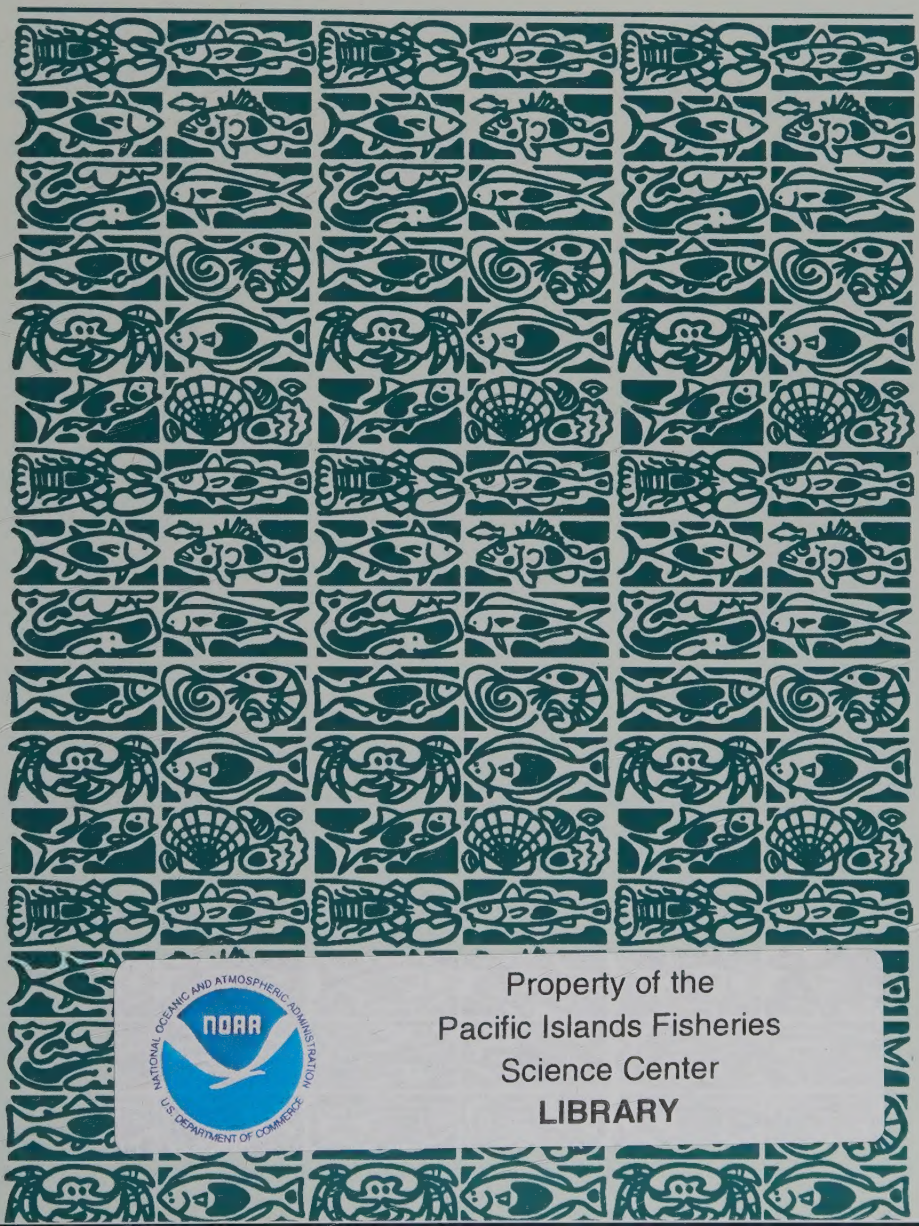

Property of the
Pacific Islands Fisheries
Science Center
LIBRARY

U.S. Department of Commerce

Gina M. Raimondo
Secretary

National Oceanic and Atmospheric Administration

Richard W. Spinrad
Administrator

National Marine Fisheries Service

Janet Coit
Assistant Administrator
for Fisheries

Fishery Bulletin

Scientific Editor
José I. Castro
National Marine Fisheries Service, NOAA
263 13th Avenue South
Saint Petersburg, Florida 33701

Managing Editor
Kathryn Dennis
Scientific Publications Office
National Marine Fisheries Service, NOAA
1845 Wasp Boulevard, Building 176
Honolulu, Hawaii 96818

Associate Editor
Cara Mayo
Scientific Publications Office
National Marine Fisheries Service, NOAA
7600 Sand Point Way NE
Seattle, Washington 98115-0070

Editorial Board

Henry L. Bart Jr.	Tulane University, New Orleans, Louisiana
Katherine E. Bemis	National Systematics Laboratory, Washington, DC
Matthew D. Campbell	National Marine Fisheries Service, Pascagoula, Mississippi
William B. Driggers III	National Marine Fisheries Service, Pascagoula, Mississippi
Gretchen L. Grammer	South Australian Research and Development Institute, Adelaide, Australia
Eric R. Hoffmayer	National Marine Fisheries Service, Pascagoula, Mississippi
Richard Langton	National Marine Fisheries Service, Walpole, Maine (retired)
J. Fernando Márquez-Farías	Universidad Autónoma de Sinaloa, Mazatlán, México
Richard S. McBride	National Marine Fisheries Service, Woods Hole, Massachusetts
Richard L. Merrick	National Marine Fisheries Service, Falmouth, Massachusetts (retired)
Richard D. Methot	National Marine Fisheries Service, Seattle, Washington
Lisa J. Natanson	National Marine Fisheries Service, Narragansett, Rhode Island (retired)
Mark S. Peterson	University of Southern Mississippi, Ocean Springs, Mississippi
André E. Punt	University of Washington, Seattle, Washington
Joseph M. Quattro	University of South Carolina, Columbia, South Carolina
John F. Walter III	National Marine Fisheries Service, Miami, Florida

***Fishery Bulletin* website: https://spo.nmfs.noaa.gov/fb.htm**

Fishery Bulletin (ISSN 0090-0656) is published quarterly by the Scientific Publications Office, National Marine Fisheries Service, NOAA, 7600 Sand Point Way NE, Seattle, WA 98115-0070.

Although the contents of this publication have not been copyrighted and may be reprinted entirely, reference to source is appreciated.

The Secretary of Commerce has determined that the publication of this periodical is necessary according to law for the transaction of public business of this Department. Use of funds for printing of this periodical has been approved by the Director of the Office of Management and Budget.

For Sale by the Superintendent of Documents, U.S. Government Publishing Office, Washington, DC 20401. Subscription price per year: $32.00 domestic and $44.80 foreign. Cost per single issue: $19.00 domestic and $26.60 foreign. **See back for order form.**

Fishery Bulletin carries original research reports on investigations in fishery science, engineering, and economics. It began as the Bulletin of the United States Fish Commission in 1881; it became the Bulletin of the Bureau of Fisheries in 1904 and the *Fishery Bulletin* of the U.S. Fish and Wildlife Service in 1941. Separates were issued as documents through volume 46; the last document was no. 1103. Beginning with volume 47 in 1931 and continuing through volume 62 in 1963, each separate appeared as a numbered bulletin. A new system began in 1963, with volume 63, in which papers are bound together in a single issue. Beginning with volume 70, number 1, January 1972, *Fishery Bulletin* became a periodical, issued quarterly. In this form, it is available by subscription from the Superintendent of Documents, U.S. Government Publishing Office, Washington, DC 20401. It is also available free in limited numbers to libraries, research institutions, and state and federal agencies and in exchange for other scientific publications.

U.S. Department of Commerce
Seattle, Washington

Volume 122
Number 4
October 2024

Fishery Bulletin

Contents

Articles

133–142 **Jacob T. Shaner, John M. Jacobs, Lance T. Yonkos, and Reginal M. Harrell**

Reevaluating fecundity of white perch (*Morone americana*) in Chesapeake Bay with modern stereological techniques

143–161 **Paul G. von Szalay, Edward A. Laman, Stan Kotwicki, Lewis A. K. Barnett, and Kotaro Ono**

Quantifying the effects of sample size and species distribution on the precision and accuracy of abundance estimates from bottom-trawl surveys in the Gulf of Alaska

162–185 **Dennis M. Allen, John J. Govoni, Kenneth W. Able, Jeffrey A. Buckel, Edward A. Hale, Eric J. Hilton, G. Todd Kellison, Timothy E. Targett, J. Christopher Taylor, and Harvey J. Walsh**

Long-term dynamics of larval and early juvenile spot (*Leiostomus xanthurus*) off the U.S. East Coast: relating ocean origins, estuarine ingress, and changing environmental conditions

186–202 **Katsuya Kimura, Ryo Misawa, and Fumihito Tashiro**

Descriptions of post-settlement juveniles of 3 greeneye species, *Chlorophthalmus nigromarginatus, C. acutifrons*, and *C. albatrossis* (Teleostei: Chlorophthalmidae), from Japan, with notes on their rapid metamorphosis after settlement

203 **Acknowledgment of reviewers**

205–208 **Guidelines for authors**

The National Marine Fisheries Service (NMFS) does not approve, recommend, or endorse any proprietary product or proprietary material mentioned in this publication. No reference shall be made to NMFS, or to this publication furnished by NMFS, in any advertising or sales promotion that would indicate or imply that NMFS approves, recommends, or endorses any proprietary product or proprietary material mentioned herein or that has as its purpose an intent to cause directly or indirectly the advertised product to be used or purchased because of this NMFS publication.

The NMFS Scientific Publications Office is not responsible for the contents of the articles.

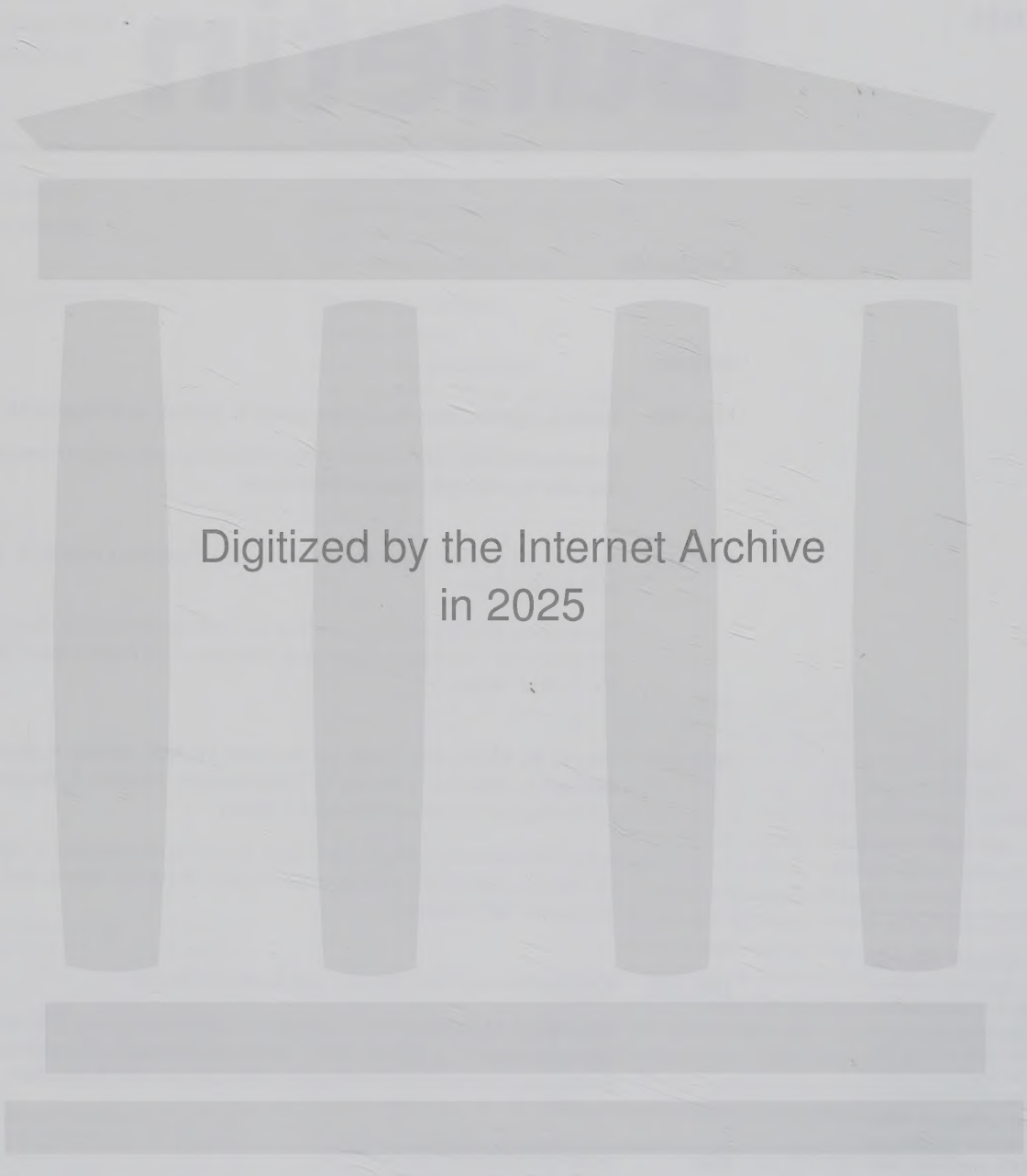

Digitized by the Internet Archive
in 2025

https://archive.org/details/fishery-bulletin_2024-10_122_4

National Marine Fisheries Service
NOAA

Fishery Bulletin
established in 1881

Spencer F. Baird
First U.S. Commissioner of Fisheries and founder of *Fishery Bulletin*

Reevaluating fecundity of white perch (*Morone americana*) in Chesapeake Bay with modern stereological techniques

Jacob T. Shaner (contact author)[1]
John M. Jacobs[2]
Lance T. Yonkos[3]
Reginal M. Harrell[4]

Email address for contact author: jacob.shaner@noaa.gov

[1] Fishing and Boating Services
Maryland Department of Natural Resources
904 South Morris Street
Oxford, Maryland 21654
Present address for contact author:
Cooperative Oxford Laboratory
National Centers for Coastal Ocean Science, NOAA
904 South Morris Street
Oxford, Maryland 21654

[2] Cooperative Oxford Laboratory
National Centers for Coastal Ocean Science, NOAA
904 South Morris Street
Oxford, Maryland 21654

[3] Department of Environmental Science and Technology
University of Maryland
1431 Animal Science/Agricultural Engineering Building
College Park, Maryland 20742

[4] Department of Environmental Science and Technology
University of Maryland
2113 Animal Science/Agricultural Engineering Building
College Park, Maryland 20742

Abstract—The white perch (*Morone americana*) is an abundant estuarine teleost in eastern North America, with its commercial and trophic importance creating a need for fecundity and recruitment data. In this study, we reevaluated the fecundity of subpopulations of white perch in Chesapeake Bay. Stereological sampling methods were used to determine if environmental changes in the Chesapeake Bay watershed over the last 60 years have altered average fecundity of this species. These methods were compared with automated gravimetric methods to determine the efficacy of using stereological fecundity sampling for white perch. The results of using both methods were statistically the same, as indicated by a Lin's concordance correlation coefficient of 0.98 and a favorable distribution on Bland–Altman plots. After the stereological methods were validated, archival histological samples from the Choptank River subestuary were evaluated for fecundity over a 4-year period of sampling. Results indicate that fecundity of white perch has been reasonably unchanged in the river system, with an average estimated fecundity of 69,379 oocytes per fish. These findings indicate the resiliency of the reproduction of white perch in mesohaline Chesapeake Bay, despite widespread environmental change.

Manuscript submitted 5 February 2024.
Manuscript accepted 14 June 2024.
Fish. Bull. 122:133–142 (2024).
Online publication date: 15 July 2024.
doi: 10.7755/FB.122.4.1

The views and opinions expressed or implied in this article are those of the author (or authors) and do not necessarily reflect the position of the National Marine Fisheries Service, NOAA.

Much has changed in the Chesapeake Bay watershed since 1961, including growth in the estimated human population by more than 10 million residents (Chesapeake Bay Program[1]). This growth has led to a cascade of effects, including changes in land use, differences in nitrogen and phosphorous inputs, and increased contamination, that influence estuarine habitats (Brush, 1997, 2001; Kemp et al., 2005). The last published investigation of fecundity of white perch (*Morone americana*) in Chesapeake Bay, in the Patuxent River sub-estuary (Mansueti, 1961), was done in 1961. Since then, research on the species has been focused on life history strategy (Kraus and Secor, 2004; McGrath and Austin, 2009; McCauley et al., 2014), reproduction and growth (Mansueti, 1964; Jackson and Sullivan, 1995; Newhard et al., 2012), and the use of white perch as indicators of ecosystem health (McLaughlin et al., 2018; Matsche et al., 2020). Given that human actions have affected the reproductive health of other resident species in the region (Blazer et al., 2013, 2014), fecundity of white perch should be reevaluated as a way to monitor reproductive potential and to ensure continued survival of this commercially valuable species.

In the last 60 years, fish fecundity sampling has become more efficient and cost effective, thanks to advances in open-source computing (Friedland et al., 2005; Klibansky and Juanes, 2008). Sampling efficiency has enabled collection of larger data sets, which provide greater detail on links between fecundity and stock recruitment (Lambert, 2008; Armstrong and Witthames, 2012) and have allowed fecundity sampling to become

[1] Chesapeake Bay Program. 2023. Population growth. [Web page available at website, accessed 6 September 2023.].

more specific to oocyte development mode (Murua et al., 2003; Witthames et al., 2009). This improvement in understanding the relationship between stock recruitment and fecundity has resulted in a more accurate picture of stock health and recruitment when metrics that include fecundity data, such as total egg production, are coupled with more traditional measurements, such as spawning stock biomass (Lambert, 2008; Morgan et al., 2009; Witthames et al., 2009). This increase in accuracy makes a strong argument for the inclusion of population-level egg production in modeling of fish stocks, even those stocks with stable recruitment, such as Chesapeake Bay white perch (Piavis and Webb[2]).

Gravimetric methods remain a popular choice for fecundity sampling given that they involve simple counting of whole oocytes in gravid specimens caught prior to spawning, with little to no sample preparation (Murua et al., 2003; Klibansky and Juanes, 2008). Therefore, early studies of reproduction of white perch relied on such methods to estimate relative fecundity (Mansueti, 1961; Taub, 1969; Zuerlein, 1981; Bur, 1986; Klauda et al., 1988). Although simple gravimetric counting has many advantages, gravimetric methods are not as effective at estimating fecundity of species in which vitellogenic and non-vitellogenic oocytes are similar in size or are uniformly mixed throughout an ovary (Murua et al., 2003). The white perch falls within this category of fish species (Jackson and Sullivan, 1995); therefore, other methods, such as stereological sampling, may be required to more accurately sample relative fecundity (Murua et al., 2003).

Stereological fecundity sampling methods for fish were developed by Emerson et al. (1990), who adapted stereometric principles used for counting lung alveoli developed by Weibel and Gomez (1962). By formulating specific equations to control for bias in oocyte size distribution and shape, Emerson et al. (1990) were able to accurately estimate fecundity in species employing both group-synchronous and asynchronous oocyte development strategies. In contrast to gravimetric methods, stereology can be used to estimate fecundity while simultaneously assessing reproductive health and oocyte developmental state (Emerson et al., 1990; Murua et al., 2003). Despite having been used with numerous species, stereological techniques have yet to be tested on white perch. If stereological methods can be validated for use with white perch, this new tool for reproductive health assessment not only will be added to the toolbox available for management of this species but also could be used in research that involves archival data to determine change over time.

In addition to monitoring general reproductive potential, monitoring for oocyte health and atresia is important for fish populations experiencing chronic stress. Research into the health of populations of white perch in Chesapeake Bay in response to anthropogenic stressors has yielded evidence of stress response in select populations (Morgan et al., 1973; McLaughlin et al., 2018; Matsche et al., 2020). Although severity and presentation of stress response has varied, noted responses to hypoxia and sediment contamination in the Choptank River watershed have included increased parasite burden, decreased white blood cell counts, and more observations of lesions (McLaughlin et al., 2018; Matsche et al., 2020). Reproductive effects of stress, however, have not been investigated beyond simple somatic index scores. Hypoxia and contamination have been determined to affect reproduction in a number of teleost species (Barton et al., 2002; Blazer et al., 2013, 2014), with specific reproductive effects that include increased atresia and greater incidence of intersex. Given the presence of these specific stressors in the habitats of white perch, it is highly possible that the reproduction of white perch in the Chesapeake Bay watershed has been affected.

We opportunistically used specimens already being collected for this health assessment work to reinvestigate fecundity in Chesapeake Bay populations of white perch by using stereological techniques. If stereological tools are accurate for this species, they not only will yield new data for the study of temporal change in reproductive potential but also will provide useful and efficient means for future studies of reproductive health in response to environmental change.

Materials and methods

Field collections for this study focused on gravid white perch from the Choptank River of Chesapeake Bay in Maryland, with an additional small sample collected from the Saluda River in South Carolina to account for geographical fecundity variation in method testing. Specimens from the Choptank River were captured by using either hook and line or standing fyke nets that collected fish for no more than 24 h (Table 2). Following capture, fish were transported live in river water with supplemental oxygen and held for 18–24 h before being euthanized with a lethal dose of buffered tricaine methanesulfonate (Syndel[3], Ferndale, WA) immediately before necropsy, as per animal use protocols of the Maryland Department of Natural Resources (UFRC, 2014). Specimens collected on the Saluda River were captured by using electrofishing techniques and were euthanized at the time of capture by severing the spinal cord, as per Maryland Department of Natural Resources animal use protocols for animals that cannot be transported alive (UFRC, 2014). Fish were checked by palpation of the abdomen for sex and spawning state at time of capture to mitigate the collection of postspawning specimens. Males and postspawning females were returned to the waters where they were captured.

Before necropsy, morphological data, including total length (TL, in millimeters) and total fish weight (in grams) prior to evisceration, were recorded. Age was determined

[2] Piavis, P., and E. Webb III. 2018. Population assessment of white perch in select regions of Chesapeake Bay, Maryland. Md. Dep. Nat. Resour., Vol. Rep. F-61-R, 46 p. [Available from Md. Dep. Nat. Resour., 580 Taylor Ave., Annapolis, MD 21401.]

[3] Mention of trade names or commercial companies is for identification purposes only and does not imply endorsement by the Maryland Department of Natural Resources or the National Marine Fisheries Service, NOAA.

after necropsy by submerging dry, whole otoliths in glycerol and counting annuli at 10× magnification. During necropsy examination, ovaries were excised, measured for mass and volume, and then sectioned and fixed in 10% neutral buffered formalin before subsamples were counted gravimetrically and stereometrically. Volume was measured by using the wet-weight method, described by Scherle (1970), in which ovaries are suspended in a tared water bath and weighed. Ovaries were sectioned by using a multiblade knife with blade spacing of 4 mm. Alternating sequential sections of 4 mm from both ovaries were used for gravimetric and stereometric analysis, with no less than 3 sections used for stereometry depending on ovary size. Because differences in oocyte distribution between ovarian regions were not considered in previous studies (Mansueti, 1961; Taub, 1969; Klauda et al., 1988; Okoye et al., 2008), a subset of sequential histological samples from 10 specimens were placed in individual histology cassettes and examined to confirm the lack of locational bias. Data confirm that oocyte size distribution was uniform throughout examined ovaries.

To test the efficacy of using stereological methods to estimate relative fecundity in white perch, data obtained from stereological counts were compared to fecundity estimated gravimetrically. Gravimetric oocyte counting was selected as the comparative method because prior fecundity estimations for populations of white perch all were made with gravimetric techniques (Taub, 1969; Zuerlein, 1981; Bur, 1986; Klauda et al., 1988; Okoye et al., 2008). For gravimetric sampling, we used techniques described by Klibansky and Juanes (2008), specifically their method for the automated counting of oocytes with ImageJ, vers. 1.53k (Schneider et al., 2012).

Gravimetric counting procedures started with collection of oocyte samples that were separated from ovarian connective tissue by using a series of sieves. From this subset, a sample of 1 g (±0.001 g) was taken, placed in 70% ethanol, and vortexed for 15 s at 1000 rpm to further separate individual oocyte particles. Following separation, oocyte samples were placed on a standard petri dish that had a diameter of 100 mm and had been painted black, and the samples were photographed with a Nikon D5100 camera that had an AF-S Micro Nikkor 60-mm lens (Nikon Corp., Tokyo, Japan). After photography, ImageJ was used to automate particle counts, with macro scripts automatically adjusting image attributes and recording number and size of particles in the sample. Particles that were larger than the 95th quartile of the size–frequency distribution were considered groups of oocytes. The area of these groups was divided by the mean particle area of the sample to estimate how many individual oocytes were present in the group.

Stereometric methods followed those of Emerson et al. (1990), as described by Murua et al. (2003), with point-counting techniques used to estimate fecundity. Stereological samples were prepared for analysis by using standard paraffin embedding protocols with sectioning done at 5-µm increments (Hinton, 1990). Before point counting, samples were checked for signs of ovulation by using light microscopy.

The white perch is a batch-spawning species with a group-synchronous oocyte development mode; therefore, oocytes are present in ovaries at multiple different developmental stages during spawning (Jackson and Sullivan, 1995). Samples with post-ovulatory oocytes were removed from consideration, as active spawning would affect the accuracy of fecundity estimates. For point counting, the grid area was adjusted to 3000 μm^2, 4× magnification was used, and a minimum of 10 full grids were counted, to ensure a balance between sampling efficiency and accuracy. Because of constraints in available equipment, the grid style was changed from the Weibel multipurpose grid as pictured in figure 4 of Murua et al. (2003), to a 10-line-by-10-line standard grid of 81 cells (Fig. 1). All method changes were tested for precision by monitoring observed coefficient of

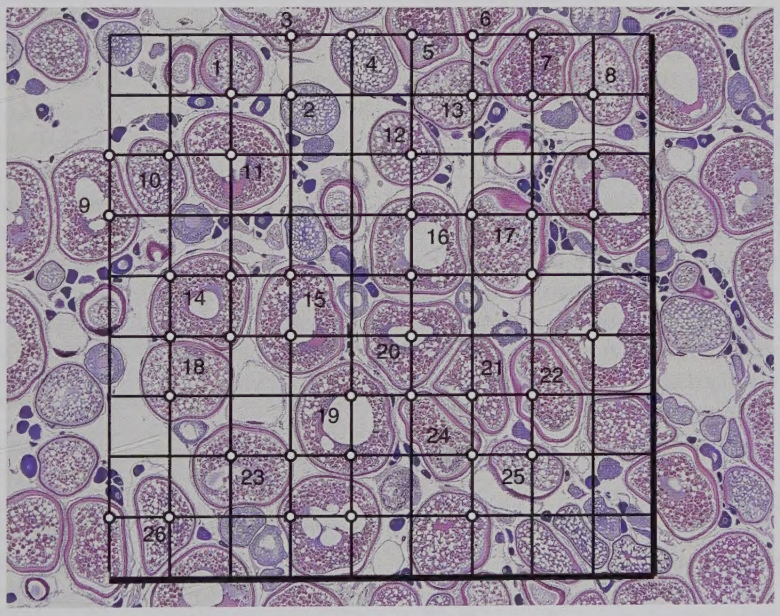

Figure 1

Image of the grid used for stereological fecundity sampling of white perch (*Morone americana*) caught from 2015 through 2018 in the Choptank River in Maryland. The grid differs from the Wiebel multipurpose grid used in other studies, but results from pilot studies indicate that the difference in grids did not affect the accuracy of estimates. The thick lines on the right side and bottom of the grid indicate exclusionary boundaries (the oocytes that overlap these boundaries were not counted), numerals indicate the number of counted whole oocytes, and white dots indicate grid intersection points that fall over oocyte tissue and were counted.

error (OCE) while sampling to verify that error rates were below 10% (West, 2012).

Following point counts, relative fecundity was calculated by multiplying the number of oocytes per unit volume by total volume of the ovaries (Emerson et al., 1990; Murua et al., 2003). Coefficients used to correct for variance in size distribution (K) and shape of oocytes (β) used by Emerson et al. (1990) were calculated for each sample by using ImageJ to count and measure particles on images taken at 4× magnification.

Method agreement was assessed by using Lin's concordance correlation coefficient (Lin, 1989) interpreted on McBride's strength of agreement criteria (McBride[4]). This assessment was undertaken in order to simultaneously measure agreement between the methods and potential bias (Lin, 1989), as opposed to using a Pearson's correlation, which can fail at assessing certain sampling biases, such as scale and location shift, when the desired outcome is reproducibility. Results from concordance correlation coefficient assessments were then combined with plotting of data by using Bland–Altman techniques and by calculating Deming and Passing–Bablok regressions to further assess potential bias (Deming, 1943; Passing and Bablok, 1983; Bland and Altman, 1986). The Bland–Atlman difference plot is a common means of visualization to compare 2 methods of collecting the same data (Bland and Altman, 1986; Westgard, 2008) and allows additional qualitative review of bias between the 2 different methods. If plotted differences approximate zero, are evenly distributed around the mean of differences, and fall within Bland–Altman accepted limits of agreement (1.96 standard deviation), it is assumed that there is no measurement bias from either method. A lack of such bias is critical for the reproducibility of data and interchangeability of methods.

Relationships between morphological data and fecundity were investigated by using linear regression techniques. Regression models were created for the entire sample and for individual years. To assess interannual variability in fecundity, analysis of variance with log transformation of fecundity data was used to compare fecundity between the 4 sampling years.

Results

Methods testing

In 2018, 42 white perch were sampled from 2 geographically isolated river systems for the purpose of testing stereological fecundity methods (Table 1). The OCE calculations indicate that a grid size of 3000 μm^2 and the minimum of 10 full grids per sample counted was sufficient to keep the OCE below 0.1. Average OCE was 0.047 for particle-area counts and 0.068 for particle-enumeration counts. In assessment of the correlation between the methods, Lin's concordance correlation coefficient was 0.98, indicating "substantial" agreement as per McBride's scale (McBride[4]). Bland–Altman plots indicate that 95% of data points are within 1.96 standard deviation confidence intervals as recommended (Fig. 2). There was no visual indication of constant bias between methods, corroborated by results from Passing–Bablok and Deming regressions (Table 1). As archival data included only dry mass ovarian weight, volumes were estimated for calculations by using the formula obtained by comparing a subset of whole ovaries measured for dry mass and wet weight:

$$V = 0.58110 + (0.96842 \times M) + 1.233,$$

where V = ovarian volume; and

M = dry mass.

Differences in fecundity estimates between the Saluda River in South Carolina and the Choptank River in Maryland were negligible. In analysis of samples collected from specimens caught in 2018 for comparison of methods, specimens from the Saluda River had an average estimated fecundity of 42,761 oocytes per fish, and specimens from the Choptank River had an average estimated fecundity of 54,406 oocytes per fish.

Table 1

Results from analysis with Lin's concordance correlation coefficient (CCC), Deming regression, and Passing–Bablok regression to compare stereological and gravimetric fecundity sampling methods used to evaluate fecundity in white perch (*Morone americana*) sampled in 2018 from the Choptank River in Maryland and the Saluda River in South Carolina. Confidence intervals are provided in parentheses. Intervals contain 0.00 for both intercepts and 1.00 for both slopes; therefore, there is no statistical evidence of bias. n=sample size.

n	Lin's CCC	Deming regression	Passing–Bablok regression
42	0.979	Intercept: −107.91 (−5786.51–5583.98) Slope: 1.01 (0.94–1.07)	Intercept: −2717.75 (−9081.37–2745.47) Slope: 1.02 (0.95–1.10)

Fecundity sampling

Following the favorable results from the methods comparison, stereological methods were used to reevaluate the fecundity of Chesapeake Bay white perch, by using the Choptank River subpopulation as a proxy for the population of the entire system. From 2015 through 2018, 182 gravid white perch were collected (Table 2). Ovarian tissue

[4] McBride, G. 2005. A proposal for strength-of-agreement criteria for Lin's concordance correlation coefficient. NIWA Client Rep. HAM2005-062, 7 p. N.Z. Natl. Inst. Water Atmos. Res., Hamilton, New Zealand. [Report on NIWA project MOH05201 prepared for the Ministry of Health.] [Available from website.]

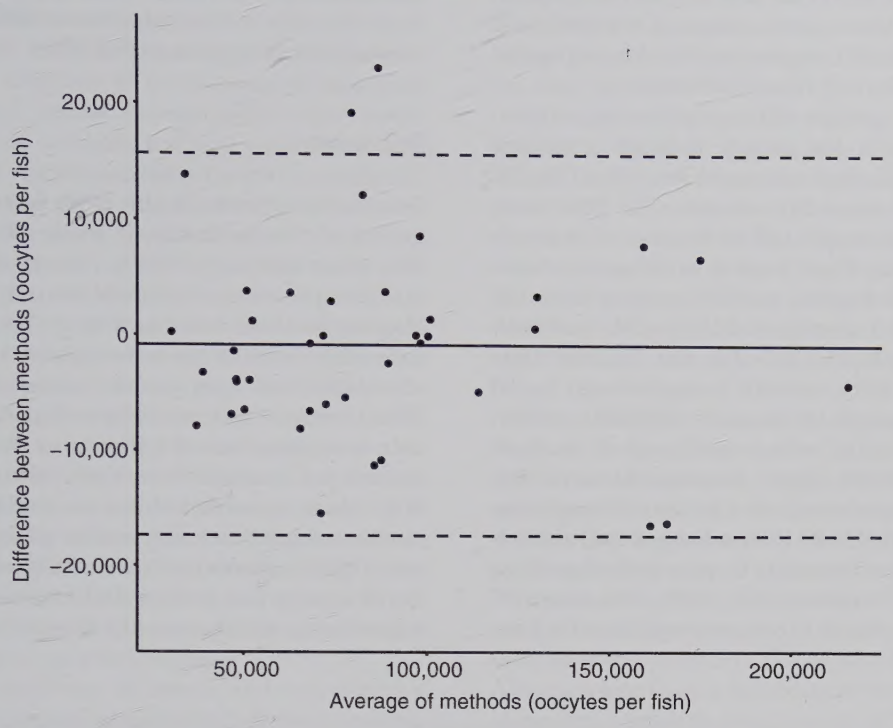

Figure 2

Bland–Altman plot comparing gravimetric and stereological sampling methods used to estimate fecundity of white perch (*Morone americana*) caught in 2018 in the Choptank River in Maryland. Dashed lines indicate 95% confidence intervals (1.96 standard deviation). The solid line indicates the mean of the differences between the 2 methods. A mean of differences near zero indicates a general lack of bias between the measurements and random variability.

Table 2

Estimated average, minimum, and maximum fecundity of white perch (*Morone americana*) caught during 2015–2018 in the Choptank River in Maryland. Hook-and-line gear were used to sample fish in 2015 at site 1 (top set of coordinates) and in 2016. Standing fyke nets were used to sample fish in 2015 at site 2 (bottom set of coordinates) and in 2017 and 2018. *n*=sample size.

			Fecundity (oocytes per fish)		
Year	Sampling location	*n*	Average	Min	Max
2015	38.9985, −75.7857; 38.7800, −75.9602	51	38,811.63	9399	13,8157
2016	38.9735, −75.8009	30	25,340.43	7691	84,345
2017	38.7800, −75.9602; 38.8072, −75.9113	35	65,520.77	28,592	146,092
2018	38.7800, −75.9602	66	117,164.30	57,184	280,537

samples from each fish were sectioned, placed on microscope slides, and archived. Mean total fish weight for all collected specimens is 140.9 g, and mean TL of fish is 211.3 mm. Mean fish age was 5 years, with a range of 2–14 years. Estimated fecundity, determined from archival histological samples, was an average of 69,379 oocytes per fish for all 4 years combined, with a maximum value of 280,537 oocytes per fish in 2018 and a minimum of 7691 oocytes per fish in 2016 (Table 2). Averages from this study fall within the range of historically reported fecundity

estimates of 50,000–150,000 oocytes per fish for populations in Chesapeake Bay and the range of reported total fecundity of 5000–320,000 oocytes per fish for all populations of this species (Setzler-Hamilton, 1991).

Results from investigations of the relationship between length and fecundity in the sample indicate a positive correlation between TL and estimated fecundity (Fig. 3). As shown in Table 2, fecundity estimates for 2018 were notably higher than fecundity values for any of the previous 3 years of sampling. Total lengths in the sample were similar in range, with lengths in 2018 ranging from 185 to 255 mm TL, with an average of 217 mm TL, and with lengths of 159–265 mm TL, 161–245 mm TL, and 189–267 mm TL in 2015, 2016, and 2017, respectively. Use of the linear model of length by fecundity yielded a moderately positive relationship, with a coefficient of multiple determination (R^2) of 0.48 (Fig. 3). Interannual variability among fish in the sample is indicated by the different average fecundity values (Table 2). Comparison of the relationship between length and fecundity by year yielded positive relationships, with R^2 values of 0.71, 0.68, 0.80, and 0.66 for 2015, 2016, 2017, and 2018, respectively. Results from the analysis of variance following log transformation of fecundity data indicate significant differences in fecundity between sampling years (P<0.001).

Discussion

Our study represents the most comprehensive investigation of the fecundity of white perch in Chesapeake Bay since the early 1960s. We used a novel approach for this species: stereological fecundity sampling. Stereological methods were proven to be efficient and accurate when results were compared to results from use of established gravimetric oocyte counting methods. This favorable outcome allowed us to expand the available fecundity data for Choptank River white perch to include information from archival histological samples. With these expanded data, we could conduct a robust, multiyear analysis of fecundity in this subpopulation of white perch. Findings from this study regarding reproductive potential further indicate the resiliency of the reproduction of Chesapeake Bay white perch in the face

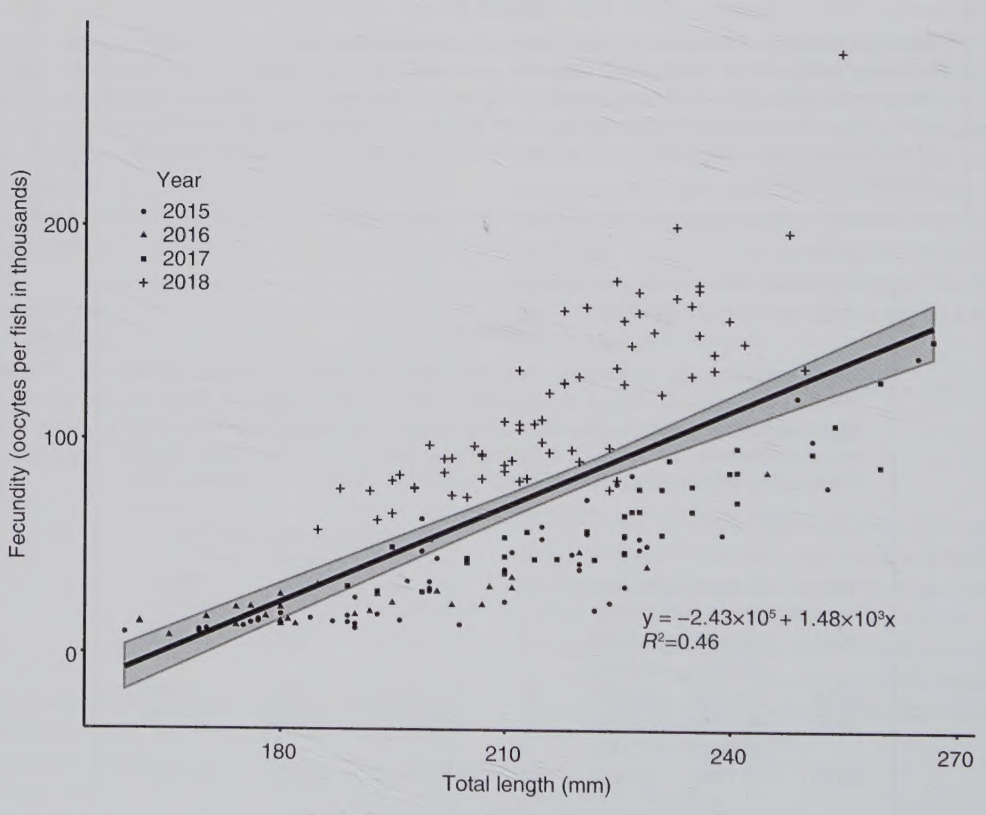

Figure 3

Relationship between estimated fecundity and total length, by year, for white perch (*Morone americana*) caught in the Choptank River in Maryland from 2015 through 2018. The shaded area indicates the estimated standard error. The equation of the line and the coefficient of multiple determination (R^2) are provided. The high fecundity values in 2018 indicate interannual variability in average fecundity of Choptank River white perch.

of environmental change and fluctuations in fishing pressure and predation over time.

When coupled with basic automation of repetitive procedures and slight changes to techniques, stereological methods appear well suited for use with white perch. Although stereological methods are well established and could be assumed to work reasonably for white perch, initial testing was needed on the basis of the oocyte development mode of white perch. Because white perch have a group-synchronous spawning strategy, ovaries of gravid fish have a well-mixed size distribution of oocytes (Jackson and Sullivan, 1995) that could confound calculations of size and shape if oocytes were not properly bounded. Results from comparisons between gravimetric and stereological methods, however, indicate that bounded gravimetric counts are just as accurate as stereometric counts and, therefore, that the size distribution of oocytes did not affect counting of whole oocytes. Although counting of whole oocytes, especially with automated image analysis, is rapid and effective (Klibansky and Juanes, 2008), performing counts stereologically has advantages, such as the abilities to cross-validate field assessments of spawning state and to investigate ovarian health.

Because of their accuracy, efficiency, and cost-effective nature, we expect stereological methods to become another tool for resource managers to more accurately assess change in reproductive potential of white perch. Despite a ubiquitous presence of the white perch in estuaries of eastern North America and the Great Lakes region, most fecundity estimates for the species were reported more than 30 years ago (Setzler-Hamilton, 1991). Having updated methods with which to retest fecundity estimates will be useful in the reevaluation of fecundity over the range of white perch, and examining fecundity stereologically will increase knowledge of reproductive health and temporal change in fecundity. Advantages of the stereological method include the abilities to simultaneously determine oocyte developmental state and sample fecundity, to monitor for reproductive health pathology, such as intersex and atresia, and to study change in fecundity over time by using archival samples. Monitoring atresia is especially important considering the relationship of this condition with environmental stress (Schreck et al., 2001; Barton et al., 2002).

In comparisons of data between the previous study conducted in the Patuxent River sub-estuary in Maryland (Mansueti, 1961) and this study, no apparent change was found in reproductive potential for white perch in Chesapeake Bay in Maryland. It is worth noting that direct comparisons are impossible because study methods for the original work were not recorded (Mansueti, 1961) and samples were not acquired from the Patuxent River for our study. Geographical isolation is an important consideration in the Chesapeake region, as white perch have discrete home ranges (McGrath and Austin, 2009), which, in conjunction with salt regimes in Chesapeake Bay, typically keep populations of white perch in the larger sub-estuaries from mixing. Therefore, a truly direct comparison between historical data would require specimens from the Patuxent River, and a truly holistic evaluation of fecundity of Chesapeake Bay white perch would require larger geographical coverage of multiple sub-estuaries of the tidal region of Maryland.

Although characteristics of the Choptank River are similar to those of the Patuxent sub-estuary, the populations in both systems are distinct and, therefore, have potentially different average reproductive potentials. We contend, however, that the Choptank River, with characteristics similar to those of the Patuxent River, serves as an effective proxy in our study. Land use in the Patuxent River watershed is markedly different, with approximately 23% of the watershed developed compared to only 5% of the watershed developed for the Choptank River (NOAA Office for Coastal Management, Coastal Change Analysis Program Landcover Atlas, available from website, accessed September 2023), but the general latitudinal and climactic locations for both sub-estuaries in the Chesapeake Bay watershed are nearly identical, making comparisons between the 2 systems a reasonable approach.

Investigating the relationship between TL and estimated fecundity was also a novel approach for populations of white perch in Chesapeake Bay (Mansueti, 1961). Although length and fecundity of the entire sample had a moderately positive relationship (R^2=0.48), relationships between length and fecundity for each year had greater correlation. Findings of interannual variability were confirmed by using analysis of variance, indicating that unknown drivers are affecting egg production.

Fecundity has been reported to vary in other species as a result of numerous factors, including food availability, fish condition, and climate (Rideout and Morgan, 2007; Lambert, 2008). Other possible explanations for the variability in fecundity found for specimens in our study are differences in reproductive potential between resident freshwater subpopulations and migratory populations in the Choptank River system. Research into the interestuarine movements of white perch in the neighboring Patuxent River has revealed the presence of resident, non-migratory freshwater population contingents (Kraus and Secor, 2004; Kerr and Secor, 2012). Although these contingents contribute to system-wide recruitment (Kraus and Secor, 2005), it is not known whether fecundity varies between migratory and resident populations. For this study, sampling in 2015–2017 included work in freshwater areas in the upper limits of the Choptank River system, increasing the potential of sampling freshwater residents. Further study would need to incorporate chemical otolith analysis to determine the source populations for individuals before it could be possible to determine whether resident populations have lower average fecundity than migratory populations.

Another explanation could be a greater influence of age, in comparison to that of length, on individual fecundity in the Choptank River population, possibly the result of a truncated age-at-length population structure due to fishing pressure. White perch are commercially collected in the Choptank River system through winter gill-net fishing (Piavis and Webb[2]). If fishing was selective for larger white

perch (>200 mm TL), as has been reported for numerous stocks with commercial fishing pressure (Bianchi et al., 2000; Ward and Myers, 2005), older females might be shorter in length but more fecund, possibly accounting for the greater fecundity (average fecundity was 117,164 oocytes per fish in 2018, versus 65,520 oocytes per fish in 2017) but not greater length (average TL was 217 mm in 2018, versus 225 mm in 2017) in specimens caught in 2018. Results from year-class investigation in the Choptank River indicate that the 2011 year class is a dominant class (Piavis and Webb[2]). Age data from this study indicate that the majority of fish collected in 2018 and 2017 were of this age class; therefore, the fish may not be growing longer but are instead producing more eggs with age.

Conclusions

In this study, we were able not only to effectively reevaluate fecundity in white perch from the Chesapeake Bay watershed but also to demonstrate the utility and accuracy of modern stereological methods of sampling for this species. The white perch is an important species in estuarine food webs in eastern North America, and the ability of this species to maintain reproductive potential and population abundance will be critical for commercially and environmentally important anadromous species of this region that use white perch as food in their early life stages (Walter and Austin, 2003). In addition, it has been demonstrated that the abundance and health of white perch are useful proxies for general habitat health (McLaughlin et al., 2018). Therefore, the ability to monitor reproductive health and production of this species can be useful in study of habitat quality for all resident species of a given mesohaline area. Given the abundance of white perch in the estuaries of eastern North America, studying changes in the reproductive potential of populations of this species over time and in relation to environmental shifts could provide insights into the health and resiliency of teleost communities in this region.

Resumen

La perca blanca (*Morone americana*) es un teleósteo estuarino abundante en el este de Norteamérica, y su importancia comercial y trófica crea la necesidad de disponer de datos sobre fecundidad y reclutamiento. En este estudio, reevaluamos la fecundidad de subpoblaciones de perca blanca en la bahía de Chesapeake. Se utilizaron métodos de muestreo estereológico para determinar si los cambios medioambientales en la cuenca de la bahía de Chesapeake durante los últimos 60 años han alterado la fecundidad media de esta especie. Estos métodos se compararon con los métodos gravimétricos automatizados para determinar la eficacia del uso del muestreo estereológico de fecundidad para la perca blanca. Los resultados de la utilización de ambos métodos fueron estadísticamente iguales, como lo indica el coeficiente de correlación de concordancia de Lin de 0.98 y una distribución favorable en los gráficos de Bland–Altman. Una vez validados los métodos estereológicos, se evaluó la fecundidad de muestras histológicas almacenadas del estuario del río Choptank durante un período de muestreo de 4 años. Los resultados indican que la fecundidad de la perca blanca se ha mantenido razonablemente inalterada en el sistema fluvial, con una fecundidad media estimada de 69,379 oocitos por pez. Estos resultados indican la resistencia de la reproducción de la perca blanca en la bahía mesohalina de Chesapeake, a pesar de los cambios ambientales generalizados.

Acknowledgments

This work was made possible by the efforts of numerous employees of the Maryland Department of Natural Resources, including K. Rosemary, M. Matsche, S. Brown, C. McCollough, and S. Lehmann, and by the efforts of J. Bulak and his team at the South Carolina Department of Natural Resources.

Literature cited

Armstrong, M. J., and P. R. Witthames.
2012. Developments in understanding of fecundity of fish stocks in relation to egg production methods for estimating spawning stock biomass. Fish. Res. 117–118:35–47.

Barton, B. A., J. D. Morgan, and M. M. Vijayan.
2002. Physiological and condition-related indicators of environmental stress in fish. *In* Biological indicators of aquatic ecosystem stress (S. M. Adams, ed.), p. 111–148. Am. Fish. Soc., Bethesda, MD.

Bianchi, G., H. Gislason, K. Graham, L. Hill, X. Jin, K. Koranteng, S. Manickchand-Heileman, I. Payá, K. Sainsbury, F. Sanchez, et al.
2000. Impact of fishing on size composition and diversity of demersal fish communities. ICES J. Mar. Sci. 57:558–571.

Bland, J. M., and D. Altman.
1986. Statistical methods for assessing agreement between two methods of clinical measurement. Lancet 327:307–310.

Blazer, V. S., A. E. Pinkney, J. A. Jenkins, L. R. Iwanowicz, S. Minkkinen, R. O. Draugelis-Dale, and J. H. Uphoff.
2013. Reproductive health of yellow perch *Perca flavescens* in selected tributaries of the Chesapeake Bay. Sci. Total Environ. 447:198–209.

Blazer, V. S., D. D. Iwanowicz, H. L. Walsh, A. J. Sperry, L. R. Iwanowicz, D. A. Alvarez, R. A. Brightbill, G. Smith, W. T. Foreman, and R. Manning.
2014. Reproductive health indicators of fishes from Pennsylvania watersheds: association with chemicals of emerging concern. Environ. Monit. Assess. 186:6471–6491.

Brush, G. S.
1997. History and impact of human activities on Chesapeake Bay. *In* Ecosystem function and human activities (R. D. Simpson and N. L. Christensen, eds.), p. 125–145. Springer, Boston, MA.
2001. Natural and anthropogenic changes in Chesapeake Bay during the last 1000 years. Hum. Ecol. Risk Assess. 7:1283–1296.

Bur, M. T.
1986. Maturity and fecundity of the white perch, *Morone americana*, in western Lake Erie. Ohio J. Sci. 86:205–207.
Deming, W. E.
1943. Statistical adjustment of data, 269 p. John Wiley and Sons, New York.
Emerson, L. E., M. G. Walker, and P. R. Witthames.
1990. A stereological method for estimating fish fecundity. J. Fish Biol. 36:721–730.
Friedland, K. D., D. Ama-Abasi, M. Manning, L. Clarke, G. Kligys, and R. C. Chambers.
2005. Automated egg counting and sizing from scanned images: rapid sample processing and large data volumes for fecundity estimates. J. Sea Res. 54:307–316.
Hinton, D. E.
1990. Histological techniques. *In* Methods for fish biology (C. B. Schreck and P. B. Moyle, eds.), p. 191–209. Am. Fish. Soc., Bethesda, MD.
Jackson, L. F., and C. V. Sullivan.
1995. Reproduction of white perch: the annual gametogenic cycle. Trans. Am. Fish. Soc. 124:563–577.
Kemp, W. M., W. R. Boynton, J. E. Adolf, D. F. Boesch, W. C. Boicourt, G. Brush, J. C. Cornwell, T. R. Fisher, P. M. Glibert, J. D. Hagy, et al.
2005. Eutrophication of Chesapeake Bay: historical trends and ecological interactions. Mar. Ecol. Prog. Ser. 303:1–29.
Kerr, L. A., and D. H. Secor.
2012. Partial migration across populations of white perch (*Morone americana*): a flexible life history strategy in a variable estuarine environment. Estuar. Coasts 35:227–236.
Klauda, R. J., J. B. McLaren, R. E. Schmidt, and W. P. Dey.
1988. Life history of white perch in the Hudson River estuary. Am. Fish. Soc. Monogr. 4:69–88.
Klibansky, N., and F. Juanes.
2008. Procedures for efficiently producing high-quality fecundity data on a small budget. Fish. Res. 89:84–89.
Kraus, R. T., and D. H. Secor.
2004. Dynamics of white perch *Morone americana* population contingents in the Patuxent River estuary, Maryland, USA. Mar. Ecol. Prog. Ser. 279:247–259.
2005. Application of the nursery-role hypothesis to an estuarine fish. Mar. Ecol. Prog. Ser. 291:301–305.
Lambert, Y.
2008. Why should we closely monitor fecundity in marine fish populations? J. Northwest Atl. Fish. Sci. 41:93–106.
Lin, L. I.-K.
1989. A concordance correlation coefficient to evaluate reproducibility. Biometrics 45:255–268.
Mansueti, R. J.
1961. Movements, reproduction, and mortality of the white perch, *Roccus americanus*, in the Patuxent estuary, Maryland. Chesap. Sci. 2:142–205.
1964. Eggs, larvae, and young of the white perch, *Roccus americanus*, with comments on its ecology in the estuary. Chesap. Sci. 5:3–45.
Matsche, M. A., V. S. Blazer, E. L. Pulster, and P. M. Mazik.
2020. High prevalence of biliary neoplasia in white perch *Morone americana*: potential roles of bile duct parasites and environmental contaminants. Dis. Aquat. Org. 141:195–224.
McCauley, M. M., R. M. Cerrato, M. Sclafani, and M. G. Frisk.
2014. Diel behavior in white perch revealed using acoustic telemetry. Trans. Am. Fish. Soc. 143:1330–1340.
McGrath, P., and H. A. Austin.
2009. Site fidelity, home range, and tidal movements of white perch during the summer in two small tributaries of the York River, Virginia. Trans. Am. Fish. Soc. 138:966–974.
McLaughlin, S. M., A. K. Leight, J. E. Spires, S. B. Bricker, J. M. Jacobs, G. A. Messick, and S. Skelley.
2018. Coastal ecosystem assessment to support NOAA's Choptank River complex habitat focus area: Tred Avon River. NOAA Tech. Memo. NOS NCCOS 251, 118 p.
Morgan, M. J., H. Murua, G. Kraus, Y. Lambert, G. Marteinsdóttir, C. T. Marshall, L. O'Brien, and J. Tomkiewicz.
2009. The evaluation of reference points and stock productivity in the context of alternative indices of stock reproductive potential. Can. J. Fish. Aquat. Sci. 66:404–414.
Morgan, R. P., R. F. Fleming, V. J. Rasin, and D. R. Heinle.
1973. Sublethal effects of Baltimore Harbor water on the white perch, *Morone americana*, and the hogchoker, *Trinectes maculatus*. Chesap. Sci. 14:17–27.
Murua, H., G. Kraus, F. Saborido-Rey, P. R. Witthames, A. Thorsen, and S. Junquera.
2003. Procedures to estimate fecundity of wild collected marine fish in relation to fish reproductive strategy. J. Northwest Atl. Fish. Sci. 33:33–54.
Newhard, J. J., J. W. Love, and J. Gill.
2012. Do juvenile white perch *Morone americana* grow better in freshwater habitats of the Blackwater River drainage (Chesapeake Bay, MD, USA)? Estuar. Coasts 35:1110–1118.
Okoye, A. O., A. S. Overton, M. Loeffler, and S. E. Winslow.
2008. White perch fecundity relationships in western Albemarle Sound, North Carolina. J. N.C. Acad. Sci. 124:46–50.
Passing, H., and W. Bablok.
1983. A new biometrical procedure for testing the equality of measurements from two different analytical methods: application of linear regression procedures for method comparison studies in clinical chemistry, Part 1. J. Clinical Chem. Lab. Med. 21:709–724.
Rideout, R. M., and M. J. Morgan.
2007. Major changes in fecundity and the effect on population egg production for three species of north-west Atlantic flatfishes. J. Fish Biol. 70:1759–1779.
Scherle, W.
1970. A simple method for volumetry of organs in quantitative stereology. Mikroskopie 26:57–60.
Schneider, C. A., W. S. Rasband, and K. W. Eliceiri.
2012. NIH Image to ImageJ: 25 years of image analysis. Nat. Methods 9:671–675.
Schreck, C. B., W. Contreras-Sanchez, and M. S. Fitzpatrick.
2001. Effects of stress on fish reproduction, gamete quality, and progeny. Aquaculture 197:3–24.
Setzler-Hamilton, E. M.
1991. White perch, *Morone americana*. *In* Habitat requirements for Chesapeake Bay living resources, 2nd ed., p. 12.1–12.20. Chesap. Res. Consort., Solomons, MD.
Taub, S. H.
1969. Fecundity of the white perch. Progress. Fish-Cult. 31:166–168.
UFRC (Use of Fishes in Research Committee).
2014. Guidelines for the use of fishes in research, 86 p. Am. Fish. Soc., Bethesda, MD.
Walter, J. F., III, and H. M. Austin.
2003. Diet composition of large striped bass (*Morone saxatilis*) in Chesapeake Bay. Fish. Bull. 101:414–423.
Ward, P., and R. A. Myers.
2005. Shifts in open-ocean fish communities coinciding with the commencement of commercial fishing. Ecology 86:835–847.
Weibel, E. R., and D. M. Gomez.
1962. A principle for counting tissue structures on random sections. J. Appl. Physiol. 17:343–348.

West, M. J.
2012. Basic stereology for biologists and neuroscientists, 206 p. Cold Spring Harbor Lab. Press, Cold Spring Harbor, NY.

Westgard, J. O.
2008. Basic method validation: training in analytical quality management for healthcare laboratories, 3rd ed., 320 p. Westgard Quality Corp., Madison, WI.

Witthames, P. R., A. Thorsen, H. Murua, F. Saborido-Rey, L. N. Greenwood, R. Dominguez, M. Korta, and O. S. Kjesbu.
2009. Advances in methods for determining fecundity: application of the new methods to some marine fishes. Fish. Bull. 107:148–164.

Zuerlein, G.
1981. The white perch, *Marone americana* (Gmelin) in Nebraska. Neb. Tech. Ser. 8, 108 p.

National Marine
Fisheries Service
NOAA

Fishery Bulletin
established in 1881

Spencer F. Baird
First U.S. Commissioner
of Fisheries and founder
of *Fishery Bulletin*

Quantifying the effects of sample size and species distribution on the precision and accuracy of abundance estimates from bottom-trawl surveys in the Gulf of Alaska

Paul G. von Szalay (contact author)[1]
Edward A. Laman[1]
Stan Kotwicki[1]
Lewis A. K. Barnett[1]
Kotaro Ono[2]

Email address for contact author: paul.von.szalay@noaa.gov

[1] Resource Assessment and Conservation Engineering Division
Alaska Fisheries Science Center
National Marine Fisheries Service, NOAA
7600 Sand Point Way NE
Seattle, Washington 98115

[2] Institute of Marine Research
P.O. Box 1870 Nordnes
5817 Bergen, Norway

Abstract—We assessed the effect of survey effort reduction on the accuracy and precision of estimates of abundance for 4 commercially or ecologically important species with differing distributions observed in a bottom-trawl survey conducted in the Gulf of Alaska. Simulations from a spatiotemporal generalized linear mixed model based on historical observations of catch densities were used to evaluate the statistical robustness, measured in terms of coefficient of variation, relative bias, and relative root mean square error, of the abundance estimates and their variances. These metrics were used to compare estimates between the traditional design-based estimator and the alternative estimator, based on a vector autoregressive spatiotemporal model, at 4 different sampling densities, representing 2 historical and 2 theoretical sampling effort levels on either side of the historical range. The recent reduction in the density of survey sampling from 820 to 550 stations had only a modest effect on the performance metrics for both estimators for arrowtooth flounder (*Atheresthes stomias*), Pacific cod (*Gadus macrocephalus*), and Pacific ocean perch (*Sebastes alutus*). However, the effect on the abundance estimates for sablefish (*Anoplopoma fimbria*) was substantial. We attribute this difference in results to the wider depth range utilized by sablefish, which preferentially occupy the relatively under-sampled deep strata (>500 m), and to the truncated survey area at the reduced sampling levels where the deepest strata (>700 m) have been eliminated.

Manuscript submitted 13 March 2024.
Manuscript accepted 16 July 2024.
Fish. Bull. 122:143–161 (2024).
Online publication date: 9 August 2024.
doi: 10.7755/FB.122.4.2

The views and opinions expressed or implied in this article are those of the author (or authors) and do not necessarily reflect the position of the National Marine Fisheries Service, NOAA.

The precision of estimates of abundance based on data from fishery-independent surveys generally increases with sample size, assuming the availability of a species to sampling remains constant. In practice, the number of sampling stations is typically known before a survey design is generated and is dictated by logistical constraints of conducting bottom-trawl surveys, including funding, staffing, time, and the ability to acquire appropriate and sufficient sampling tools and platforms. The goal of a survey design is, therefore, to optimize the geographical distribution of the predetermined number of sampling stations to achieve the highest possible precision and accuracy for survey data products. Furthermore, it is often assumed that sampling effort will remain constant over time when a survey time series is initiated. However, a potential problem for survey continuity arises if circumstances compel alteration of sampling effort because variability in sample size can change the precision of abundance estimates (Cochran, 1977). Large-scale surveys (spanning areas larger than approximately 30,000 km^2), which tend to be relatively long in duration (>1–2 months), are especially prone to unavoidable reductions in survey effort because there is a smaller margin with which to accommodate unforeseen tightening of logistical constraints for them (ICES, 2020).

It is well-known that fisheries resource management agencies, both in the United States and internationally, have had to contend with unavoidable reductions in survey effort for a variety of reasons. These reasons include vessel breakdowns, reduction in survey area due to development of offshore wind farms, failure to acquire a sufficient number of survey vessels or staff, bad weather, and failure to obtain sampling permits in all parts of the survey area, among others (Peel et al., 2013; ICES, 2020). An illustrative example is the change in survey effort made by the NOAA Alaska Fisheries Science Center for the bottom-trawl survey that the organization has conducted during summer in the Gulf of Alaska (GOA) since 1984, using a stratified

random survey design to assess the distribution and abundance of groundfish species for fisheries management (von Szalay and Raring, 2018). Traditionally, the survey effort consisted of 3 survey vessels sampling approximately 820 stations from 59 different strata extending from nearshore waters to a depth of 1000 m. However, a variety of factors in recent years, such as funding limitations and difficulties with acquiring 3 suitable charter vessels, have resulted in a reduction of the survey effort to only 2 survey vessels sampling 550 stations from 54 strata extending as deep as only 700 m (von Szalay, 2015). Therefore, the reduction in survey effort also resulted in a reduction in survey area, similar to the consequences of offshore wind farm development and other marine spatial management actions that cause preclusion of sampling (ICES, 2023).

In this study, we assessed the effect of variability in sampling density on estimates of the biomass of species targeted in the GOA bottom-trawl survey. Specifically, we performed a simulation analysis to quantify the effect of changes in sampling density on the accuracy and precision of estimates of biomass, as a measure of abundance, and their associated variances for 4 commercially and ecologically important species that represent diverse geographical distribution patterns: Pacific cod (*Gadus macrocephalus*), Pacific ocean perch (*Sebastes alutus*), arrowtooth flounder (*Atheresthes stomias*), and sablefish (*Anoplopoma fimbria*). The statistical robustness of the biomass estimates was evaluated by using a simulation framework, recently developed by Kotwicki and Ono (2019), in which distributions of fish population density are simulated with a spatiotemporal generalized linear mixed model based on historical catch and environmental survey data. We set up this operating model so that the "true" distribution of abundance and the results of simulated surveys with different sampling densities were represented. Three performance metrics, including coefficient of variance (CV), relative bias, and relative root mean square error (rRMSE), were used to measure the quality of the simulated estimates of biomass and its variance. Using these metrics, we compared estimates from the use of both the traditional design-based biomass estimator (Wakabayashi et al., 1985) and the recently developed estimator based on a vector autoregressive spatiotemporal (VAST) model (Thorson, 2019), across 4 plausible sampling densities, including the 2 levels of sampling effort that have been used in the past and 1 level on each side of the historical range.

Materials and methods

Survey characteristics

The GOA (Fig. 1) forms the northeastern border of the Pacific Ocean and consists of complex bathymetric features ranging from jagged, mountainous pinnacles to flat, muddy areas (Zimmermann et al., 2019). These features provide a variety of habitats in a complex ecosystem. The stratified random sampling design of the standard biennial GOA bottom-trawl survey historically has covered an area of approximately 320,000 km^2 that includes the continental shelf and upper slope from the Islands of Four Mountains east to Dixon Entrance and extends from nearshore waters to a depth of 1000 m (von Szalay and Raring, 2018). In years when survey effort has been unavoidably reduced from the historic 3 charter vessels to 2 vessels, the survey area has been concomitantly reduced to depths shallower than 700 m and to around 30% fewer stations than in those years in which 3 vessels were used. In a bottom-trawl survey with unreduced survey effort, the bulk of survey stations are located on the continental shelf because it accounts for over 80% of the survey area, and the stations on the approximately 20-km-wide continental slope that borders the shelf is sampled only at depths between 200 and 1000 m.

During the bottom-trawl surveys conducted in the GOA by the Resource Assessment and Conservation Engineering Division of the Alaska Fisheries Science Center, approximately 820 locations across 59 strata traditionally have been sampled in years with standard effort (i.e., when 3 vessels were used) and around 550 stations across 54 strata have been sampled in years with reduced effort (when 2 vessels were used). Survey effort in 2001, 2013, and 2017–2023 was reduced because of unavoidable funding limitations as well as challenges in acquisition of 3 qualified charter vessels. Abundance estimates typically have been generated by using the design-based estimator developed by Wakabayashi et al. (1985). The same standard trawl gear has been used for this survey since 1990: a Poly Nor'Eastern 4-seam bottom trawl with 24.2-m roller gear constructed with 36-cm rubber bobbins separated by 10-cm rubber disks (Stauffer, 2004). Surveys begin in the western GOA and proceed east into southeast Alaska. The targeted duration for tows of the trawl net is 15 min at a speed of 1.54 m/s (3 kt). The catch per unit of effort (CPUE), in terms of weight per swept area, typically is estimated by using the area-swept method (e.g., Alverson and Pereyra, 1969), in which the effort is defined as the product of the distance fished and the average distance between wing tips of the trawl gear (von Szalay and Raring, 2018).

A 5-by-5-km grid of sampling units (stations) superimposed on the survey area is used to delineate stations in combination with predetermined stratum designations. Each unique grid cell within a stratum represents a potential survey station. Some stations have been excluded from the pool of stations eligible for survey selection because they are known to be untrawlable with our standard survey trawl gear. Grid cells along the boundaries of the survey area are truncated by the coastline and the deepest edge of the sampling domain and, therefore, have an area smaller than a standard 25-km^2 grid cell.

Following the stratified random sampling design used since the inception of the GOA bottom-trawl survey in 1984, with the survey area divided into 59 strata defined by water depth, bottom terrain (e.g., shelf, gully, and slope),

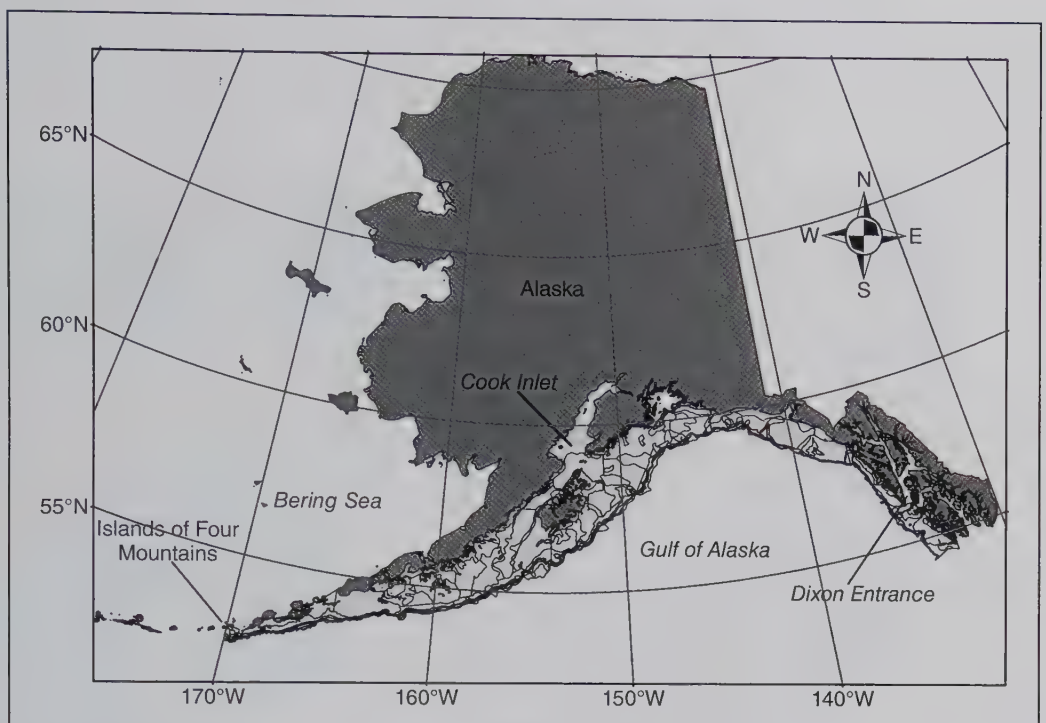

Figure 1

Map showing the 59 strata of the bottom-trawl survey conducted biennially in the Gulf of Alaska by the NOAA Alaska Fisheries Science Center. The survey area includes the portion of the continental shelf from the Islands of Four Mountains eastward approximately 2800 km to Dixon Entrance and from nearshore waters to a depth of 1000 m. The total survey area encompasses approximately 320,000 km^2. The stratum boundaries have been fixed since the inception of the survey in 1984.

and statistical management areas (von Szalay and Raring, 2018), we determined the allocation of stations among the strata for species k using a modified Neyman optimal allocation strategy (Cochran, 1977):

$$n_{hk} = \frac{\frac{nN_h s_{hk} a_h}{\sqrt{c_h}}}{\sum_h \frac{N_h s_{hk} a_h}{\sqrt{c_h}}}, \quad (1)$$

where n_{hk} = the sample size for species k in stratum h;
n = the total sample size;
N_h = the population size for stratum h;
s_{hk} = the standard deviation of species k in stratum h;
a_h = the area of stratum h; and
c_h = the cost to tow a trawl in stratum h.

Sampling effort among strata for each of the 10 survey years between 1996 and 2015 and each of 50 principal groundfish species in the GOA was based on stratum variances and their respective areas from the 12 consecutive surveys conducted between 1990 and 2015. A cost variable in terms of the time required to complete a trawl tow in a given stratum was also used to penalize strata that are deeper and for which there is a higher probability of unacceptable gear performance. The mean sample size over the 10 survey years between 1996 and 2015 for each stratum and species was calculated and subsequently weighted by the commercial value of each species to obtain the final allocation assignments. The sample sizes were rounded to whole numbers representing the number of stations allocated to each stratum, with an additional constraint that 2 samples were required for each stratum.

Simulated distributions of catch per unit of effort

Simulated CPUE distributions of Pacific cod, Pacific ocean perch, arrowtooth flounder, and sablefish were created by fitting a spatiotemporal delta model to historical GOA survey data from 1996 to 2015, through the use of the package R-INLA (vers. 18.07.12; available from website, accessed October 2018; Rue et al., 2009) in the statistical computing environment R (vers. 3.6.1; R Core Team, 2019); this package accounts for both environmental covariates and spatiotemporal dependency in catches (Kotwicki and Ono, 2019) (Fig. 2). The delta model has 2 components: one that models the species occurrence and another that models positive CPUE.

Species occurrence at locations s and year t, $\pi_t(s)$, was modeled by using a binomial generalized linear mixed

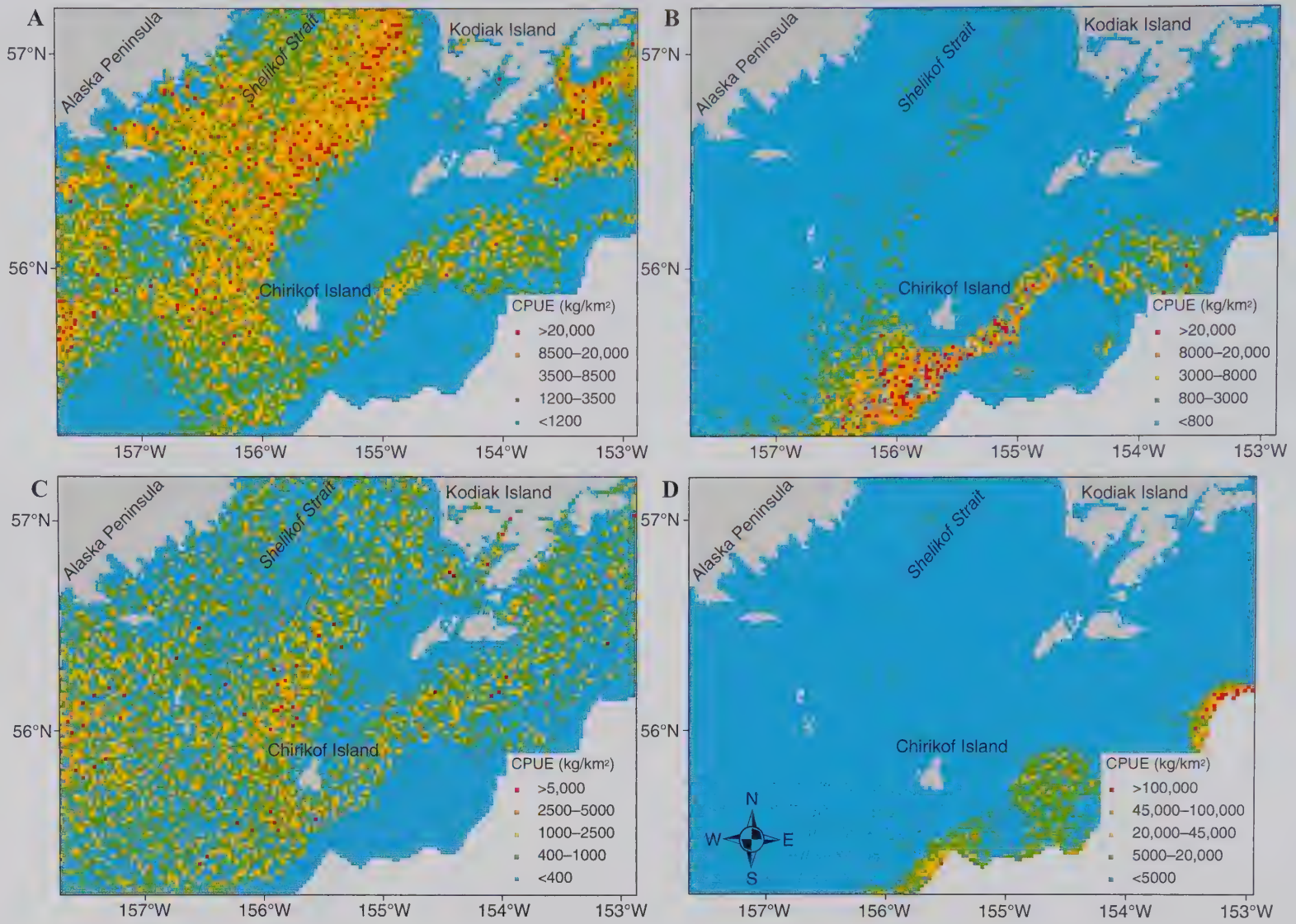

Figure 2

Simulated distributions of catch per unit of effort (CPUE) for (**A**) arrowtooth flounder (*Atheresthes stomias*), (**B**) Pacific ocean perch (*Sebastes alutus*), (**C**) Pacific cod (*Gadus macrocephalus*), and (**D**) sablefish (*Anoplopoma fimbria*) in 2015 at the entrance to Cook Inlet in southcentral Alaska. The simulations were created by fitting a spatiotemporal delta model that accounts for both environmental covariates and spatiotemporal dependency in catches to historical data from a bottom-trawl survey conducted in the Gulf of Alaska. Each pixel on the map is 2 km^2 and represents the CPUE realized when a station is sampled at that location in the simulated surveys conducted in this study.

model with the logit link function (see Lindgren et al., 2011):

$$\text{logit}\left(\pi_t(s)\right) = X_t(s)b + \omega_t(s), \text{ where} \quad (2)$$

$$\omega_t(s) \sim Normal\left(\rho_1\omega_{t-1}(s), \Sigma_1\right),$$

and $X_t(s)$ = the matrix of covariates at locations s and year t;
b = the vector of regression coefficients;
ω = the spatiotemporal variation that follows a first-order autoregressive process;
ρ_1 = the degree of autocorrelation in encounter probability between successive years; and
Σ_1 = the spatial covariance modeled as a Mátern function with smoothness of 1.

The covariates used in this study were log(*depth*), (log(*depth*))^2, *bottom temperature*, *bottom temperature* squared, *surface temperature*, *surface temperature* squared, and a fixed year effect (Kotwicki et al., 2005, 2015).

The non-zero species density at a set of locations s during year t, $\mu_t(s)$, was modeled by using a lognormal distribution:

$$\log\left(\mu_t(s)\right) = Z_t(s)a + \delta_t(s), \text{ where} \quad (3)$$

$$\delta_t(s) \sim Normal\left(\rho_2\delta_{t-1}(s), \Sigma_2\right),$$

and $Z_t(s)$ = a matrix of covariates at locations s during year t;
a = the vector of regression coefficients;
δ_t = the spatial field for year t assumed to follow a first-order autoregressive process;
ρ_2 = autocorrelation of the first-order autoregressive process in which the current value is based on the immediately preceding value; and
Σ_2 = the spatial covariance modeled as a Mátern function with smoothness of 2.

Annual distributions of simulated CPUE within the survey area were predicted over a nominal grid with a 2-km resolution on the basis of a single random sample from the posterior predictive distribution of the models while accounting for the sampling process. Simulated CPUE was calculated as the product of sampled fish occurrence and sampled density. Sampled fish occurrence was estimated by using a Bernoulli trial with the probability determined by the parameter samples taken from the posterior predictive distribution (in practice, a random Markov chain Monte Carlo run was chosen, and parameter values were taken from it). Sampled density was estimated by using a sample from a Gaussian distribution on the link scale with the mean and variance derived from parameter values taken from a randomly chosen Markov chain Monte Carlo run (the sample value was exponentiated by using the natural exponential function to convert it to real space).

With this approach, predictions accounted for all sources of uncertainty included in the model and created a noisier CPUE distribution that was more reflective of "true" patterns than the mean Markov chain Monte Carlo prediction. Environmental covariate values were determined by kriging with the semivariogram model that best fit the historical survey data (Kotwicki and Ono, 2019), as implemented by the function autofitVariogram in the R package automap (vers. 1.0-16; Hiemstra et al., 2009). All geographic coordinates were converted into an Albers projection in order to preserve distances prior to analysis.

Simulation of surveys

The grid with the finer resolution of 2 km for CPUE distribution was superimposed on the grid with a resolution of 5 km for GOA surveys prior to generation of the simulated surveys. Accordingly, each GOA survey station (i.e., 25-km^2 grid cell) contained between 4 and 7 of the 2-km^2 grid cells with density data. The allocated stations within each stratum were randomly selected without replacement from the 2-km-resolution grid described previously in the "Simulated distributions of catch per unit of effort" section. A total of 100 replicate surveys with the traditional stratified random sampling design were simulated by using the modeled CPUE distributions for each of the 10 survey years between 1996 and 2015. Simulations at 4 different levels of survey effort representing 1, 2, 3, and 4 survey vessels sampling 280, 550, 820, and 1094 stations, respectively, were used as input for 2 different estimators: Wakabayashi's design-based estimator (Wakabayashi et al., 1985) and Thorson's (2019) model-based VAST estimator. All analyses were conducted in R, vers. 3.6.1 (R Core Team, 2019).

The station allocations among strata for the 2-vessel and 3-vessel simulation scenarios were based on the sampling allocation realized during the GOA surveys conducted in 2013 and 2007, respectively. Consequently, the 5 deepest strata (those at depths between 700 and 1000 m) were not sampled in the 1-vessel and 2-vessel simulation scenarios. In contrast, all 59 strata were sampled under the 3-vessel and 4-vessel scenarios. The number of stations allocated by stratum in the 1-vessel scenario was half that in the 2-vessel scenario, subject to rounding and ensuring a minimum of 2 stations per stratum. The station allocation for the 4-vessel scenario was generated by using the Alaska Fisheries Science Center's traditional station allocation program for the GOA survey with an effort level of 1094 stations.

Design-based estimator

The mean CPUE $\left(\bar{x}_{hk}\right)$ and its standard deviation (s_{hk}) of stratum h for species k was calculated and used to generate the survey mean CPUE $\left(\overline{X}_k\right)$ and its variance $\left(S^2_{\bar{x}k}\right)$ for a stratified random sampling design according to Wakabayashi et al. (1985):

$$\overline{X_k} = \frac{1}{N}\sum_{h=1}^{H_r} N_h \bar{x}_{hk}, \text{ and} \quad (4)$$

$$S^2_{\bar{x}_k} = \sum_{h=1}^{H_t} \left(\frac{N_h}{N}\right)^2 \left(\frac{N_h - n_h}{N_h}\right) \left(\frac{s^2_{hk}}{n_h}\right), \quad (5)$$

where N = the total number of 5-by-5-km grid cells in the survey area;
N_h = the number of 5-by-5-km grid cells in stratum h;
H_r = the 55 strata for the surveys with reduced survey effort and 1 or 2 vessels; and
H_t = the 59 strata for the traditional surveys with full survey effort and 3 or 4 vessels.

The true biomass was calculated as the product of the trawlable area of the survey area in the GOA and the arithmetic mean of simulated CPUE (with observation error) from all 65,863 trawlable grid cells. The true variance was calculated for each year as the variance of the replicate simulated biomass estimates:

$$\sigma^2_T = \frac{\Sigma_S (B_S - B_T)^2}{N}, \quad (6)$$

where σ^2_T = the "true" variance of the abundance index based on 100 simulated surveys;
N = the total number of simulated surveys (100);
Σ_S = the sum over the 100 simulated surveys;
B_S = the estimated biomass realized in simulation survey s; and
B_T = the "true" biomass estimated from simulated density maps.

Model-based estimator

The model-based estimator was a spatiotemporal delta model consisting of a binomial model for the probability of encounter and a user-selected model for positive catch rates, as implemented in the R package VAST, vers. 3.3.0 (Thorson, 2019). In a report on their recent work, Thorson et al. (2021) noted that the choice of distributional assumptions can have a substantial effect on the scale of the biomass index estimated from such spatiotemporal models. A range of assumptions to determine which provided the best fit and accuracy were tested in a previous study (von Szalay et al., 2023), in which alternate observation error distributions for positive catch rates were compared. On the basis of the results of that study (Suppl. Table) (online only), we used a delta-gamma distribution for the observation error for positive catch rates and applied the epsilon correction for retransformation bias in the VAST package (Thorson and Kristensen, 2016).

The delta models included *year* as a fixed effect, a spatial random field for each model component (encounter probability and positive catch rate), and independent spatiotemporal random fields for the positive catch rate component. The spatiotemporal term for encounter probability was not estimated because of a lack of consistent convergence among replicate simulated surveys. A model resolution of 500 knots was used, and bilinear interpolation was implemented to extrapolate from knot locations in order to generate predictions at each location in the same 2-km-resolution grid used by the operating model. Anisotropy was estimated.

All models were run with the VAST package (Thorson et al., 2015) and the tools available in FishStatsUtils (vers. 2.6.0; available from website, accessed August 2022).

Performance metrics

Three metrics were used to evaluate the relative performance of the design-based and model-based abundance estimators at the 4 survey effort levels: CV, relative bias, and rRMSE. Each metric was applied to estimates of biomass and its associated variance and was calculated separately for each year and species. Bias of biomass and its variance was defined as the mean of the deviations between the respective value of each simulation and the true value. The relative bias (RB) of these estimates was calculated within each year and species as follows:

$$RB = \frac{\frac{1}{n}\sum_{i=1}^{n}(\theta_i - \theta_{True})}{\theta_{True}}, \quad (7)$$

where θ_i = the value (biomass or variance) of the ith simulation replicate; and
θ_{True} = the true value (biomass or variance), over 100 simulation replicates.

The CV was defined as follows:

$$CV = \frac{\sqrt{Var(\theta)}}{\theta_{True}}, \text{ where} \quad (8)$$

$$Var(\theta) = \frac{1}{n}\sum_{i=1}^{n}(\theta_i - \theta_{mean})^2,$$

and $Var(\theta)$ = the mean of the square deviations between the value (biomass or variance) of each simulation and the mean biomass or variance.

The mean square error was defined as the sum of the bias squared and variance, and the rRMSE was calculated as follows:

$$rRMSE = \frac{\sqrt{Bias^2 + Var}}{\theta_{True}}, \quad (9)$$

where $Bias$ = the absolute bias as defined by the numerator of Equation 7.

These performance metrics were used as measures of quality of the estimates of biomass and associated variance derived from the simulations. Thresholds were established according to the recommendations by the second Workshop on Unavoidable Survey Effort Reduction (ICES, 2023) to place the values of the performance metrics into 1 of 3 categories:

- desirable and reliable estimate of biomass and variance (metric value <0.20);
- acceptable estimate of biomass and variance (metric value of 0.20–0.40); and
- poor and unreliable estimate of biomass and variance (metric value >0.40).

These 3 categories were, in turn, used to evaluate how estimates of biomass or variance changed with sample size (e.g., from acceptable to desirable or from poor to desirable). For reference, a CV of 0.50 indicates that the bounds of the 95% confidence interval for an estimate of either biomass or variance are ±100%, clearly indicating an unacceptable level of uncertainty.

Results

Realized survey effort reduction from 3 vessels to 2 vessels

Results differed qualitatively between the deep-dwelling sablefish and the other 3 species analyzed, as estimates of the abundance of sablefish were more sensitive to changes in sampling effort as well as to concomitant changes in sampling area. The effect of the reduction in survey effort from 3 vessels (820 stations) to 2 vessels (550 stations) on all 3 performance metrics for biomass estimates was small for both the design-based and model-based estimators for arrowtooth flounder, Pacific cod, and Pacific ocean perch (Figs. 3–5). For these 3 species, all 3 performance metrics remained well within the desirable range for both estimators (<0.20), given that the CV increased only modestly from already low levels (0.060–0.150) to slightly higher levels (0.070–0.160) for the design-based estimator and that the CV was essentially unchanged (change of <0.002) for the model-based estimator. Similarly, the increase in relative bias was modest, as it rose from already low levels (0.000–0.050) to only slightly higher levels (0.003–0.040) for both estimators and all 3 species (Table 1).

For the design-based estimator, the effect of the change in survey effort on the CV and relative bias of the estimates of variance for arrowtooth flounder, Pacific cod, and Pacific ocean perch was generally similar to the effect on those same metrics of the biomass estimates, with only modest increases in both metrics when the survey effort was reduced (Figs. 6–8). The median CVs of the variance estimates from the design-based estimator increased modestly

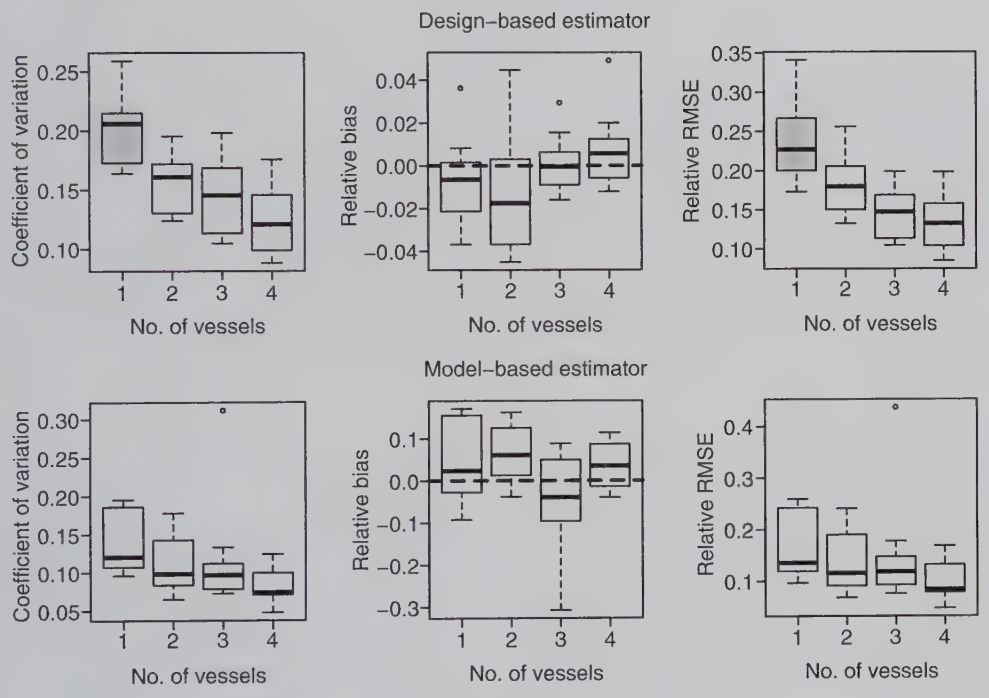

Figure 3

Relative performance of the design-based estimator and the estimator based on a vector autoregressive spatiotemporal model in estimation of biomass of Pacific ocean perch (*Sebastes alutus*) in simulated bottom-trawl surveys of the Gulf of Alaska at 4 survey effort levels. Each box plot represents the distribution of a performance metric, coefficient of variation, relative bias, or relative root mean square error (RMSE), for a survey effort level (number of vessels) over the 10 survey years between 1996 and 2015. In each box plot, the thick black line is the median. The upper and lower parts of each box represent the first and third quartiles (the 25th and 75th percentiles). The whiskers extend above and below the box no more than 1.5 times the interquartile range. Data points that appear beyond the end of the whiskers are outliers. The white and light gray colors of individual boxes indicate that performance metric values are within the ranges at which estimates are classified as desirable (<0.20) and acceptable (0.20–0.40), respectively.

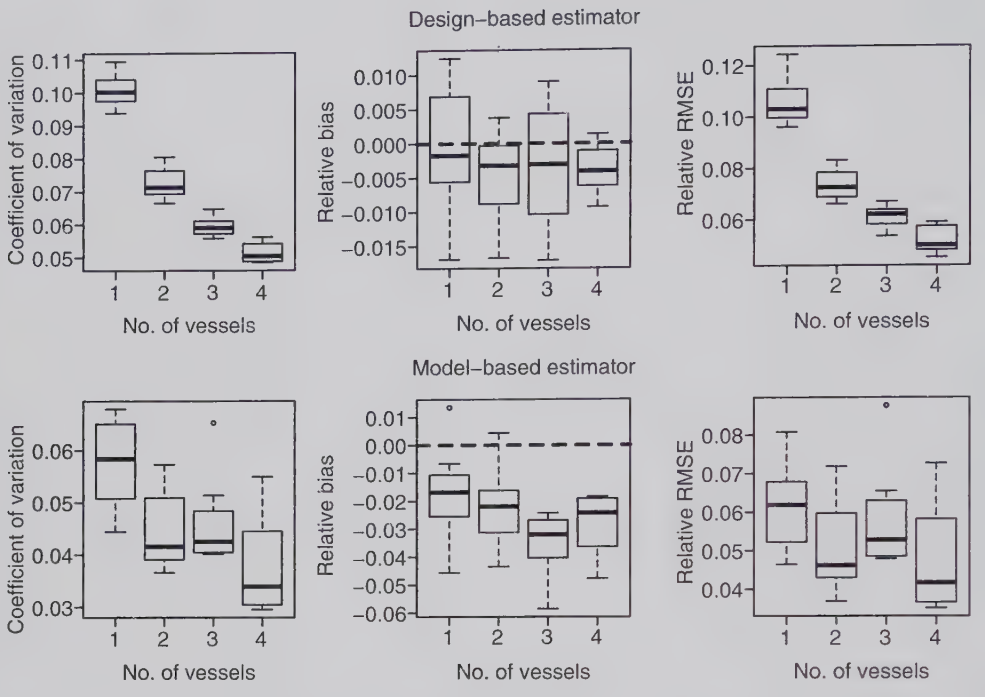

Figure 4

Relative performance of the design-based estimator and the estimator based on a vector autoregressive spatiotemporal model in estimation of biomass of Pacific cod (*Gadus macrocephalus*) in simulated bottom-trawl surveys of the Gulf of Alaska at 4 survey effort levels. Each box plot represents the distribution of a performance metric, coefficient of variation, relative bias, or relative root mean square error (RMSE), for a survey effort level (number of vessels) over the 10 survey years between 1996 and 2015. In each box plot, the thick black line is the median. The upper and lower parts of each box represent the first and third quartiles (the 25th and 75th percentiles). The whiskers extend above and below the box no more than 1.5 times the interquartile range. Data points that appear beyond the end of the whiskers are outliers. All metric values in this figure are below the threshold at which estimates are classified as desirable (<0.20).

from 0.15 to 0.17 for Pacific cod and from 0.23 to 0.25 for arrowtooth flounder but decreased from 0.45 to 0.39 for Pacific ocean perch, resulting in estimates of variance categorized as either desirable (Pacific cod) or acceptable for all of these species. The relative bias, which was comparatively low (<0.02) for variance estimates for arrowtooth flounder and Pacific cod and was –0.10 for Pacific ocean perch, was unchanged for estimates for Pacific cod and Pacific ocean perch but increased slightly (0.00 to –0.01) for estimates for arrowtooth flounder.

The CVs for variance estimates from the model-based estimator at the 3-vessel effort level were considerably higher for arrowtooth flounder (0.10) and Pacific cod (0.11) than the corresponding CVs of the biomass estimates for these species (0.044 and 0.043, respectively). Only for Pacific ocean perch was the CV of the variance estimate in a lower quality category than that for the biomass estimate with this estimator: the variance estimate was deemed acceptable with a CV of 0.28, and the biomass estimate was categorized as desirable with a CV of 0.100. The CV of variance estimates increased modestly (from 0.28 to 0.32) for Pacific ocean perch, decreased modestly (from 0.11 to 0.09) for Pacific cod, and was unchanged for arrowtooth flounder, but the quality category did not change for any of the species. The relative bias for variance estimates from the model-based estimator was relatively low (0.00–0.12) and generally comparable to the corresponding values for the biomass estimates from this estimator. It decreased to 0.00 from the already low level of 0.03 for Pacific cod, increased from 0.00 to 0.12 for Pacific ocean perch, and was unchanged at 0.09 for arrowtooth flounder (Table 1).

Unlike the comparatively modest effects observed for arrowtooth flounder, Pacific cod, and Pacific ocean perch, the effect on the CV and relative bias of biomass estimates observed for sablefish was unexpectedly high under this survey effort reduction scenario (Fig. 9). Although the CV of the biomass estimate for sablefish was relatively constant between the 2 effort levels for the design-based estimator (0.200 versus 0.210), the relative bias of the biomass estimate changed from a negligible value at the 3-vessel effort level to a large and negative value (–0.550, low enough to categorize the biomass estimate as poor) at the

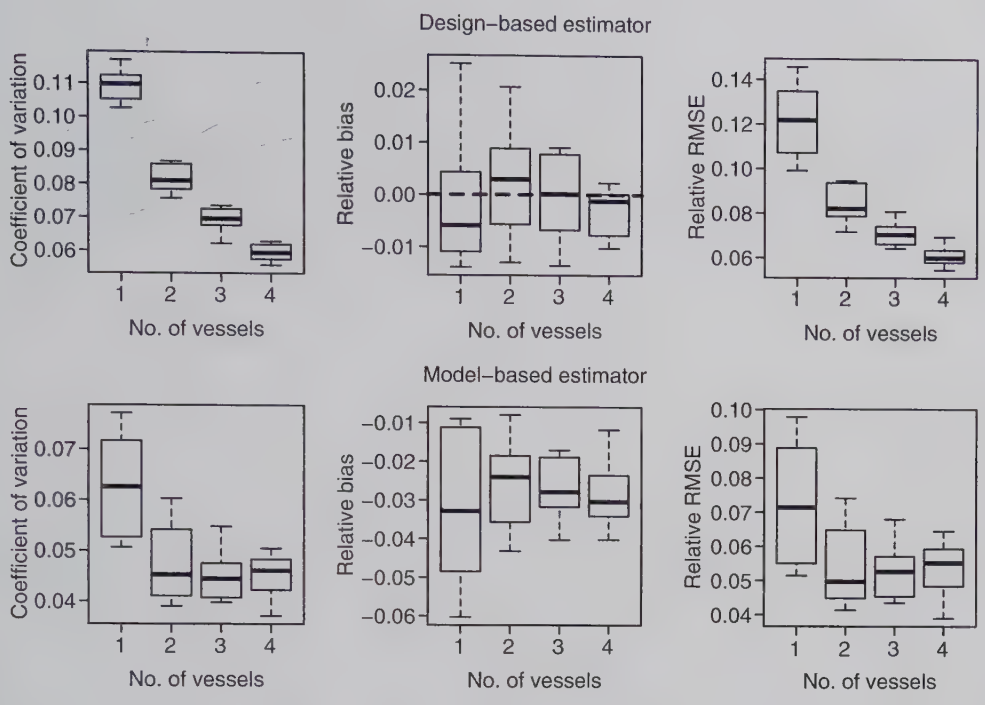

Figure 5

Relative performance of the design-based estimator and the estimator based on a vector autoregressive spatiotemporal model in estimation of biomass of arrowtooth flounder (*Atheresthes stomias*) in simulated bottom-trawl surveys of the Gulf of Alaska at 4 survey effort levels. Each box plot represents the distribution of a performance metric, coefficient of variation, relative bias, or relative root mean square error (RMSE), for a survey effort level (number of vessels) over the 10 survey years between 1996 and 2015. In each box plot, the thick black line is the median. The upper and lower parts of each box represent the first and third quartiles (the 25th and 75th percentiles). The whiskers extend above and below the box no more than 1.5 times the interquartile range. Data points that appear beyond the end of the whiskers are outliers. All metric values in this figure are below the threshold at which estimates are classified as desirable (<0.20).

2-vessel effort level. For the model-based estimator, the CV (0.600–1.300) and relative bias (0.450–0.750) were high, and meant the estimates were in the poor category, at both survey effort levels (Table 1). Although the effect of the effort reduction on the CV and relative bias of variance estimates was also relatively high for sablefish, the values for these performance metrics already put the variance estimates in the poor category at the 3-vessel effort level and the classification remained there at the 2-vessel effort level for both estimators (Fig. 10, Table 1).

Hypothetical survey effort reduction from 4 vessels to 1 vessel

As expected, the effect on the CV was more pronounced between the 2 hypothetical survey effort levels—1 vessel (280 stations) and 4 vessels (1094 stations)—than it was for the realized survey reduction from 3 vessels to 2 vessels, especially for estimates from the design-based estimator. The median CV of the biomass estimates for arrowtooth flounder, Pacific cod, and Pacific ocean perch from this estimator increased from a range of 0.050–0.120 to a higher and slightly wider range of 0.100–0.210 when the survey effort was reduced from 4 vessels to 1 vessel. However, even in this most extreme scenario for reduction in survey effort, the CV remained in the range that indicates desirable estimates for 2 of the 3 species (arrowtooth flounder and Pacific cod) and only slightly exceeded the range for desirable estimates for 1 species (Pacific ocean perch). The increase in the median CV of biomass estimates from the model-based estimator was even more modest, going from already low values and a relatively narrow range (0.030–0.090) to only slightly higher values and a wider range (0.058–0.120), with all values within the range that indicates desirable estimates at both effort levels. Similar to the values for the 2-vessel and 3-vessel effort levels, the relative bias was small and well within the range for desirable estimates (<0.03) for both estimators and all 3 species at both the 1-vessel and 4-vessel effort levels (Table 1).

The effect on the median CV and relative bias of the variance estimates from the design-based estimator for arrowtooth flounder, Pacific cod, and Pacific ocean perch

Table 1

Comparison of mean values of 3 performance metrics for the traditional design-based estimator and the alternative estimator, based on a vector autoregressive spatiotemporal model, used to estimate biomass and its variance for arrowtooth flounder (*Atheresthes stomias*) (ATF), Pacific cod (*Gadus macrocephalus*) (COD), Pacific ocean perch (*Sebastes alutus*) (POP), and sablefish (*Anoplopoma fimbria*). The values of metrics, coefficient of variation (CV), relative bias, and relative root mean square error (rRMSE), are compared across 4 levels of survey effort. Data used in analysis are from the bottom-trawl surveys conducted in the Gulf of Alaska during 1996–2015 by the NOAA Alaska Fisheries Science Center. The lowest rRMSE value for each species is indicated with an asterisk (*).

		Survey effort: no. of stations (no. of vessels)							
		Design-based estimator				Model-based estimator			
Species	Performance metric	280 (1)	550 (2)	820 (3)	1094 (4)	280 (1)	550 (2)	820 (3)	1094 (4)
Estimates of biomass									
ATF	CV	0.110	0.080	0.070	0.060	0.063	0.044	0.044	0.045
	Rel. bias	−0.007	0.003	0.000	−0.001	−0.032	−0.025	−0.030	−0.031
	rRMSE	0.120	0.080	0.070	0.060	0.070	0.049*	0.052	0.054
COD	CV	0.100	0.072	0.059	0.050	0.058	0.042	0.043	0.033
	Rel. bias	−0.002	−0.003	−0.003	−0.004	−0.016	−0.021	−0.032	−0.025
	rRMSE	0.100	0.072	0.060	0.050	0.062	0.046	0.052	0.041*
POP	CV	0.210	0.160	0.150	0.120	0.120	0.100	0.100	0.090
	Rel. bias	−0.005	−0.020	0.000	0.005	0.010	0.040	−0.050	0.030
	rRMSE	0.220	0.170	0.150	0.120	0.130	0.100	0.100	0.090*
Sablefish	CV	0.230	0.210	0.200	0.230	0.550	1.300	0.600	1.900
	Rel. bias	−0.500	−0.550	0.000	0.030	0.100	0.750	0.450	1.400
	rRMSE	0.600	0.580	0.200*	0.240	0.570	1.550	0.750	2.400
Estimates of variance in biomass									
ATF	CV	0.33	0.25	0.23	0.21	0.30	0.10	0.10	0.75
	Rel. bias	−0.07	−0.01	0.00	0.00	0.24	0.09	0.09	−0.18
	rRMSE	0.35	0.26	0.23	0.22	0.39	0.19*	0.19*	0.79
COD	CV	0.22	0.17	0.15	0.13	0.18	0.09	0.11	0.13
	Rel. bias	−0.03	−0.02	−0.02	0.00	−0.02	0.00	0.03	0.10
	rRMSE	0.23	0.18	0.15	0.13	0.21	0.09*	0.13	0.18
POP	CV	0.51	0.39	0.45	0.35	0.34	0.32	0.28	0.30
	Rel. bias	−0.12	−0.10	−0.10	−0.04	0.00	0.12	0.00	0.20
	rRMSE	0.52	0.39	0.45	0.35	0.34	0.36	0.28*	0.35
Sablefish	CV	0.89	0.89	0.71	0.81	1.50	1.52	1.15	1.80
	Rel. bias	−0.50	−0.48	−0.30	−0.42	−0.55	−0.56	−0.47	−0.57
	rRMSE	1.02	0.96	0.75*	0.88	1.60	1.65	1.25	1.85

was also considerably greater between the 2 hypothetical survey effort levels than between the 2 realized survey effort levels (Figs. 6–8). As expected, the increases in both the CV and the relative bias of variance estimates from the design-based estimator were consistent and substantially greater for all of these species under the hypothetical reduction scenario than under the reduction in survey effort from 3 vessels to 2 vessels. The CV of variance estimates increased from a value indicating desirable estimates (0.13) to a value indicating acceptable estimates (0.22) for Pacific cod, remained at levels indicating acceptable estimates (0.21 and 0.33) for arrowtooth flounder, and increased from a value indicating acceptable estimates (0.35) to a value indicating poor estimates (0.51) for Pacific ocean perch. The relative bias in variance estimates from the design-based estimator increased from levels that indicate that estimates were well within the desirable category (0.00–0.04) to considerably higher levels (0.03–0.12) (Table 1).

The effect of this effort reduction scenario on the CV and relative bias of variance estimates, however, was inconsistent and not always intuitive for the model-based estimator. The CV of variance estimates increased modestly for Pacific ocean perch (from 0.30 to 0.34) and Pacific cod (from 0.13 to 0.18); therefore, the category for the quality of estimates did not change for either of these species. In contrast, the CV unexpectedly decreased from 0.75 to 0.30 for arrowtooth flounder because of an outlier value at the 4-vessel effort level (with the outlier excluded, the CV is 0.10 at this effort level), resulting in an

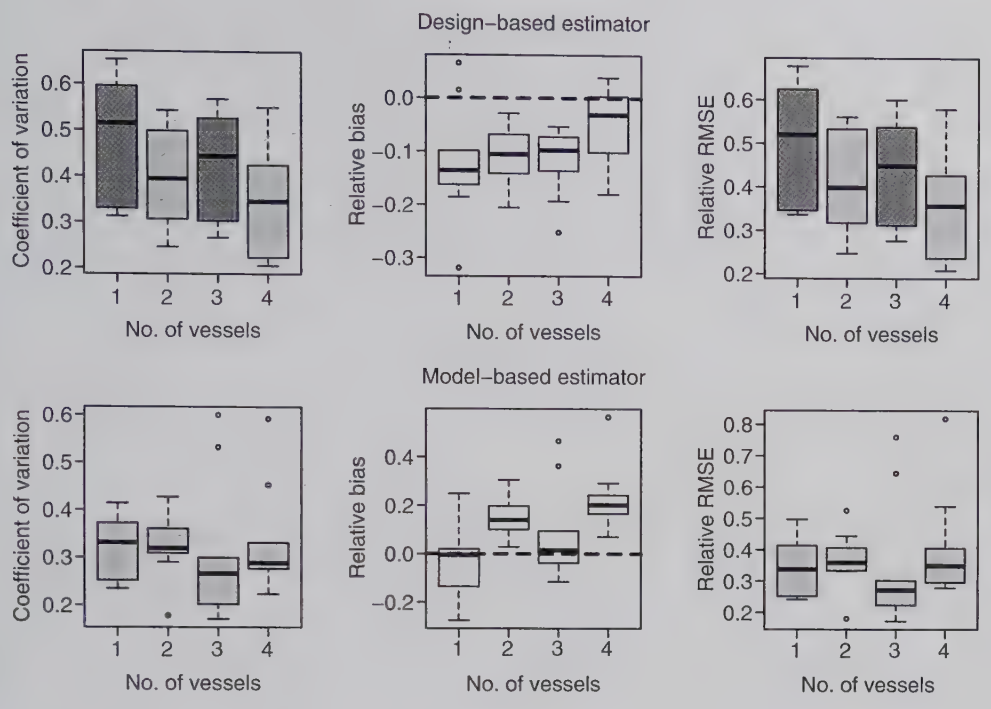

Figure 6

Relative performance of the design-based estimator and the estimator based on a vector autoregressive spatiotemporal model in estimation of variance in biomass of Pacific ocean perch (*Sebastes alutus*) in simulated bottom-trawl surveys of the Gulf of Alaska at 4 survey effort levels. Each box plot represents the distribution of a performance metric, coefficient of variation, relative bias, or relative root mean square error (RMSE), for a survey effort level (number of vessels) over the 10 survey years between 1996 and 2015. In each box plot, the thick black line is the median. The upper and lower parts of each box represent the first and third quartiles (the 25th and 75th percentiles). The whiskers extend above and below the box no more than 1.5 times the interquartile range. Data points that appear beyond the end of the whiskers are outliers. The white, light gray, and dark gray colors of individual boxes indicate that metric values are within the ranges at which estimates are classified as desirable (<0.20), acceptable (0.20–0.40), and unreliable (>0.40), respectively.

improvement in the quality of variance estimates from the poor to the acceptable category (Table 1). Furthermore, relative bias increased for arrowtooth flounder (from 0.18 to 0.24), resulting in a change in the categorization of estimates from desirable to acceptable, but relative bias decreased for both Pacific cod (from 0.10 to 0.02) and Pacific ocean perch (from 0.20 to 0.00), with estimates for both species at both effort levels considered desirable.

For sablefish, no effect on the CV of biomass estimates from the design-based estimator is discernable under this effort reduction scenario, with the same value (0.230), which indicates acceptable estimates, found for both effort levels. However, as with the scenario in which survey effort was reduced from 3 vessels to 2 vessels, relative bias was very low and indicates that the quality of biomass estimates is desirable at the high (4-vessel) effort level (0.030) but large and negative (–0.500, low enough to categorize the estimates as poor) at the low (1-vessel) level. For estimates of both biomass and variance from the model-based estimator, CV (0.55–1.90) and relative bias (0.10–1.40) were both generally high and put estimates in the poor category at both survey effort levels except for one outlier value for relative bias of biomass estimates (0.100) at the 1-vessel level (Table 1).

Trends in total error across all survey effort levels

As expected, the total error of the biomass estimates for the design-based estimator, as measured by using the rRMSE, consistently decreased with increasing sampling density for arrowtooth flounder, Pacific cod, and Pacific ocean perch, although the quality of estimates remained in the desirable category for all species and at all effort levels, except for Pacific ocean perch at the 1-vessel effort level (0.220). Because the CVs responded more to differences in effort level than the relative bias values, the CV was the primary source of variation in the rRMSE with effort level. The magnitude of the decline in the rRMSE

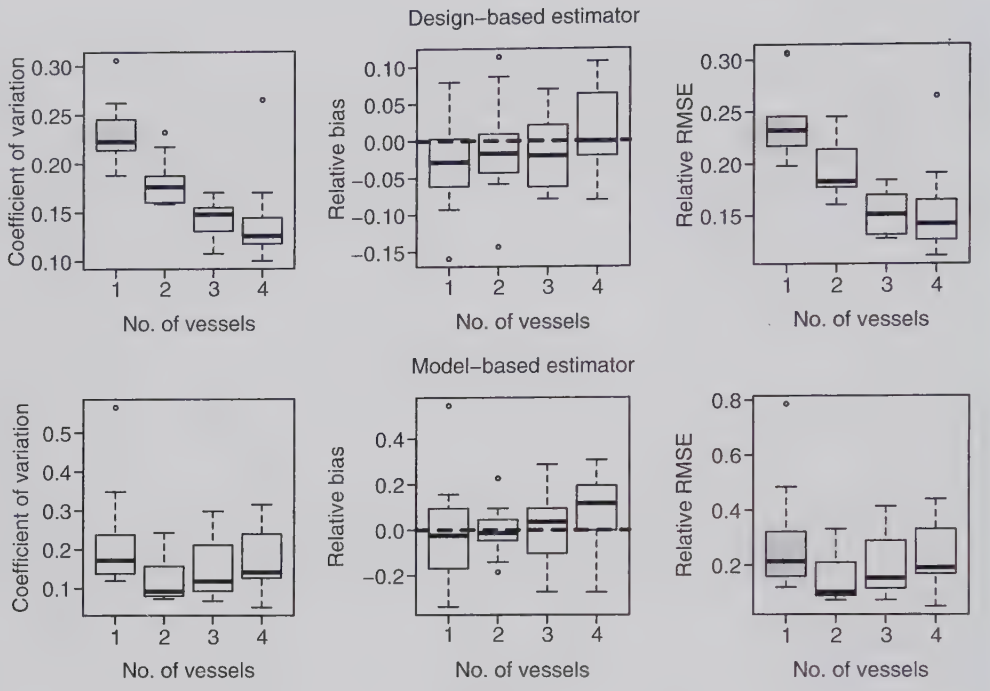

Figure 7

Relative performance of the design-based estimator and the estimator based on a vector autoregressive spatiotemporal model in estimation of variance in biomass of Pacific cod (*Gadus macrocephalus*) in simulated bottom-trawl surveys of the Gulf of Alaska at 4 survey effort levels. Each box plot represents the distribution of a performance metric, coefficient of variation, relative bias, or relative root mean square error (RMSE), for a survey effort level (number of vessels) over the 10 survey years between 1996 and 2015. In each box plot, the thick black line is the median. The upper and lower parts of each box represent the first and third quartiles (the 25th and 75th percentiles). The whiskers extend above and below the box no more than 1.5 times the interquartile range. Data points that appear beyond the end of the whiskers are outliers. The white and light gray colors of individual boxes indicate that metric values are within the ranges at which estimates are classified as desirable (<0.20) and acceptable (0.20–0.40), respectively.

between the 1-vessel and 4-vessel effort levels was relatively similar for all 3 species, ranging from 45% (from 0.220 to 0.120) for Pacific ocean perch to 50% (from 0.100 to 0.050) for Pacific cod (Figs. 3–5). For sablefish, the rRMSE was similar and indicates poor estimates for the 1-vessel and 2-vessel effort levels (0.580–0.600). It reached a minimum at the borderline of the desirable and acceptable categories for estimate quality (0.200) for the 3-vessel effort level and was at an intermediate value (0.240) that indicates acceptable estimates for the 4-vessel level (Table 1). The lack of a decreasing trend in the rRMSE with increasing sampling density for sablefish was due to a large and abrupt increase in relative bias for effort levels with fewer than 3 vessels and to the nonintuitive increase in CV at the 4-vessel effort level (Fig. 9).

The rRMSE of the variance estimates from the design-based estimator consistently decreased with increasing sampling density for arrowtooth flounder and Pacific cod but not for Pacific ocean perch and sablefish (Figs. 6–8 and 10). For Pacific ocean perch, the decreasing trend was interrupted slightly between the 2-vessel and 3-vessel levels but resumed between the effort levels with 3 vessels and 4 vessels, reaching a minimum at the 4-vessel level. For sablefish, the pattern of the rRMSE of the variance estimates from the design-based estimator was similar to that for the corresponding biomass estimates but indicates that variance estimates are firmly in the poor category at all effort levels (0.75–1.02).

Although the rRMSE of biomass estimates from the model-based estimator did not decline as consistently with increasing sampling density for arrowtooth flounder, Pacific cod, and Pacific ocean perch as the rRMSE of estimates from the design-based estimator, the magnitudes of the rRMSE were consistently lower for the model-based estimator than for the design-based estimator at all effort levels, indicating that the model-based estimator was generally the better performing estimator (Table 1, Figs. 3–5). However, this trend was not found for sablefish, for which the magnitudes of the rRMSE of biomass estimates were substantially higher

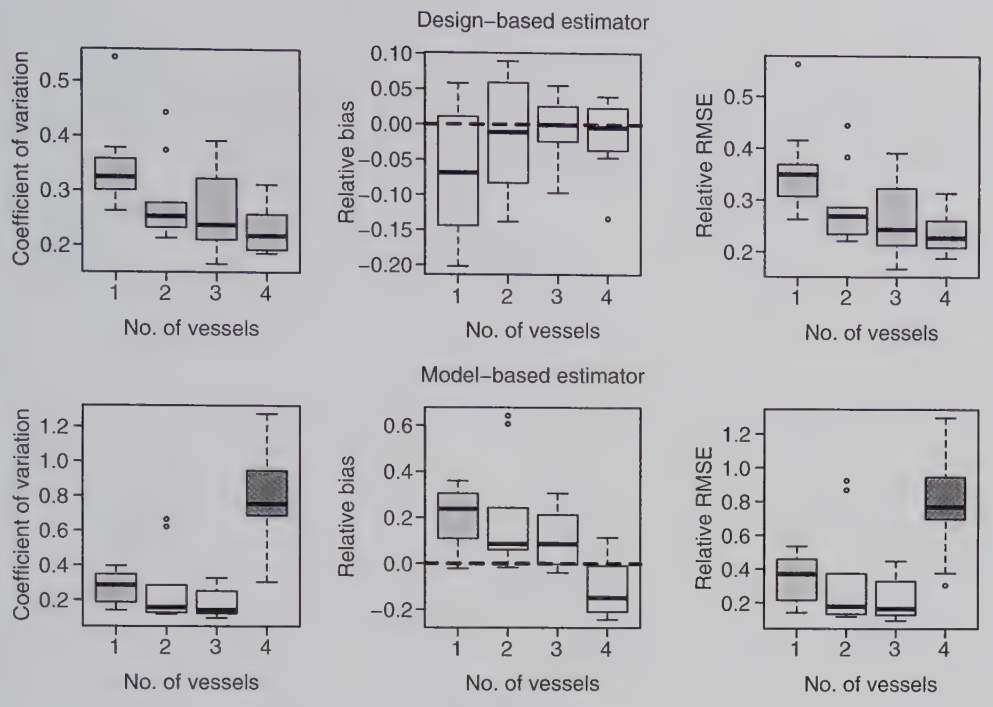

Figure 8

Relative performance of the design-based estimator and the estimator based on a vector autoregressive spatiotemporal model in estimation of variance in biomass of arrowtooth flounder (*Atheresthes stomias*) in simulated bottom-trawl surveys of the Gulf of Alaska at 4 survey effort levels. Each box plot represents the distribution of a performance metric, coefficient of variation, relative bias, or relative root mean square error (RMSE), for a survey effort level (number of vessels) over the 10 survey years between 1996 and 2015. In each box plot, the thick black line is the median. The upper and lower parts of each box represent the first and third quartiles (the 25th and 75th percentiles). The whiskers extend above and below the box no more than 1.5 times the interquartile range. Data points that appear beyond the end of the whiskers are outliers. The white, light gray, and dark gray colors of individual boxes indicate that metric values are within the ranges at which estimates are classified as desirable (<0.20), acceptable (0.20–0.40), and unreliable (>0.40), respectively.

for the model-based estimator at all but 1 of the 4 effort levels (the 1-vessel level) (Table 1). Also, as with the design-based estimator, there was no decline in the rRMSE with sampling density for the model-based estimator for this species. Both estimators performed poorly for sablefish compared to their performances for the other 3 species (Fig. 9).

The rRMSE values of variance estimates were somewhat similar and consistently indicate that the quality of estimates from the design-based and model-based estimators is desirable or acceptable for the arrowtooth flounder and Pacific cod, except at the 4-vessel effort level for arrowtooth flounder, where the value for the model-based estimator unexpectedly spiked to its highest level (0.79) (Figs. 7–8). For Pacific ocean perch, the rRMSE of variance estimates from the model-based estimator was smaller than that of estimates from the design-based estimator at all sampling densities, but there was no clear trend in the rRMSE with increasing sampling density for either estimator (Fig. 6). The rRMSE values for estimates for Pacific ocean perch at all survey effort levels consistently indicate not only that estimates from the design-based estimator range from barely acceptable (0.35–0.39) to poor (0.45–0.52) but also that estimates from the model-based estimator are acceptable (0.28–0.36). Although the design-based estimator consistently outperformed the model-based estimator at all effort levels for sablefish, the rRMSE values were unacceptably high for both estimators, indicating that neither estimator performed well for this species (Table 1, Fig. 10).

Discussion

The recent reduction of sampling density from 820 to 550 stations for the bottom-trawl survey conducted in the GOA (von Szalay, 2015) was expected to only modestly affect the 3 performance metrics for design-based and

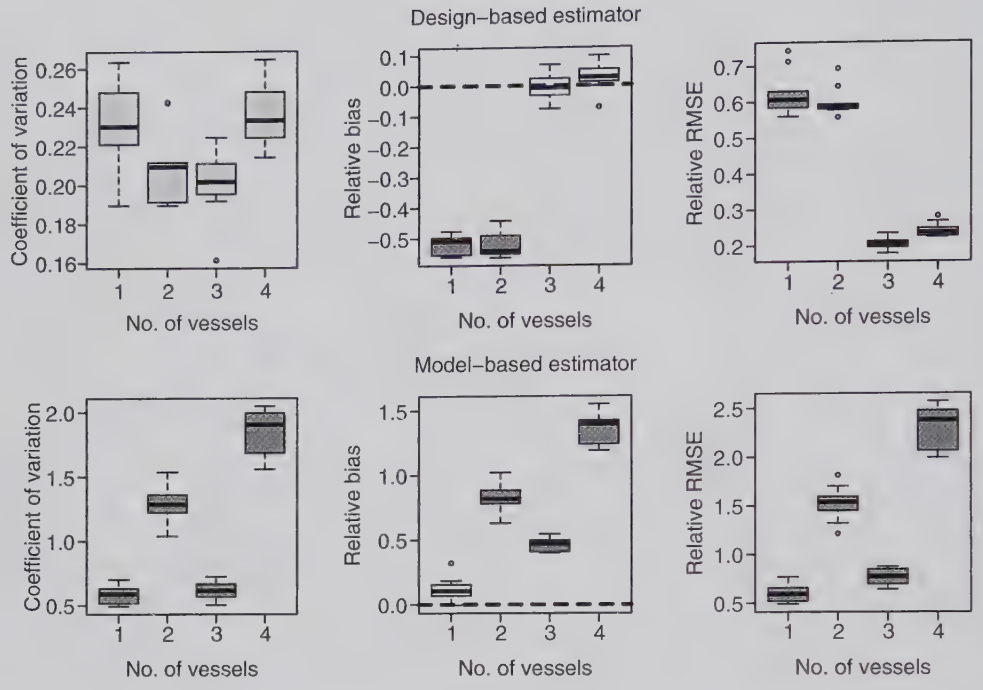

Figure 9

Relative performance of the design-based estimator and the estimator based on a vector autoregressive spatiotemporal model in estimation of biomass of sablefish (*Anoplopoma fimbria*) in simulated bottom-trawl surveys of the Gulf of Alaska at 4 survey effort levels. Each box plot represents the distribution of a performance metric, coefficient of variation, relative bias, or relative root mean square error (RMSE), for a survey effort level (number of vessels) over the 10 survey years between 1996 and 2015. In each box plot, the thick black line is the median. The upper and lower parts of each box represent the first and third quartiles (the 25th and 75th percentiles). The whiskers extend above and below the box no more than 1.5 times the interquartile range. Data points that appear beyond the end of the whiskers are outliers. The white, light gray, and dark gray colors of individual boxes indicate that metric values are within the ranges at which estimates are classified as desirable (<0.20), acceptable (0.20–0.40), and unreliable (>0.40), respectively.

model-based estimators of biomass and variance, and the results of this study support this hypothesis for 3 of the 4 species examined: arrowtooth flounder, Pacific cod, and Pacific ocean perch. This outcome is consistent with the findings of similar simulation studies on sampling effort (Xu et al., 2015; Meng et al., 2019). For example, Xu et al. (2015) analyzed the relationship between performance metrics and effort levels in a simulation study to optimize sampling effort for a survey with a stratified random design, and they achieved relatively high precision and accuracy of abundance indices for most species at a broad range of effort levels, indicating that the quality of abundance indices can be robust despite changes in effort levels. However, the effect on the performance metrics for sablefish was substantial (rRMSE changed from a value indicating that the quality of estimates is desirable [0.200] to a value indicating that the quality is poor [0.580]); in particular, the relative bias for biomass estimates from the design-based estimator changed from unbiased (0.000) to highly biased (–0.550).

Effect on estimates for sablefish

The disproportionate effect of reduced sampling density on abundance indices for sablefish in comparison to those for the other species analyzed in our study can be attributed to differences in depth distribution. Of the 4 species examined in our study, the sablefish occupies the broadest and deepest range of depths, from less than 100 m to 1500 m (Kimura et al., 1998). In contrast, the Pacific ocean perch, which occupies the next widest depth range, rarely occurs at depths greater than 500 m (von Szalay and Raring, 2016). Furthermore, the depth distribution of sablefish is size-specific because fish migrate ontogenetically to deep water, where the largest fish live and, hence, a substantial portion of the biomass of sablefish occurs (Jacobson et al., 2001). For example, approximately 37% of the total biomass of GOA sablefish was estimated to occur in the deepest stratum (700–1000 m) sampled by the GOA bottom-trawl survey in 2015 (von Szalay and Raring, 2018). Because this deepest stratum was eliminated from

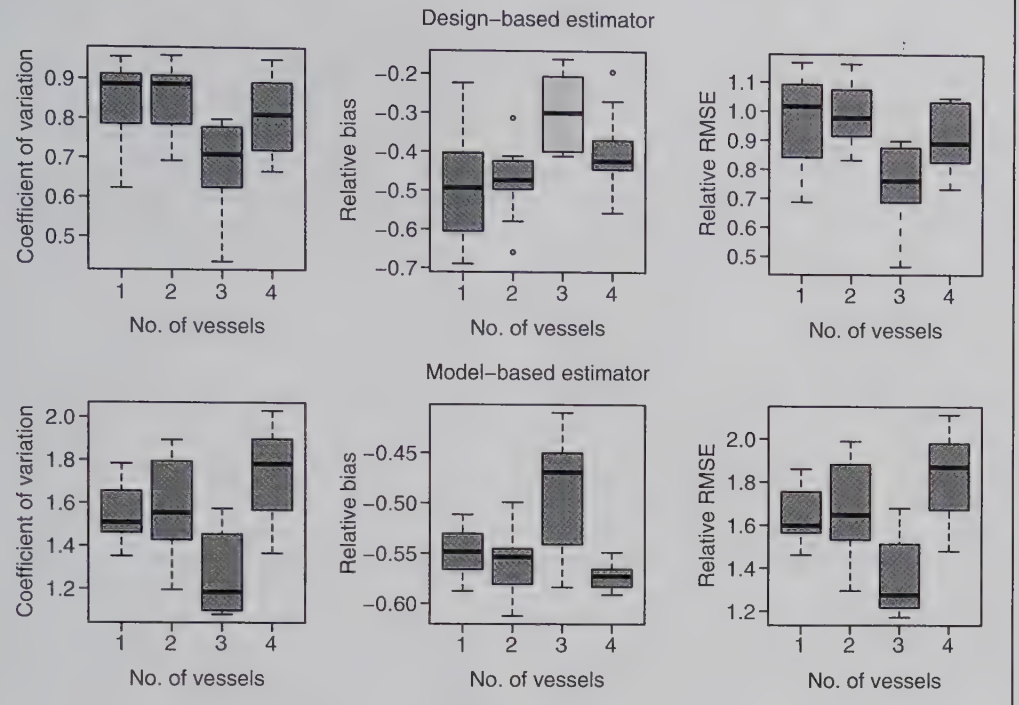

Figure 10

Relative performance of the design-based estimator and the estimator based on a vector autoregressive spatiotemporal model in estimation of variance in biomass of sablefish (*Anoplopoma fimbria*) in simulated bottom-trawl surveys of the Gulf of Alaska at 4 survey effort levels. Each box plot represents the distribution of a performance metric, coefficient of variation, relative bias, or relative root mean square error (RMSE), for a survey effort level (number of vessels) over the 10 survey years between 1996 and 2015. In each box plot, the thick black line is the median. The upper and lower parts of each box represent the first and third quartiles (the 25th and 75th percentiles). The whiskers extend above and below the box no more than 1.5 times the interquartile range. Data points that appear beyond the end of the whiskers are outliers. The light and dark shades of gray of individual boxes indicate that metric values are within the ranges at which estimates are classified as acceptable (0.20–0.40) and unreliable (>0.40), respectively.

the sampling protocol when the effort for this survey was changed from 3 vessels to 2 vessels, a large portion of the sablefish population in the GOA is not sampled at the reduced effort level, causing the increase in the relative bias of estimates found for this species. The estimates for the other 3 species are not affected by the removal of this stratum from the sampling protocol because these species do not occur at the depths in that stratum. Therefore, survey teams should consider evaluating how changes in sampling density affect not only survey data products but also survey footprint and, therefore, spatial availability of the survey in different years.

Estimates of biomass and variance for sablefish were considerably more affected by the reduction in survey effort from 3 vessels to 2 vessels than estimates for any of the other species. In addition, the quality of estimates from both the design-based and model-based estimators for this species was consistently the worst by far on the basis of values for all 3 performance metrics. This difference in estimate quality for sablefish can be explained in part by the much wider depth distribution of this species, with a large portion of the biomass of the GOA population occurring in the 3 deepest depth strata, all on the continental slope (Fig. 2) (von Szalay and Raring, 2016). Two main factors cause the modified Neyman allocation scheme to effectively result in under-sampling of these strata. First, the sampling allocation is proportional to stratum area, an approach that is not ideal because it is preferable to allocate resources with the aim to reduce variance in survey estimates (Oyafuso et al., 2022). Second, because the strata on the continental slope are narrow and encompass small areas, relatively few stations are allocated to the slope strata (Equation 3). For species like sablefish, which have large concentrations of biomass in these strata, the taking of fewer samples there reduces the quality of estimates of abundance and variance.

Other factors also cause under-sampling of strata. The number of stations allocated is inversely proportional to the cost of sampling a stratum. The cost, measured in terms of the time required to both find a viable towing location and

the time spent conducting a trawl tow in a given stratum, is greater for deep strata on the continental slope than for strata on the comparatively shallow continental shelf. This difference in cost also leads to less sampling allocation to strata where biomass of sablefish is high. Therefore, including cost of sampling in the allocation algorithm should be considered in conjunction with the value of the data because consideration of cost alone may result in inadequate sampling of valuable species. The relatively low sampling effort on the continental slope is also due to necessary trade-offs among species, an inherent aspect of the design of all multispecies surveys. Because a dedicated longline survey for sablefish on the continental slope already exists (Sigler and Zenger, 1989), and because of the extremely high commercial value of this species, sablefish receive no weight when optimal sampling allocations are calculated for each species and a weighted average, based on commercial value, is generated. This tack is taken to prevent the sablefish from unnecessarily dominating the sampling allocation scheme at the expense of other species that lack a dedicated survey.

The consistently poor performance of the model-based estimator for sablefish at all effort levels and for estimates of both biomass and variance can likely be attributed to the effectively unbalanced sampling design for this species, a design that results in under-sampling in some areas for the reasons discussed earlier in this section (Fig. 2). The unbalanced nature of the stratified random design with respect to sablefish is analogous to the poor performance of the same estimator when coupled with a survey design in which the survey stations, rather than fish distributions, were heavily concentrated in just a few strata (von Szalay et al., 2023). Although the stratified random sampling design was far superior to all the other designs to which it was compared when coupled with a design-based estimator, it did not perform well when coupled with the model-based estimator, which is sensitive to highly unbalanced sampling.

Effect on estimates for Pacific ocean perch

With the exception of the variance estimate from the model-based estimator for arrowtooth flounder at the 4-vessel effort level, both estimators performed relatively well for arrowtooth flounder and Pacific cod. In contrast, variance estimates were only marginally acceptable to unacceptable for Pacific ocean perch, at all sampling densities, although values of the 3 performance metrics for biomass estimates were almost always better than those for the corresponding variance estimates. Of these 3 species, Pacific cod consistently had the best biomass and variance estimates, and Pacific ocean perch consistently had the worst estimates, on the basis of rRMSE values.

The comparatively poor estimates for Pacific ocean perch can be attributed to the relatively patchy spatial distribution of this species compared with those of the other 2 species (Lunsford et al., 2001; Clausen and Fujioka, 2007). The bulk of the biomass of Pacific ocean perch is confined to a relatively small depth interval between 150 and 300 m, in a narrow band along the upper continental slope, and the distribution of this species within this band is patchy (von Szalay and Raring, 2016). Furthermore, the traditional stratified sampling design coupled with a design-based estimator used for the GOA bottom-trawl survey has been shown to be suboptimal for Pacific ocean perch, for which larger sample sizes in patchy areas of high density are required to reduce variance estimates of biomass (von Szalay et al., 2023). This problem could potentially be addressed through implementation of a hybrid survey design that incorporates an element of adaptive sampling in areas where catches of Pacific ocean perch are very large. However, a more consistent approach for multispecies surveys, such as the GOA bottom-trawl survey, would be to use a different sampling design altogether.

One approach is to consider other stratification methods as alternatives to the traditional Neyman allocation scheme, in which stratum boundaries are defined by depth as well as by management area. In one alternate stratification procedure, which is not constrained by predefined strata boundaries, abundance and variability from historical survey data are used to derive an empirical metric (an *information score*) for fine-tuning the traditional stratification process. This method of stratification can be used to ensure that more sampling is done in areas of high fish density and has proven to be particularly effective at reducing both the CV and the rRMSE of estimates for Pacific ocean perch vis-á-vis the traditional Neyman approach (von Szalay et al., 2023). The improvements in both the CV and rRMSE were particularly noteworthy for the variance estimates (at the 3-vessel level of survey effort), which changed from borderline acceptable to highly reliable (CV: from 0.40 to 0.03; rRMSE: from 0.40 to 0.10). Variance homogeneity within strata was considerably greater with stratification based on information scores than with the traditional stratification coupled with the Neyman allocation algorithm. This improvement in homogeneity can be attributed to the variance component of the information score, which allows variance to be targeted more directly, and consequently makes the stratification method based on information scores more efficient than the traditional stratification approach.

The method for stratification based on information scores also can be used to ensure adequate sampling in areas of high density but low temporal variance. This additional focus on areas of high density contrasts with the modified Neyman allocation approach, which can be used to account for only variance, stratum area, and a cost variable but not directly for density. Consequently, in the extreme case of a stratum with consistently high but uniform fish density, no sampling stations would be allocated with the Neyman allocation scheme.

Comparison of results from estimators

The model-based estimator consistently outperformed the design-based estimator in terms of both CV and rRMSE of biomass estimates at all sampling densities for arrowtooth flounder, Pacific cod, and Pacific ocean perch. To a

lesser extent, the opposite was true for relative bias, on the basis of which the design-based estimator consistently outperformed. However, because relative bias was consistently low for all of these species, its contribution to the rRMSE of biomass estimates was much smaller than the contribution of the CV; therefore, the model-based estimator performed best overall. An important short-term implication of this finding is that the relatively modest negative effect on the rRMSE of the recent reduction in survey effort can be completely mitigated by switching to spatiotemporal model-based methods, such as those in the VAST package, to estimate biomass.

Although the model-based estimator did not outperform the design-based estimator as consistently at all sampling densities for variance estimates as it did for biomass estimates, it did so at the only 2 sampling densities implemented in practice and likely to be implemented in the future, the 2-vessel and 3-vessel effort levels, for arrowtooth flounder, Pacific cod, and Pacific ocean perch. Therefore, the model-based estimator can also be used to mitigate the negative effect on variance estimates resulting from the recent reduction of sampling density in the GOA. The advantage of the model-based approach is so large that, on the basis of CV and rRMSE, it provides better biomass and variance estimates for Pacific ocean perch, even at the low 1-vessel effort level, than the design-based estimator and provides approximately the same quality of biomass estimates for arrowtooth flounder and Pacific cod at the 3-vessel effort level.

In contrast to its performance for arrowtooth flounder, Pacific cod, and Pacific ocean perch, the model-based estimator did not perform well for sablefish, even at the 3-vessel and 4-vessel effort levels at which sampling included the deepest strata. This difference in performance is likely due to the relatively high concentration of large fish (>70 cm in fork length) along the narrow strata on the continental slope. The model in the VAST package has been shown to perform very poorly when coupled with an unbalanced sampling design for arrowtooth flounder, Pacific cod, and Pacific ocean perch (von Szalay et al., 2023). It is likely that the high concentration of biomass of sablefish along the narrow continental slope has a similar effect on VAST estimates as an unbalanced survey design because the knots created in the VAST model to extrapolate fish density are often spaced too far from the sampling locations to generate valid density estimates. In the case of sablefish, the knots tend to be concentrated on or near the continental slope where fish density is greatest. This concentration is problematic because, as discussed earlier in the "Effect on estimates for sablefish" section, the stratified random sampling design results in under-sampling of this part of the survey area. Similarly, a VAST model coupled with an unbalanced survey design for a more evenly distributed species, such as arrowtooth flounder, also performs poorly when the bulk of sampling locations are concentrated in just a few strata. This poor performance occurs because the sampling locations tend to be located close to just a few knots where fish density may not be representative of the entire survey area.

Effect of climate change on validity of sampling design

Although the findings of this study indicate that the effects on the quality of biomass and variance estimates for most species are only modest when survey effort is reduced by as much as a third from historical maxima, this benign outcome is predicated on the validity of using historical survey data as the basis for allocating sampling locations in a stratified random sampling design. This assumption may be problematic because of shifts in distribution of fish species that may occur under climate change, with future distributions deviating from historical norms as species migrate in response to increased water temperatures and other variables (Hobday and Evans, 2013; Maureaud et al., 2021; Hollowed et al., 2022). For example, if fish move abruptly to strata that previously had low abundance, the data used as input for the Neyman allocation scheme will not reflect the new distribution, and these strata consequently will be under-sampled. In order to maintain the quality of abundance estimates in this scenario, it may be necessary to maintain or increase the overall sampling effort to characterize distribution shifts and use new survey data as an input for the sampling design process.

Conclusions

The reduction of sampling density from 820 to 550 stations for the GOA bottom-trawl survey only modestly affected the 3 performance metrics for biomass and variance estimates from both the design-based and model-based estimators for arrowtooth flounder, Pacific cod, and Pacific ocean perch. However, the effect on the relative bias of abundance indices for sablefish was profound. The performance metric of rRMSE consequently put the quality of abundance estimates for sablefish firmly in the poor category, meaning that estimates are unreliable at the reduced sampling densities. The disproportionate effect of reduced sampling density on estimates of abundance for sablefish can be attributed to the wider and deeper depth distribution of this species compared with those of the other 3 species, and estimates for this species are more sensitive to changes in survey effort as well as to concomitant changes in sampling area.

Resumen

Se evaluó el efecto de reducir el esfuerzo de prospección sobre la exactitud y precisión de las estimaciones de abundancia de 4 especies comerciales o ecológicamente importantes con distribuciones diferentes observadas en una prospección de arrastre de fondo realizado en el Golfo de Alaska. Se utilizaron simulaciones de un modelo mixto lineal generalizado espaciotemporal con base en observaciones históricas de las densidades de capturas para evaluar la robustes estadística, medida en términos de coeficiente de variación, sesgo relativo y error cuadrático medio relativo, de las estimaciones de abundancia y sus

varianzas. Estas métricas se utilizaron para comparar las estimaciones entre el estimador tradicional basado en el diseño y el estimador alternativo, basado en un modelo vectorial autorregresivo espaciotemporal, en 4 densidades de muestreo diferentes, que representan 2 niveles de esfuerzo de muestreo históricos y 2 teóricos a cada lado del intervalo histórico. La reciente reducción en la densidad de la prospecion de 820 a 550 estaciones sólo tuvo un efecto modesto en las medidas de rendimiento de ambos estimadores para el lenguado *Aesthes stomias*, el bacalao del Pacífico (*Gadus macrocephalus*) y la perca *Sebastes alutus*. Sin embargo, el efecto sobre las estimaciones de abundancia del bacalao negro (*Anoplopoma fimbria*) fue considerable. Atribuimos esta diferencia de resultados al mayor rango de profundidad utilizado por el bacalao negro, que ocupa preferentemente los estratos profundos relativamente poco muestreados (>500 m), y al área de estudio truncada en los niveles de muestreo reducidos, en los que se han eliminado los estratos más profundos (>700 m).

Acknowledgments

We are deeply grateful for J. Thorson's development of the R package VAST and for the valuable feedback and inspiration provided by the working group formed during the International Council for the Exploration of the Sea Workshop on Unavoidable Survey Effort Reduction. We also greatly appreciate the labor-intensive work of the many scientists and volunteers who have contributed to the GOA bottom-trawl surveys over the years. Finally, we thank M. Siple, P. Hulson, and 2 anonymous reviewers for their informative comments and suggestions, which helped to substantially improve the readability and clarity of this paper.

Literature cited

Alverson, D. L., and W. T. Pereyra.
1969. Demersal fish explorations in the northeastern Pacific Ocean—an evaluation of exploratory fishing methods and analytical approaches to stock size and yield forecasts. J. Fish. Res. Board Can. 26:1985–2001.

Clausen, D. M., and J. T. Fujioka.
2007. Variability in trawl survey catches of Pacific ocean perch, shortraker rockfish, and rougheye rockfish in the Gulf of Alaska. *In* Biology, assessment, and management of North Pacific rockfishes. Alsk. Sea Grant Coll. Program Rep. AK-SG-07-01 (J. Heifetz, J. Dicosimo, A. J. Gharrett, M. S. Love, V. M. O'Connell, and R. D. Stanley, eds.), p. 411–428. Univ. Alsk. Fairbanks, Fairbanks, AK.

Cochran, W. G.
1977. Sampling techniques, 3rd ed., 428 p. John Wiley and Sons, New York.

Hiemstra, P. H., E. J. Pebesma, C. J. W. Twenhöfel, and G. B. M. Heuvelink.
2009. Real-time automatic interpolation of ambient gamma dose rates from the Dutch radioactivity monitoring network. Computer Geosci. 35:1711–1721.

Hobday, A. J., and K. Evans.
2013. Detecting climate impacts with oceanic fish and fisheries data. Clim. Change 119:49–62.

Hollowed, A. B., A. C. Haynie, A. J. Hermann, K. K. Holsman, A. E. Punt, and C. S. Szuwalski.
2022. Implications of climate change on the Bering Sea and other cold water systems. Deep-Sea Res., II 201:105110.

ICES (International Council for the Exploration of the Sea).
2020. ICES Workshop on Unavoidable Survey Effort Reduction (WKUSER). ICES Sci. Rep. vol. 2, issue 72, 92 p. [Available from website.]
2023. Workshop on Unavoidable Survey Effort Reduction 2 (WKUSER2). ICES Sci. Rep. vol. 5, issue 13, 115 p. [Available from website.]

Jacobson, L. D., J. Brodziak, and J. Rogers.
2001. Depth distributions and time-varying bottom trawl selectivities for Dover sole (*Microstomus pacificus*), sablefish (*Anoplopoma fibria*), and thornyheads (*Sebastoloubs alascanus* and *S. altivelis*) in a commercial fishery. Fish. Bull. 99:309–327.

Kimura, D. K., A. M. Shimada, and F. R. Shaw.
1998. Stock structure and movement of tagged sablefish, *Anoplopoma fimbria*, in offshore northeast Pacific waters and the effects of El Niño-Southern Oscillation on migration and growth. Fish. Bull. 96:462–481.

Kotwicki, S., and K. Ono.
2019. The effect of random and density-dependent variation in sampling efficiency on variance of abundance estimates from fishery surveys. Fish Fish. 20:760–774.

Kotwicki, S., T. W. Buckley, T. Honkalehto, and G. Walters.
2005. Variation in the distribution of walleye pollock (*Theragra chalcogramma*) with temperature and implications for seasonal migration. Fish. Bull. 103:574–587.

Kotwicki, S., J. K. Horne, A. E. Punt, and J. N. Ianelli.
2015. Factors affecting the availability of walleye pollock to acoustic and bottom trawl survey gear. ICES J. Mar. Sci. 72:1425–1439.

Lindgren, F, H. Rue, and J. Lindström.
2011. An explicit link between Gaussian fields and Gaussian Markov random fields: the stochastic partial differential equation approach. J. R. Stat. Soc. 73:423–498.

Lunsford, C. R., L. Haldorson, J. T. Fujioka, and T. J. Quinn II.
2001. Distribution patterns and survey design considerations of Pacific ocean perch (*Sebastes alutus*) in the Gulf of Alaska. *In* Spatial processes and management of marine populations. Alsk. Sea Grant Coll. Program Rep. AK-SG-01-02 (G. H. Kruse, N. Bez, A. Booth, M. W. Dorn, S. Hills, R. N. Lipcius, D. Pelletier, C. Roy, S. J. Smith, and D. Witherell, eds.), p. 281–302. Univ. Alsk. Fairbanks, Fairbanks, AK.

Maureaud, A. A., R. Frelat, L. Pécuchet, N. Shackell, B. Mérigot, M. L. Pinsky, K. Amador, S. C. Anderson, A. Arkipkin, A. Auber, et al.
2021. Are we ready to track climate-driven shifts in marine species across international boundaries? A global survey of scientific bottom trawl data. Global Change Biol. 27:220–236.

Meng, X., J. Wang, C. Zhang, Y. Xue, B. Xu, and Y. Ren.
2019. Effects of sampling transect number on estimation of abundance index for bottom trawl surveys of fisheries resources in the Yellow River estuary. J. Fish. China 43:1507–1517. [In Chinese.]

Oyafuso, Z. S., L. A. K. Barnett, M. C. Siple, and S. Kotwicki.
2022. A flexible approach to optimizing the Gulf of Alaska groundfish bottom trawl survey design for abundance estimation. NOAA Tech. Memo. NFMS-AFSC-434, 142 p.

Peel, D., M. V. Bravington, N. Kelly, S. N. Wood, and I. Knuckey.
2013. A model-based approach to designing a fishery-independent survey. J. Agric. Biol. Environ. Stat. 18:1–21.

R Core Team.
2019. R: a language and environment for statistical computing. R Foundation for Statistical Computing, Vienna, Austria. [Available from website, accessed March 2020.]
Rue, H., S. Martino, and N. Chopin.
2009. Approximate Bayesian inference for latent Gaussian models by using integrated nested Laplace approximations (with discussion). J. R. Stat. Soc., B 71:319–392.
Sigler, M. F., and H. H. Zenger Jr.
1989. Assessment of Gulf of Alaska sablefish and other groundfish based on the domestic longline survey, 1987. NOAA Tech. Memo. NMFS F/NWC-169, 54 p.
Stauffer, G.
2004. NOAA protocols for groundfish bottom trawl surveys of the Nation's fishery resources. NOAA Tech. Memo. NMFS-F/SPO-65, 205 p.
Thorson, J. T.
2019. Guidance for decisions using the Vector Autoregressive Spatio-Temporal (VAST) package in stock, ecosystem, habitat and climate assessments. Fish Res. 210:143–161.
Thorson, J. T., and K. Kristensen.
2016. Implementing a generic method for bias correction in statistical models using random effects, with spatial and population dynamics examples. Fish. Res. 175:66–74.
Thorson, J. T., A. O. Shelton, E. J. Ward, and H. J. Skaug.
2015. Geostatistical delta-generalized linear mixed models improve precision for estimated abundance indices for West Coast groundfishes. ICES J. Mar. Sci. 72:1297–1310.
Thorson, J. T., C. J. Cunningham, E. Jorgensen, A. Havron, P.-J. F. Hulson, C. C. Monnahan, and P. von Szalay.
2021. The surprising sensitivity of index scale to delta-model assumptions: recommendations for model-based index standardization. Fish. Res. 233:105745.
von Szalay, P. G.
2015. The impact of sample size reduction on the precision of biomass estimates in the Gulf of Alaska. NOAA Tech. Memo. NMFS-AFSC-297, 17 p.
von Szalay, P. G., and N. W. Raring.
2016. Data report: 2015 Gulf of Alaska bottom trawl survey. NOAA Tech. Memo. NMFS-AFSC-325, 249 p.
2018. Data report: 2017 Gulf of Alaska bottom trawl survey. NOAA Tech. Memo. NMFS-AFSC-374, 260 p.
von Szalay, P. G., S. Kotwicki, L. A. K Barnett, L. J. Rugolo, and K. Ono.
2023. Reducing uncertainty in survey abundance estimates by considering alternative designs and estimators: a case study with 3 species in the Gulf of Alaska. Fish. Bull. 121:50–66.
Wakabayashi, K., R. G. Bakkala, and M. S. Alton.
1985. Methods of the U.S.–Japan demersal trawl surveys. *In* Results of cooperative U.S.–Japan groundfish investigations in the Bering Sea during May–August 1979 (R. G. Bakkala and K. Wakabayashi, eds.), p. 7–29. Int. North Pac. Fish. Comm., Bull. 44. [Available from website.]
Xu, B., C. Zhang, Y. Xue, Y. Ren, and Y. Chen.
2015. Optimization of sampling effort for a fishery-independent survey with multiple goals. Environ. Monit. Assess. 187:252.
Zimmermann, M., M. M. Prescott, and P. J. Haeussler.
2019. Bathymetry and geomorphology of Shelikof Strait and the western Gulf of Alaska. Geosciences 9:409.

National Marine Fisheries Service
NOAA

Fishery Bulletin
established in 1881

Spencer F. Baird
First U.S. Commissioner of Fisheries and founder of *Fishery Bulletin*

Long-term dynamics of larval and early juvenile spot (*Leiostomus xanthurus*) off the U.S. East Coast: relating ocean origins, estuarine ingress, and changing environmental conditions

Dennis M. Allen (contact author)[1]
John J. Govoni[2]
Kenneth W. Able[3]
Jeffrey A. Buckel[2]
Edward A. Hale[4]
Eric J. Hilton[5]
G. Todd Kellison[6]
Timothy E. Targett[7]
J. Christopher Taylor[8]
Harvey J. Walsh[9]

Email address for contact author: dallen@baruch.sc.edu

[1] Baruch Marine Field Laboratory
University of South Carolina
P.O. Box 1630
Georgetown, South Carolina 29440

[2] Department of Applied Ecology
Center for Marine Sciences and Technology
North Carolina State University
303 College Circle
Morehead City, North Carolina 28557

[3] Marine Field Station
Rutgers University
800 Great Bay Boulevard
Tuckerton, New Jersey 08087

[4] College of Earth, Ocean and Environment
University of Delaware
1044 College Drive
Lewes, Delaware 19958

[5] Virginia Institute of Marine Science
William and Mary
1370 Greate Road
Gloucester Point, Virginia 23062

[6] Southeast Fisheries Science Center
National Marine Fisheries Service, NOAA
101 Pivers Island Road
Beaufort, North Carolina 28516

[7] School of Marine Science and Policy
College of Earth, Ocean, and Environment
University of Delaware
1044 College Drive
Lewes, Delaware 19958

[8] National Centers for Coastal Ocean Science
National Ocean Service, NOAA
101 Pivers Island Road
Beaufort, North Carolina 28516

[9] Northeast Fisheries Science Center
National Marine Fisheries Service, NOAA
28 Tarzwell Drive
Narragansett, Rhode Island 02882

Abstract—Ichthyoplankton data sets based on collections from estuaries in South Carolina, North Carolina, Virginia, Delaware, and New Jersey and from ocean cruises off the U.S. East Coast were examined to determine spawning locations in the ocean, cross-shelf distributions of larvae, and movements of spot (*Leiostomus xanthurus*) into estuaries. Spot spawn during fall and winter near the edge of the continental shelf, primarily south of Cape Hatteras in North Carolina. We documented additional spawning of spot north of Cape Hatteras, close to the coast, in summer and fall. Larval and early juvenile spot enter estuaries from November through May in South Carolina and North Carolina and from January through June in Virginia, Delaware, and New Jersey. Numbers of spot per volume of water sampled decreased from south to north among estuaries and in the ocean. Interannual variations in abundance were high, and no long-term trends were determined. Over the decades, median annual lengths of ingressing larval and juvenile spot decreased as annual mean water temperature increased in South Carolina and North Carolina. The timing of ingress was positively correlated with water temperature. Continued increases in water temperature on the East Coast will likely lead to additional changes in oceanic distribution and ingress patterns of spot. Our findings indicate the value of synthesizing information from long-term studies conducted across broad geographic scales.

Manuscript submitted 25 March 2024.
Manuscript accepted 30 July 2024.
Fish. Bull. 122:162–185 (2024).
Online publication date: 20 August 2024.
doi: 10.7755/FB.122.4.3

The views and opinions expressed or implied in this article are those of the author (or authors) and do not necessarily reflect the position of the National Marine Fisheries Service, NOAA.

The spot (*Leistomus xanthurus*) is among the most abundant demersal fish species in the estuaries of the Atlantic and Gulf coasts of the United States and in the coastal ocean. As consumers of infauna and as prey for a range of piscivores, juvenile and adult spot play important ecological roles in shallow-water systems (Able and Fahay, 2010). Adults are harvested recreationally and commercially throughout their range (Hildebrand and Cable, 1930; Summers et al., 1985); however, harvests on the U.S. East Coast have been declining (ASMFC[1]). Although a considerable body of scientific literature is available on the biology and ecology of spot (Hales and Van Den Ayyle[2]), there is a need for a bet-

[1] ASMFC (Atlantic States Marine Fisheries Commission). 2022. ASMFC stock status overview, 53 p. ASMFC, Washington, D.C. [Available from website.]

[2] Hales, L. S., and M. J. Van Den Avyle. 1989. Species profiles: life histories and environmental requirements of coastal fishes and invertebrates (South Atlantic): spot. U.S. Fish Wildl. Serv. Biol. Rep. 82 (11.91). U.S. Army Corps Eng. TR EL-82-4, 24 p. [Available from website.]

ter understanding of its life history, the factors determining temporal dynamics, and the status of populations. One shortcoming is the lack of broadscale, long-term knowledge of the recruitment dynamics of this species.

Along the East Coast, adult spot spend spring and summer in estuaries and the coastal ocean from New Jersey to Florida. In the fall, adults with ripening gonads occur near estuarine inlets (Hildebrand and Schroeder, 1928) before migrating across the continental shelf to spawn (Hildebrand and Cable, 1930). The presence of early-stage larvae indicates that spot spawn near the edge of the shelf between North Carolina and Cape Canaveral, Florida, from late fall to early spring (Powles and Stender[3]; Lewis and Judy, 1983; Warlen and Chester, 1985). Adult spot make offshore migrations when water temperatures are suitable for spawning. In the laboratory, spot spawn when water cools to between 17.5°C and 25.0°C (Hettler and Powell, 1981), with maximum egg production at 20°C (Powell and Gordy, 1980). Larvae hatch at ~1.6 mm standard length (SL) in about 2 d (Powell and Gordy, 1980).

Spot dominate larval fish collections in winter in ocean waters south of Cape Hatteras (SoCH) in North Carolina, and it is in these waters below this point where they reach maximum abundance on the offshore continental shelf in winter (Powell and Robbins, 1994). The presence of small spot larvae (<4.0 mm SL) offshore of North Carolina indicates that most spawning occurs SoCH (Quattrini et al., 2005). Most spawning takes place where waters of the outer continental shelf mix with waters of the Gulf Stream (Govoni and Pietrafesa, 1994; Govoni and Spach, 1999). Larval spot ranging from 2.8 to 5.9 mm SL have been collected in the region of the Charleston Gyre off South Carolina, where shelf and Gulf Stream waters are mixed and wrapped around eddies; larvae also have occurred in Gulf Stream waters within the core of eddies on the outer continental shelf (J. Govoni, personal commun.). Larval spot grow as they move across the shelf (Lewis and Judy, 1983; Warlen and Chester, 1985). Off North Carolina, larvae of different sizes were more abundant in different areas: small larvae in Gulf Stream and outer shelf waters, medium larvae (4.0–7.5 mm SL) inside the outer shelf mixing zone, and large larvae (>7.5 mm SL) in the mid-shelf water mass (Walsh, 2007).

Advection or transport of larval spot has both a cross-shelf (zonal) component and an along-shore (meridional) component (Hare et al., 1999). It is widely recognized that zonal movement of larvae occurs with prevailing currents that are directed southwestward and are inshore of spawning areas near Gulf Stream fronts (Haight[4]; Werner et al., 1999; Blanton et al., 2003; Walsh, 2007). Newly hatched larvae are moved toward shore by Gulf Steam intrusions (Govoni and Pietrafesa, 1994) or eddies that strand on the shelf (Govoni et al., 2013).

Meridional transport moves larvae from ocean areas SoCH to waters north of Cape Hatteras (NoCH). Larvae entrained into the Gulf Stream by mixing and exchange with shelf waters at the Gulf Stream front (Govoni and Spach, 1999) can be transported northeastward. Larvae carried by the Gulf Stream could be moved into slope and shelf waters NoCH. Some young larvae remain in the Gulf Stream and have been collected off the coast of New England (Hare et al., 2001). Conversely, larvae in coastal waters off Virginia can be transported south into Onslow Bay, North Carolina (Stegmann and Yoder, 1996; Stegmann et al., 1999; Hare et al., 2001).

Some of the complexities of the transport of larval spot are a result of the nonuniform distribution of larvae in the water column (Hare and Govoni, 2005). Vertical position is important in their transport, zonally, across the shelf toward the East Coast by advection. Larvae and early juveniles in shelf waters <200 m deep are more abundant in the middle and deepest layers than in shallow layers (Hare and Govoni, 2005), and they are transported shoreward by residual lateral water movement at those depths (Pietrafesa and Janowitz, 1988; Hare et al., 1999). Investigating fish assemblages on the continental shelf off Georgia, Marancik et al. (2005) determined that transport of larvae could not be explained solely by 2-dimensional physical factors. Spatial and temporal variations occur in physical properties of shelf waters on multiple scales. Combined with largely unknown changes in behavior by developing larvae, the directions and rates of movement between spawning areas and estuaries remain difficult to resolve.

The age of larval and early juvenile spot (LEJ) collected in estuaries has provided some insights about transport duration. The youngest LEJ spot in Beaufort Inlet, in North Carolina, during 1978–1980 were 40 d old, and the average age was 59 d (Warlen and Chester, 1985). In North Inlet estuary, in South Carolina, during the winter–spring of 1981, the youngest larvae were about 60 d old and the average age was about 80 d (Beckman and Dean, 1984). Variations in both transport duration and environmental conditions across the shelf might account for much of the variation in ages and lengths observed among planktonic stages of spot found outside inlets and inside estuaries.

Larval and early juvenile spot arrive at inlets along the East Coast as far south as the Indian River Lagoon in southcentral Florida (Reyier and Shenker, 2007). Larval and early juvenile spot have been reported from inlets near St. Augustine, Florida (Korsman et al., 2017), the central coast of Georgia (Rogers et al., 1984), an estuary in northern South Carolina (Allen and Barker, 1990), various estuaries in North Carolina (Hettler and Chester, 1990; Hettler and Barker, 1993), Chesapeake Bay in Virginia (Olney and Boehlert, 1988; Ribeiro et al., 2015), the eastern shore of Maryland (Love et al., 2009), Delaware Bay

[3] Powles, H., and B. W. Stender. 1976. Observations on composition, seasonality and distribution of ichthyoplankton from MARMAP cruises in the South Atlantic Bight in 1973. Mar. Resour. Res. Inst., S.C. Wildl. Mar. Resour. Dep., Tech. Rep. 11, 47 p. [Available from website.]

[4] Haight, F. J. 1942. Coastal currents along the Atlantic coast of the United States. U.S. Dep. Commer., Coast Geod. Survey, Spec. Publ. 230, 73 p. Gov. Print. Off., Washington, DC. [Available from website.]

(de Sylva et al.[5]; Ribeiro et al., 2015), and Little Egg Inlet in New Jersey (Able and Fahay, 2010). Although LEJ spot were not documented in early ichthyoplankton surveys in Rhode Island (Herman, 1963; Bourne and Govoni, 1988), recent reports indicate rare occurrences in Connecticut (Millstone Environmental Laboratory[6]) and Rhode Island (Schneider[7]).

The most complete understanding of the arrival of spot into estuaries has come from studies along the coast of North Carolina, where larvae and early juveniles reach inlets from late fall through spring (Warlen and Chester, 1985; Flores-Coto and Warlen, 1993; Ross, 2003). Studies in North Carolina have addressed distributions of LEJ spot from the outer shelf to the inner estuary (Lewis and Judy, 1983), ocean movements outside and through inlets (Pietrafesa and Janowitz, 1988; Hettler and Hare, 1998), differences in patterns between neighboring inlets (Hettler and Barker, 1993), demographics of early life stages within estuaries (Flores-Coto and Warlen, 1993), and temporal dynamics within estuaries (Warlen and Burke, 1990; Hettler et al., 1997; Joyeux, 1999). However, a large gap persists in our understanding of the broader spatiotemporal dynamics associated with the ingress of spot into estuaries on a coast-wide scale.

Given the ecological and economic importance of spot in estuarine systems, understanding connections between the ocean and estuaries and how they are influenced by the environment is extremely important. A review of the most recent stock assessment of spot (ASMFC[8]) listed several research priorities that justify this study. The following priorities were identified: 1) examining historical estuarine and oceanic ichthyoplankton data sets to investigate the magnitude of spawning and potential use of larval abundance time series in future assessments, 2) investigating environmental effects (e.g., temperature and large-scale oceanic cycles, such as the Atlantic Multidecadal Oscillation [AMO]) on recruitment of spot, and 3) developing a better understanding of patterns of larval migration into nursery grounds.

The goals of this study were 1) to synthesize and interpret ocean-based ichthyoplankton survey data regarding the origins and transport of larvae across the continental shelf; 2) to determine and compare long-term patterns of ingress for larval and juvenile spot at multiple estuaries on the East Coast; 3) to explore relationships between spot abundance, size, and phenology and environmental conditions of estuaries and coastal waters during ingress; and 4) to consider effects of changing water temperatures on spawning, ocean transport processes, ingress, and landings of adult spot.

Materials and methods

Size classes

We designated 3 size classes for describing and comparing patterns of distribution of planktonic stages of spot in the ocean: small (nominal yolk sac and preflexion, ≤4.9 mm SL), medium (nominal flexion, 5.0–8.9 mm SL), and large (nominal postflexion, 9.0–20.0 mm SL). Specimens >16 mm SL, referred to herein as *early juveniles*, usually had a complete set of fins. Because 2 or 3 size classes often occurred in the same collection, we generally refer to the spot in this study as *larvae and early juveniles* of the species. Spot collected in estuarine ichthyoplankton collections included some specimens >28 mm SL; however, because their transition to the demersal phase had occurred (Hodson et al., 1981) and because they likely were not recent arrivals to estuaries, they were excluded from our analyses. In analyses of estuarine collections, we included all larvae and juveniles ≤27 mm SL.

Ocean

Data for larval spot from the ocean region NoCH (between 35°15′N and 42°0′N) came from 4 sampling programs conducted by the NOAA Northeast Fisheries Science Center. Details for the 4 programs, Marine Resources Monitoring, Assessment and Prediction (1977–1987), Herring and Sand Lance Program (1988–1994), Georges Bank Global Ocean Ecosystems Dynamics (1995–1999), and Ecosystem Monitoring (1999–present), can be found in Walsh et al. (2015). The basic station protocols were very similar among programs, providing consistency in sampling (Jossi and Marak, 1983; Ejsymont and Sherman, 2000). Samples were collected both day and night by using 61-cm-wide bongo nets (Table 1). Oblique tows were taken at 1.5 kt (0.77 m/s) with a minimum duration of 5 min, and nets were fished from the surface either to within 5 m of the seabed or to a maximum depth of 200 m. The volume of water filtered was measured with mechanical flowmeters mounted across the mouth of each net.

Shelf-wide station coverage extended from Cape Hatteras to the Gulf of Maine. A variety of sampling strategies were employed, including those that involved transects, fixed stations, and stations selected through a stratified random design. Most collections were processed at the Morski Instytut Rybacki in Szczecin, Poland, and the remaining collections were processed at

[5] de Sylva, D. P., F. A. Kalber Jr., and C. N. Shuster Jr. 1962. Fishes and ecological conditions in the shore zone of the Delaware River estuary, with notes on other species collected in deeper water. Univ. Del. Mar. Lab., Info. Ser. Publ. 5, 164 p. [Available from website.]

[6] Millstone Environmental Laboratory. 2021. Annual ecological report 2020: monitoring the marine environment of Long Island Sound at Millstone Power Station, Waterford, Connecticut, 205 p. Millstone Environ. Lab., Dom. Energy Nuclear Conn., Waterford, CT. [Available from the Millstone Power Station Environ. Lab., 314 Rope Ferry Rd. (Rte. 156), Waterford, CT 06358.]

[7] Schneider, E. 2021. Personal commun. Rhode Island Div. Mar. Fish., 3 Fort Wetherill Rd., Jamestown, RI 02835.

[8] ASMFC (Atlantic States Marine Fisheries Commission). 2017. 2017 spot stock assessment peer review, 9 p. Atlantic States Mar. Fish. Comm., Arlington, VA. [Available from website.]

Table 1

Gear, tow type, mesh size, and years sampled for the ichthyoplankton collections used to assess the occurrence and length distributions of larval and early juvenile spot (*Leiostomus xanthurus*) during research cruises in the ocean north of Cape Hatteras in North Carolina (between 35°15′N and 42°0′N) and south of Cape Hatteras (below 35°15′N).

Region	Gear	Tow type	Mesh size (μm)	Years
North of Cape Hatteras	61-cm bongo	Oblique	505	1977–1994
	61-cm bongo	Oblique	333	1988, 1995–2018
South of Cape Hatteras	1-m Tucker trawl	Surface	333	1992
	Issacs-Kidd trawl	Midwater	Unknown	1979–1982
	1-by-2-m frame net	Neuston	950	1973, 1992–1995
	20-by-40-cm frame net	Neuston	947	1973–1975, 1977–1982, 1985, 1986, 1995
	61-cm bongo	Neuston	333	1988
		Neuston	505	1973, 1975–1982, 1985, 1986, 1988, 1992, 1993
		Neuston	838	1988
		Oblique	333	1988, 1990–1996, 1998–1999
		Oblique	505	1988, 1990, 1991
		Surface	333	1990–1995
		Surface	505	1990–1991
		Unknown	505	1973–1980, 1982, 1985, 1995

the Narragansett Laboratory (Narragansett, RI) or the James J. Howard Marine Sciences Laboratory (Highlands, NJ) of the Northeast Fisheries Science Center or at the Atlantic Reference Centre (St. Andrews, Canada). A minimum of 50 randomly selected LEJ spot were measured to the nearest 0.1 mm SL. The total number of LEJ spot, concentration (number of spot per 100 m^3), minimum SL, and maximum SL were available for 1 bongo-net collection at each station.

Data for larvae from the region SoCH (south of 35°15′N) came from 2 sources: the plankton archives at the Beaufort Laboratory of the NOAA Southeast Fisheries Science Center and the Marine Resources Research Institute of the South Carolina Department of Natural Resources. Collection gear and tow types used in sampling programs SoCH are provided in Table 1. The collections and data obtained from the Marine Resources Research Institute were from ichthyoplankton sampling programs conducted by the Southeast Fisheries Science Center, nominally between February 1973 and April 1995: Marine Resources Monitoring, Assessment, and Prediction and Southeast Area Monitoring, Assessment, and Prediction (Collins and Stender, 1989). The number of collections per date and the locations of tows varied among years. Collections were made with tows of 61-cm-wide bongo nets (with mesh sizes of either 333 μm or 505 μm) at stations over the inner (minimum depth of 9 m), middle, and outer continental shelf from just south of Cape Canaveral to off Cape Lookout in North Carolina. The total number of LEJ spot, minimum SL, and maximum SL were available for 1 bongo-net collection at each station on all dates.

Ichthyoplankton collections and data obtained from the Southeast Fisheries Science Center came from the South Atlantic Bight Recruitment Experiment and other cruises conducted before and after the South Atlantic Bight Recruitment Experiment. Samples were collected primarily during the fall and winter in 1988 and 1990–1999 (Table 1). Collections were made with tows of a 61-cm-wide bongo net (with mesh sizes of either 333 μm or 505 μm) within 3 m of the surface and obliquely through the water column. Surface tows were also made with a 1-m-wide Tucker trawl net (with a mesh size of 333 μm). The volume of water filtered in bongo-net and Tucker-trawl collections was measured with a mechanical flowmeter mounted across the mouth of each net. Collections were also made by towing a neuston net with a 1-by-2-m frame (and a mesh size of 950 μm), with the top of the frame 0.25 m above the water's surface. Collections occurred primarily from off Charleston, South Carolina, to Cape Hatteras and targeted fish species that spawn on the shelf and, as juveniles, use estuarine habitats. Cross-shelf transects bisecting the cuspate bays SoCH were the predominate sampling strategy for many of the cruises. In addition, concentration of spot (number of spot per 100 m^3) was available for 1 bongo-net and 3 Tucker-trawl tows at each station.

Data from sampling in the ocean were grouped for analyses into 2 regions, NoCH and SoCH. Collections were made during all 12 months in each region (Table 2). Effort varied among months and years in both regions. The number of years during which collections were made within a given month varied from 13 to 41 NoCH and from 1 to 14 SoCH (Table 2). The total number of collections NoCH (number of samples [n]=28,280) was more than 9 times greater than that SoCH (n=3098) (Table 2). The full data set (with information from all collections) was used to describe seasonal patterns for the 2 regions based on presence or absence of and minimum and maximum lengths of

Table 2

Summary of monthly data used to assess the occurrence and length distributions of larval and early juvenile (LEJ) spot (*Leiostomus xanthurus*) collected during cruises north of Cape Hatteras in North Carolina (NoCH, between 35°15′N and 42°0′N) and south of Cape Hatteras (SoCH, below 35°15′N) between 1973 and 2018. The following information is presented for each month: the total number of years in which collections were made, the total number of collections with and without LEJ spot, the percentage of all collections with LEJ spot, the number of individuals caught in all collections taken that month, and the minimum and maximum lengths (standard lengths, in millimeters) of LEJ spot collected during the month.

Region	Month	No. of years collections made	No. of collections with LEJ spot	No. of collections without LEJ spot	Percentage of collections with LEJ spot	No. of specimens	Min. length	Max. length
NoCH	Jan.	25	23	1759	1.2	121	4	13
	Feb.	36	29	2417	1.2	138	3	17
	Mar.	39	36	2503	1.4	418	2	18
	Apr.	41	8	2874	0.3	33	7	19
	May	34	19	2961	0.6	57	2	20
	Jun.	31	11	2199	0.5	237	1	4
	Jul.	13	1	1021	<0.1	1	4	4
	Aug.	28	12	2658	0.4	118	1	3
	Sep.	35	39	1837	2.1	299	1	9
	Oct.	36	1	3008	0.4	2	6	11
	Nov.	37	8	3550	0.2	20	2	13
	Dec.	17	1	1305	<0.01	1	7	7
SoCH	Jan.	12	153	327	32	4276	2	17
	Feb.	14	184	485	28	5800	2	21
	Mar.	10	29	184	14	480	4	17
	Apr.	10	32	310	9	269	2	11
	May	7	0	244	0	0		
	Jun.	3	0	61	0	0		
	Jul.	3	0	73	0	0		
	Aug.	6	0	243	0	0		
	Sep.	9	1	277	<0.01	1	4	4
	Oct.	2	2	58	3	2	2	3
	Nov.	1	2	46	4	13	4	6
	Dec.	5	110	277	28	1137	2	12

LEJ spot. The decision to include all mesh sizes was based on studies comparing lengths of larval fish collected in nets with different meshes that were deployed at the same time. Johnson and Morse (1994) reported that the smallest larvae (2–3 mm SL) of 6 species were collected in nets with mesh sizes of both 333 µm and 505 µm. Only these 2 mesh sizes were used in the NoCH collections. Powell et al. (2000) noted that, although the smallest larvae caught in 333-µm-mesh nets (<3 mm SL) were not caught in 947-µm-mesh nets, 3–4 mm SL larvae were present in the collections made with nets with a mesh size of 947 µm. Most collections SoCH were made with nets with mesh sizes of 333 µm and 505 µm. The results of both studies indicate differences in the concentrations of larvae in most collections made by using nets with these mesh sizes.

Accordingly, concentrations of spot collected in the ocean were determined by using a subset of samples. Only collections made with 61-cm bongo nets with 333-µm-mesh nets towed obliquely through the entire water column were used to examine spatial and environmental patterns during the oceanic life stages. Concentrations were binned into 2-month sampling periods: January–February, March–April, May–June, July–August, September–October, and November–December. Individual size classes were compared between the 2 regions with samples for the 2-month periods. Analysis of variance was done in Matlab[9] (vers. 9.12; MathWorks Inc., Natick, MA) to determine if concentrations of spot among collections in the 2 regions were significantly different for each size class.

Cross-shelf (distance from shore) and environmental (sea-surface temperature and sea-surface salinity) patterns for the waters where spot were collected, by size class, were examined by using quotient analysis. Quotient analysis is relatively robust for data sets containing many values of 0, allowing regional analyses despite the rarity of spot larvae in collections NoCH (Bernal et al., 2007). With this analysis, the ratio of the proportion of

[9] Mention of trade names or commercial companies is for identification purposes only and does not imply endorsement by the National Marine Fisheries Service, NOAA.

larval occurrence to the proportion of observations was determined within environmental bins (distance from shore, temperature, and salinity) to discover where larvae were collected with higher (or lower) frequency than would be expected if larvae were evenly distributed. Quotient values >1 and above the upper confidence interval indicate a relatively higher occurrence of larvae, based on the number of observations, than expected. Quotient values just above or below 1 and below the upper confidence interval and above the lower confidence interval indicate occurrence at the expected level (van der Lingen et al., 2001). We examined the distance from shore (in kilometers), sea-surface temperature (in degrees centigrade), and sea-surface salinity for the locations where spot were collected for each of the 3 size classes of larvae (using Matlab).

Estuaries

Ichthyoplankton sampling in estuaries in South Carolina, North Carolina, Virginia, Delaware, and New Jersey resulted in data on abundance, lengths, and timing of ingress (phenology) of LEJ spot and on environmental parameters during ingress. Locations of the estuarine sampling sites are shown in Figure 1, and descriptions of the sampling gear, deployment strategies, and timing of collections for each site are provided in Table 3.

North Inlet estuary is a shallow, ocean-dominated salt marsh system with an extensive network of tidal creeks. Semidiurnal tides, with a mean tidal range of 1.4 m, maintain salinities at a range of 30–34 in the core of the estuary through most of the year. Water temperatures in the well-mixed salt marsh creeks of this system are usually 8–12°C

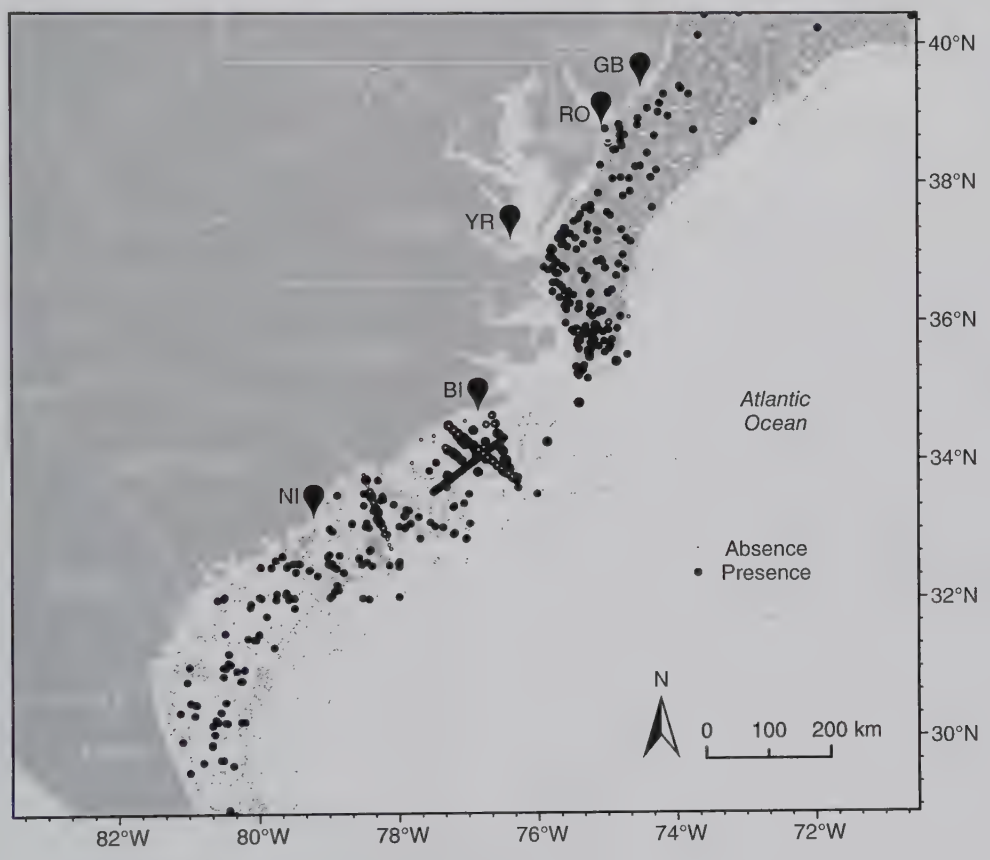

Figure 1

Map of presence (large black dots) and absence (small gray dots) of larval and early juvenile (LEJ) spot (*Leiostomus xanthurus*) in ocean-based collections made during 1973–2018 along the U.S. East Coast from central Florida to central New Jersey and included in this study. Although collections occurred north into the Gulf of Maine, so few LEJ spot were collected there (all far offshore) that these data were not plotted. The distribution of points represents all collections made during the cruises and sampling programs identified in Table 1. The dots in the lines that cross each other off the coast of North Carolina represent closely spaced sampling stations in roughly perpendicular transects. Balloons indicate the locations of the 5 estuaries where collections occurred: North Inlet (NI) in South Carolina, Beaufort Inlet (BI) in North Carolina, York River (YR) in Virginia, Roosevelt Inlet (RO) in Delaware, and Great Bay (GB) in New Jersey.

Table 3

Characterization of the estuarine sampling programs and data sets for collections of larval and early juvenile (LEJ) spot (*Leiostomus xanthurus*) in estuaries in South Carolina (SC), North Carolina (NC), Virginia (VA), Delaware (DE), and New Jersey (NJ) during 1982–2017. Net size is the area of the mouth of the net. The sampling frequency at North Inlet was once every 2 weeks. Period of occurrence is based on the months of earliest and latest occurrences of spot at each estuary for all years of sampling combined. Number of dates includes both the number of samples in which LEJ spot occurred and the number of all samples collected over all of the years at each site. Percentage of dates is the frequency of occurrence in the time series.

Estuary	Gear	Net size	Mesh size (µm)	Period	No. of years	Time of day	Sampling frequency and period	Period of occurrence	No. of dates (% of dates)
North Inlet, SC	Rectangular net on epibenthic sled	0.13 m^2	365	1982–2017	36	Day	Biweekly, all year	1 Nov.–31 May	246/515 (48%)
Beaufort Inlet, NC	Rectangular net	2 m^2	1000	1985–2017	31	Night	Weekly, only 1 Nov.–31 May	1 Nov.–31 May	668/949 (70%)
York River, VA	Ring net	0.79 m^2	1000	2008–2014	7	Night	Weekly, all year	1 Jan.–30 June	91/187 (49%)
Roosevelt Inlet, DE	Ring net	0.79 m^2	1000	2006–2010	5	Night	Weekly, all year	1 Jan.–30 June	44/136 (32%)
Little Egg Inlet, NJ	Ring net	0.79 m^2	1000	1989–2017	29	Night	Weekly, all year	1 Jan.–30 June	63/707 (9%)

in winter and 26–30°C in summer (Allen et al.[10]). The sampling location was in Town Creek about 2 km from the inlet. Depth at the time of sampling during the daytime mid-ebb tides was 2.5–4.0 m, and surface current velocities were usually 1.0–1.2 m/s. Tows were made with a net, which had a diameter of 0.5 and a mesh size of 365 µm, fitted to the vertically oriented rectangular frame (mouth) of an epibenthic sled. Three consecutive (replicate) tows were made from a boat in the direction of the current along a 150-m path on every sampling date (Table 3).

Beaufort Inlet is the location of tidal exchange between the ocean and Back Sound, Bogue Sound, and several estuarine systems. Samples were collected from a fixed platform on Pivers Island Bridge in Beaufort, North Carolina (Table 3), about 1.5 km inside Beaufort Inlet. The bridge spans a channel that is 40 m wide and 7 m deep. An estimated 10% of the water entering Beaufort Inlet flows through this channel (Checkley et al., 1999). Tidal range was about 1 m. The seasonal temperature range was 8–30°C. Larvae were collected at night with a 2-m^2 rectangular plankton net that had a mesh size of 1000 µm and was fitted with a flowmeter. Four sequential (replicate) net deployments were made at maximum flood velocity. The net was deployed just below the surface during nighttime flood tides.

The site in the York River at Gloucester Point, Virginia, is located about 11 km from the river mouth and 47 km from the entrance to Chesapeake Bay. At this location, the river is 700 m wide and 4 m deep. During this study, water temperature ranged from 2°C to 29°C, salinity ranged from 14 to 24, and current velocity ranged from 0.2 to 0.8 m/s (Chesapeake Bay National Estuarine Research Reserve in Virginia, Virginia Institute of Marine Science, Virginia Estuarine and Coastal Observing System [VECOS], available from website, accessed July 2024). On each date of sampling, 3 consecutive (replicate) deployments were done with a 1-m-diameter ring net, which was fitted with a flowmeter and had a net mesh size of 1000 µm, from the pier (at the Virginia Institute of Marine Science) during a nighttime flood tide; the 3 deployments were timed with one at peak flood tide, one before peak flood, and another after peak flood.

Roosevelt Inlet, near Lewes, Delaware, is located at the mouth of the Broadkill River, about 5 km from the mouth of Delaware Bay. At this sampling location, the river is 60 m wide and 3 m deep. Water temperature varied from 1°C to 28°C, salinity ranged from 4 to 33, and tidal water velocity ranged from 0.3 to 0.5 m/s (Ribeiro et al., 2015). On each sampling date, 3 consecutive (replicate) deployments were done with a flowmeter-fitted, 1000-µm-mesh, 1-m-diameter ring net from a pier on flooding tides at night.

Little Egg Inlet, in New Jersey, connects the Great Bay–Little Egg Harbor estuarine system to the ocean. This polyhaline estuary has a broad, seasonal temperature range of –2–28°C, average water depth of 1.7 m, and a moderate tidal range of about 1 m (Kennish, 2003). Sheepshead Creek, located about 2.5 km from Little Egg Inlet, is among the several thoroughfares or "creeks" that run through a peninsula and serve to connect Great Bay and Little Egg Harbor. Portions of the flood tide waters from the ocean are diverted into the mouth of Little Sheepshead Creek, where the average depth is about 1.5 m

[10] Allen, D. M., W. B. Allen, R. F. Feller, and J. S. Plunkett (eds.). 2014. Site profile of the North Inlet–Winyah Bay National Estuarine Research Reserve, 312 p. North Inlet–Winyah Bay Natl. Estuar. Res. Reserve, Georgetown, SC. [Available from website.]

(Chant et al., 2000). Sampling was done from the bridge at Little Sheepshead Creek on flooding tides at night, with 3 consecutive (replicate) deployments of a 1000-µm-mesh, 1-m-diameter ring net fitted with a flowmeter.

Differences in the gear, timing, and frequency of the sampling among the 5 estuaries (Table 3) were considered in comparing the data sets. Sampling at North Inlet estuary differed most from that in the other estuaries, with tow collections low in the water column and close to the bottom, a net area and mesh size that were smaller than those of the gear used at other sites, and sampling done during the day. In a comparison of LEJ spot in collections at North Inlet estuary during simultaneous deployments (day and night, ebb and flood) of the epibenthic sled (mesh size: 365 µm) and fixed nets (mesh size: 1000 µm, similar to the mesh size of nets used for collections in Virginia, Delaware, and New Jersey), concentrations in the sled towed during the day were 2–4 times less than concentrations in a 0.79-m^2 fixed net used to sample during the flooding tide the same night (senior author, unpubl. data). Because the concentrations of LEJ spot in South Carolina appear to be biased low, comparisons of concentrations in South Carolina with those in other states should be made with this bias in mind. The potential effect on concentrations and fish lengths of using a much larger net (with a mouth area of 2 m^2) in North Carolina, compared to the 0.79-m^2 nets used in Virginia, Delaware, and New Jersey, was not tested.

Length distributions in South Carolina were similar among all types of gear used at different tide stages and times of day (senior author, unpubl. data). Accordingly, the use of length distributions, the timing of occurrence (phenology), and temporal patterns of abundance of LEJ spot in South Carolina in comparisons of estuaries is considered valid and strong. The 1000-µm-mesh nets used at the other estuaries are appropriate for collecting larval fish with lengths >3 mm (Powell et al., 2000), well below the length of the smallest spot that have been documented in estuaries.

Because the ingress of LEJ spot was usually between November and May in South Carolina and North Carolina and between January and June in northern estuaries, periods of ingress rather than calendar years were used to define years for comparisons within and among estuaries. The first day of the month of earliest occurrence and the last day of the month of last occurrence in each time series were established as the end points of the period of occurrence (POC) at each estuary. The POCs used for comparing abundance and lengths during ingress among years were as follows: 1 November–31 May in South Carolina and North Carolina and 1 January–30 June in Virginia, Delaware, and New Jersey. Although LEJ spot usually first occurred in estuaries in South Carolina and North Carolina in November or December, the calendar year starting on 1 January of that POC was used to identify the year class. For example, if the first LEJ spot were collected in 1991 (before 1 January 1992), they were included in the analysis for the 1992 POC year class. If no larvae occurred before 1 January, zeros for all sampling dates back to the beginning of the POC (1 November in South Carolina and North Carolina) were used in the calculation of abundance for that year. This approach enabled direct comparisons of ingress periods for each year class among estuaries.

Data were not grouped by calendar year for any analyses; therefore, the term *annual* always refers to the POC for that estuary. Mean annual concentrations for each estuary were based on the number of LEJ spot per cubic meter of water filtered in all collections between the designated start and end dates of the POC. In North Carolina, sampling ceased in late April or in mid-May during 16 of the 31 years (mostly during 1987–1997). However, in years when sampling occurred until the end of May, no or very few LEJ spot were collected during those final 2 weeks of the designated POC. All collections in North Carolina between 1 November and the last date sampled until May 31 were used in calculations for comparisons of abundance and length among years.

To determine interannual differences and long-term trends in the timing of ingress into estuaries for LEJ spot, we used the cumulative summation procedure to generate phenological metrics (Greve et al., 2005). Four metrics were selected to examine the timing of occurrence in the estuaries: early, middle, late, and peak dates within the POCs. Determination of the timing of these phenological events was based on abundance data. Calculations for the phenology analyses required a common time line for all estuaries. Calendar dates corresponding to the events were converted to day numbers 1–365 with 1 November as day 1 for all estuaries, even though ingress into the estuaries NoCH did not occur until January. To avoid bias associated with the tails (actual first and last dates of ingress) of the annual abundance curves, the earliest and latest dates of occurrence of larvae and juveniles each year were determined by summing concentrations for all dates within POCs and determining the dates on which 15% (early), 50% (middle), and 85% (late) of the total annual concentration (sum for all dates) were reached (Greve et al., 2005). The peak occurrence date for each year was the actual date on which the highest concentration was observed. Years in which larvae did not occur on at least 3 dates were not included in the analyses of these phenological metrics. Duration was defined as the number of days between the early (15%) and late (85%) dates of occurrence each year.

Water temperature and salinity measurements were made at the time of the ichthyoplankton collections on almost every date at all estuaries. Mean annual values were based on all sampling dates from the first to the last date of spot occurrences (i.e., during the POC for that estuary) each year. These mean annual values of water temperature and salinity were used in correlation analyses with abundance, phenology, and fish length at each estuary.

Relationships between climate events and the abundances and timing (phenological metrics) of LEJ spot were explored for each estuary. North Atlantic Oscillation (NAO) annual index data were obtained from the National Center for Atmospheric Research (indices produced by the Climate Analysis Section in Boulder, Colorado, based on Hurrell et al. (2003), available from website, accessed July 2024). Atlantic Multidecadal Oscillation data were obtained from the Earth System Research Laboratory

(Enfield et al., 2001; data available from website, accessed July 2024). Indices used for the El Niño–Southern Oscillation (ENSO) were obtained from the Oceanic Niño Index generated by the Climate Prediction Center of the National Weather Service (data available from website, accessed July 2024). Average index values for the period from December through February were used to create climate event metrics for use in the correlation analyses. The designated period for the climate indices overlapped with the beginning of ingress of LEJ spot at all estuaries.

All statistical analyses and plots were configured by using SigmaPlot, vers. 10.0 (Grafiti, Pala Alto, CA). Abundance data for estuaries were converted to number of spot per cubic meter for analyses. Because abundance data were not normally distributed, a Kruskal–Wallis one-way analysis of variance on ranks was used to explore relationships between annual (POC) mean concentrations of spot at estuaries in South Carolina, North Carolina, and New Jersey, the estuaries with at least 29 years of data. Pairwise multiple comparisons were conducted with Tukey's honestly significant difference tests. Analyses with the Spearman's rank correlation coefficient were used to explore relationships between abundance, length, phenological metrics, climate index, water temperature, and salinity data within each of the 5 estuaries. Comparisons between annual median lengths of spot for pairs of estuaries with years in common were conducted by using Mann–Whitney rank sum tests. Linear regression was used to explore long-term trends in abundance, length, phenological metrics, water temperature, and salinity data at individual estuaries.

Results

Ocean

Larval and early juvenile spot were collected in the ocean from central Florida to Maine and from the coast to the edge of the continental shelf, but their occurrence north of New Jersey was very rare and is not shown in Figure 1. Overall, monthly estimates of frequency of occurrence in collections (number of samples with larvae per total number of samples) were low (average <0.1%) NoCH compared with estimates for collections SoCH (12.5%) (Table 2). Spot occurred NoCH during all 12 months. Frequencies of occurrence of 1.2–1.4% in January, February, and March represent the 3-month period of most frequent occurrence during the year. The highest frequency of occurrence (2.1%) was in September, and the lowest (0.01%) was in December (Table 2). Spot occurred SoCH only from September through April. Frequencies of occurrence of 28% in December, 32% in January, and 28% in February represent the 3-month period of most frequent occurrence SoCH. Spot were absent in SoCH samples from May through August, and occurrences in September and October were very low (Table 2).

During the months when LEJ spot were collected with oblique bongo-net tows in both regions, mean concentrations were significantly greater SoCH than NoCH for all 3 size classes whenever larvae occurred in both regions (Fig. 2). Small spot larvae were present NoCH during all 2-month sampling periods (Fig. 2A) and had the highest mean concentrations from May through October (Fig. 2A). Medium and large larvae were present NoCH in all 2-month sampling periods except in July–August (Fig. 2, B and C). Medium larvae were most abundant in January–February (Fig. 2B), and the highest concentrations of large larvae occurred in January–February and March–April (Fig. 2C). South of Cape Hatteras, small and medium spot larvae

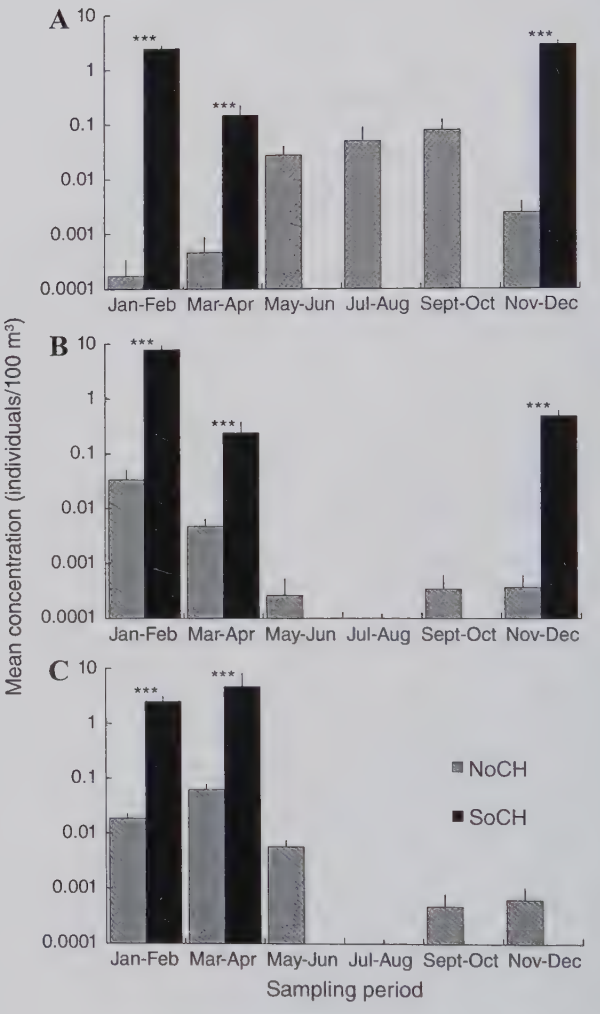

Figure 2

Mean concentration of (**A**) small (≤4.9 mm standard length [SL]), (**B**) medium (5.0–8.9 mm SL), and (**C**) large (9.0–20.0 mm SL) larval and early juvenile spot (*Leiostomus xanthurus*) collected from 1973 through 2018 during oblique tows of 61-cm-wide bongo nets (with a mesh size of 333 µm). Collections occurred in 2 ocean regions: north of Cape Hatteras (NoCH, between 35°15′N and 42°0′N) in North Carolina and south of Cape Hatteras (SoCH, below 35°15′N). Asterisks (***) indicate significant differences ($P \leq 0.05$) in mean concentration between regions during 2-month periods. Error bars indicate the standard errors of the means. Data for the 3 size classes were analyzed independently.

were abundant during the 2-month sampling periods of November–December, January–February, and March–April (Fig. 2, A and B). Small larvae were most abundant in November–December and January–February, and medium larvae were most abundant in January–February. Large larvae occurred SoCH only from January through April, and concentrations were higher there than NoCH throughout the year (Fig. 2C).

Results from quotient analyses indicate that spot larvae were produced at different locations across the continental shelf (east–west) in the 2 regions and in water masses with different environmental conditions (Fig. 3). North of

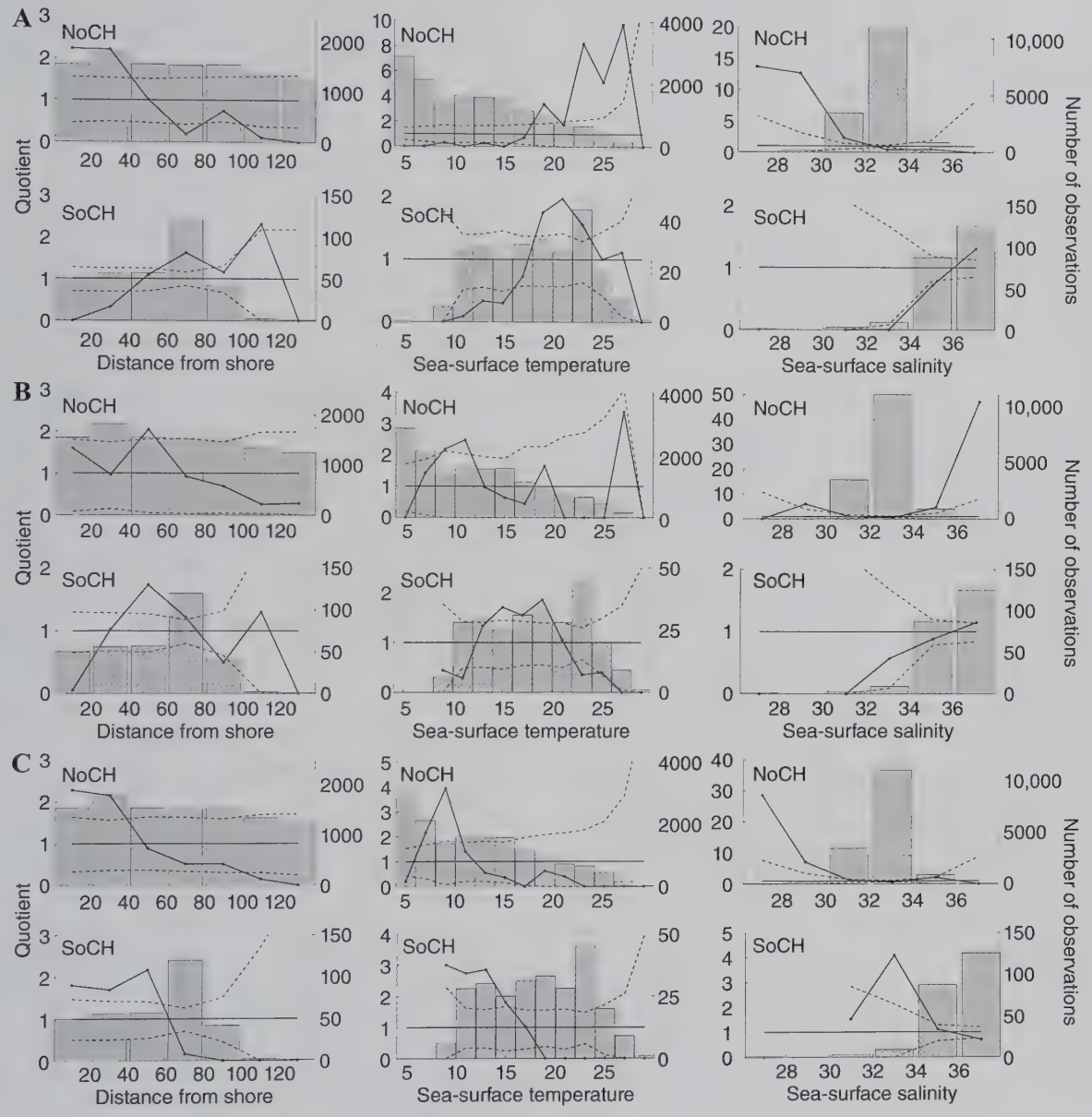

Figure 3

Ratio of the proportion of occurrence of larval spot (*Leiostomus xanthurus*) to the proportion of observations (quotient) for each bin of distances from shore, sea-surface temperatures, and sea-surface salinities from sampling on the U.S. East Coast during 1973–2018, by size class of spot: (**A**) small (≤4.9 mm standard length [SL]), (**B**) medium (5.0–8.9 mm SL), and (**C**) large (9.0–20.0 mm SL). The gray bars indicate total numbers of observations by bin. Collections were made by using oblique tows of 61-cm-wide bongo nets (with a mesh size of 333 µm) in 2 regions, north of Cape Hatteras (NoCH, between 35°15′N and 42°0′N) in North Carolina and south of Cape Hatteras (SoCH, below 35°15′N). The solid lines connect the data points for ratios. The dashed lines are the upper and lower confidence intervals for the null hypothesis (i.e., even distribution across the sampling bins).

Cape Hatteras, small larvae occurred significantly more frequently on the inner shelf (<40 km from the coast) in warm coastal water, with sea-surface temperatures generally greater than 18°C and salinities less than 32 (Fig. 3A). South of Cape Hatteras, small larvae occurred significantly more frequently on the outer shelf (>60 km from the coast) in offshore water masses, with sea-surface temperatures between 19°C and 24°C and salinities greater than 34 (Fig. 3A). Medium larvae NoCH were generally on the middle to inner shelf in multiple water masses (Fig. 3B). In the region NoCH, medium larvae were in 1) warmer (≥15°C) water masses in September–December, 2) colder (<15°C) and saltier (>34) water masses in January–February, and 3) colder (<15°C) and fresher (<34) water masses in March–April (Fig. 3B). In the region SoCH, medium larvae occurred significantly more frequently on the middle shelf (40–70 km from shore) (Fig. 3B), with sea-surface temperatures between 14°C and 20°C (Fig. 3B). Large larvae occurred NoCH more frequently on the inner shelf (Fig. 3C), and, SoCH, large larvae occurred on the inner shelf and middle shelf where water temperature and salinity were lowest (Fig. 3C).

Estuaries

Larval and early juvenile spot entered estuaries in South Carolina and North Carolina from November through May, and they entered estuaries in Virginia, Delaware, and New Jersey from January through June (Fig. 4). Within those POCs, frequency of occurrence varied among states: 48% in South Carolina, 70% in North Carolina, 49% in Virginia, 32% in Delaware, and 9% in New Jersey (Table 3). Early life stages of spot occurred during each of the 31 years in North Carolina, 35 of 36 years in South Carolina, all 7 years in Virginia, and all 5 years in Delaware, but they occurred during only 15 of 29 years in New Jersey.

Mean annual (POC) concentrations varied considerably among estuaries, and they differed by 3 orders of magnitude between the most (North Carolina) and least (New Jersey) abundant sites (Fig. 5). Long-term mean concentrations based on all years sampled at the sites were as follows: 0.4220 individuals/m^3 in South Carolina, 0.6312 individuals/m^3 in North Carolina, 0.0146 individuals/m^3 in Virginia, 0.0042 individuals/m^3 in Delaware, and 0.0004 individuals/m^3 in New Jersey. An overall difference in median concentrations of LEJ spot was observed among sites (Kruskal–Wallis analysis of variance on ranks: n=29, P<0.001). Results from pairwise comparisons of mean annual concentrations when using the years in common indicate no difference in ranks between estuaries in North Carolina and South Carolina (n=29, q=2.32). Differences were observed between estuaries in North Carolina and New Jersey (n=29, q=10.19) as well as between those in South Carolina and New Jersey (n=29, q=7.87).

Interannual variation in mean concentrations were high at all estuaries. Minimum (non-zero) and maximum mean annual (POC) concentrations differed by a factor of 32 in South Carolina, 15 in North Carolina, 34 in Virginia, 42 in Delaware, and 65 in New Jersey (Fig. 5). Results from linear regression analysis indicate no long-term trends for annual mean concentrations in any of the estuaries.

The highest concentration of LEJ spot for a single day during POCs at the 5 estuaries (total of 2494 collections) was 33.1546 individuals/m^3 in North Carolina in 2005, and the next highest was 11.0775 individuals/m^3 in South Carolina in 1984. Maximum concentrations for a single day were 0.0517 individuals/m^3 in Virginia, 0.1388 individuals /m^3 in Delaware, and 0.0282 individuals/m^3 in New Jersey. In 2005, mean POC concentrations in both North Carolina (1.9990 individuals/m^3) and South Carolina (1.2860 individuals/m^3) were the highest among all years. In 1991, the only year during which no spot were collected in South Carolina, concentrations in North Carolina were the second lowest (0.2180 individuals/m^3).

Mean annual (POC) water temperature increased between 1981 and 2017 in South Carolina (coefficient of determination [r^2]=0.17, P=0.007) and between 1987 and 2017 in North Carolina (r^2=0.39, P<0.001). No trend in temperature was observed in New Jersey (1989–2017) or during the shorter periods of sampling in Virginia and Delaware (Fig. 6). No correlations were found between mean annual concentrations of LEJ spot and mean temperature during the periods of occurrence within the estuaries. No long-term trends in salinity were found, and no correlations between salinity and mean annual concentrations of larvae were identified for any of the estuaries.

No correlations were found between mean annual water temperatures and the climate indices except for a positive relationship in North Carolina between mean annual water temperature and the AMO index (n=31, coefficient of correlation [r]=0.48, P=0.006). Mean annual concentrations of LEJ spot were not correlated with corresponding annual indices for ENSO, NAO, or AMO at any of the 5 estuaries.

The timing of the early (date when 15% of total annual abundance was reached) and late (date when 85% of total annual abundance was reached) occurrences of LEJ spot differed between estuaries south and north of Cape Hatteras. The date of early arrival (mean based on all years) was in late January in North Carolina and in early February in South Carolina (Table 4). The earliest mean dates in Virginia, Delaware, and New Jersey occurred in early to mid-March. The dates of late arrival were in mid-March in South Carolina and North Carolina and from late-April to mid-May in Virginia, Delaware, and New Jersey (Table 4). Similarly, middle dates and peak dates of ingress were earlier in North Carolina and South Carolina than at the northern sites. Average periods of duration were shortest in North Carolina and South Carolina (Table 4).

Positive relationships were found between many pairs of phenological metrics in North Carolina, South Carolina, and New Jersey, the 3 sites with the longest time series (Table 5). For example, the timing of the early and middle (date when 50% of the total annual abundance was reached) occurrences as well as the timing of middle and late dates across the years were positively correlated within each of these 3 estuaries. Dates of peak ingress were positively correlated with the dates of early, middle,

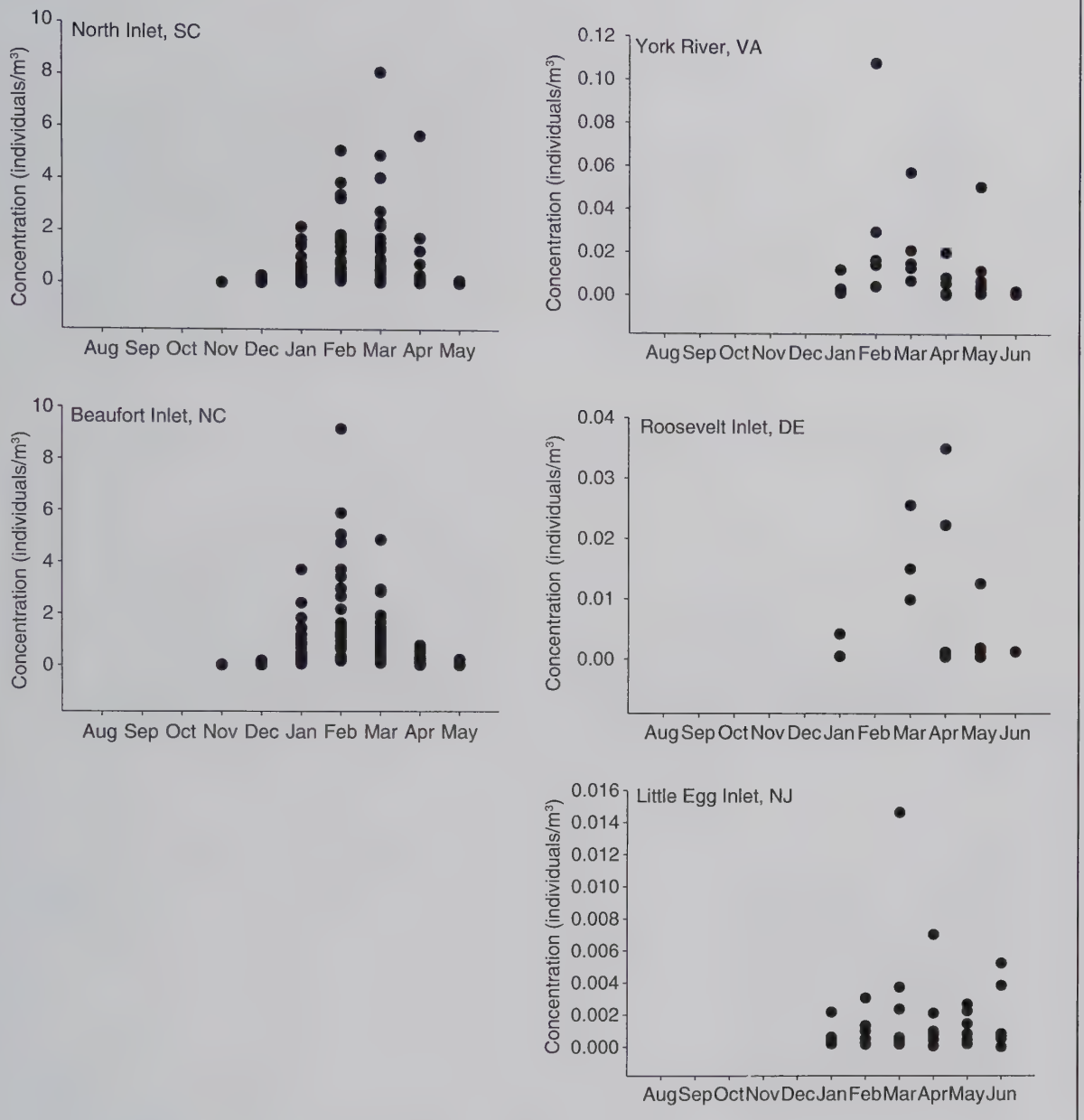
North Inlet, SC
Concentration (individuals/m³)
Aug Sep Oct Nov Dec Jan Feb Mar Apr May
York River, VA
Aug Sep Oct Nov Dec Jan Feb Mar Apr May Jun
Beaufort Inlet, NC
Roosevelt Inlet, DE
Little Egg Inlet, NJ

Figure 4

Average monthly concentrations of larval and early juvenile (LEJ) spot (*Leiostomus xanthurus*) in estuaries in South Carolina (SC), North Carolina (NC), Virginia (VA), Delaware (DE), and New Jersey (NJ) during 1982–2017. Each vertical set of points is based on the mean concentration of LEJ spot collected that month over all years. Note that the scales on the *y*-axes vary among estuaries.

and late arrivals in South Carolina and New Jersey and with middle dates and late dates in North Carolina across the years (Table 5).

Long-term trends were not found for the timing of early or middle dates or for the durations of the ingress periods at any of the estuaries; however, long-term trends were found for late dates of arrival, which occurred later in South Carolina (n=33, r^2=0.11, P=0.06), North Carolina (n=31, r^2=0.40, P<0.001), and New Jersey (n=12, r^2=0.55, P<0.01) than in the other estuaries, and for peak dates, which occurred later in North Carolina (n=31, r^2=0.21, P<0.01) than at other sites.

Positive correlations were found between early, middle, and peak dates of ingress and water temperatures in South Carolina, Virginia, and New Jersey and between peak date and water temperature in North Carolina

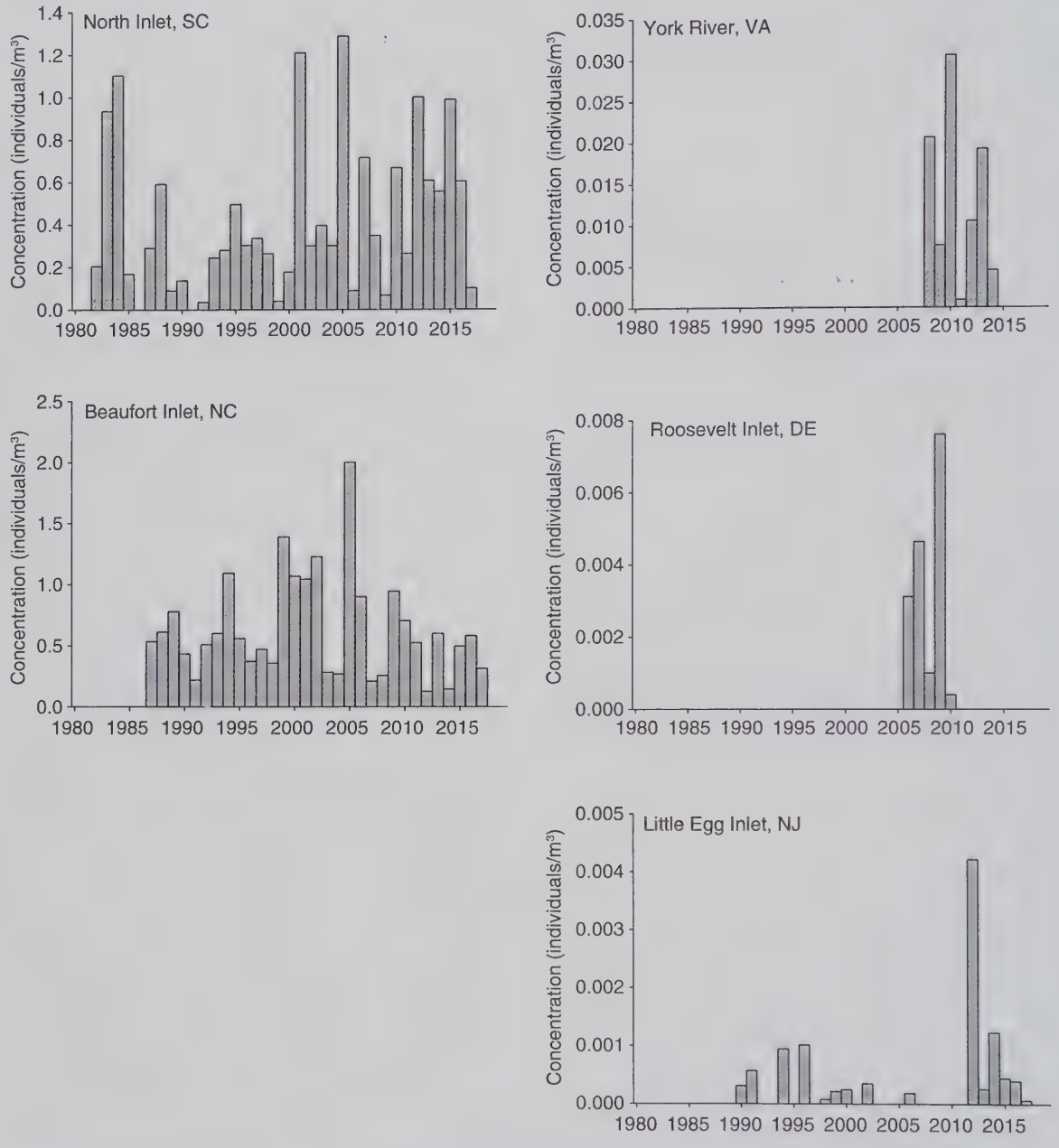

Figure 5

Average annual concentrations of larval and early juvenile spot (*Leiostomus xanthurus*) in estuaries in South Carolina (SC), North Carolina (NC), Virginia (VA), Delaware (DE), and New Jersey (NJ) from 1982 through 2017. Annual values are for a period of occurrence (POC) rather than a calendar year. The POCs used for comparing abundance during estuarine ingress of spot among years were as follows: 1 November–31 May in South Carolina and North Carolina and 1 January–30 June in Virginia, Delaware, and New Jersey. Values are the means of concentrations for all collection dates that year. Note that the scales on the *y*-axes vary among estuaries.

(Table 5). Negative correlations were found between salinity and early and middle dates in North Carolina (Table 5).

Relationships between early, middle, and peak dates of ingress and the indices for ENSO, NAO, or winter AMO were not determined for most of the estuaries. The exceptions were the negative correlations between winter AMO and duration of ingress in both South Carolina (n=33, r=–0.38, P=0.03) and Virginia (n=7, r=–0.75, P=0.04).

Length distributions were similar in South Carolina, North Carolina, Virginia, and Delaware with the majority of ingressing LEJ spot measuring 12–17 mm SL (Fig. 7). Spot were smaller in New Jersey with LEJ spot

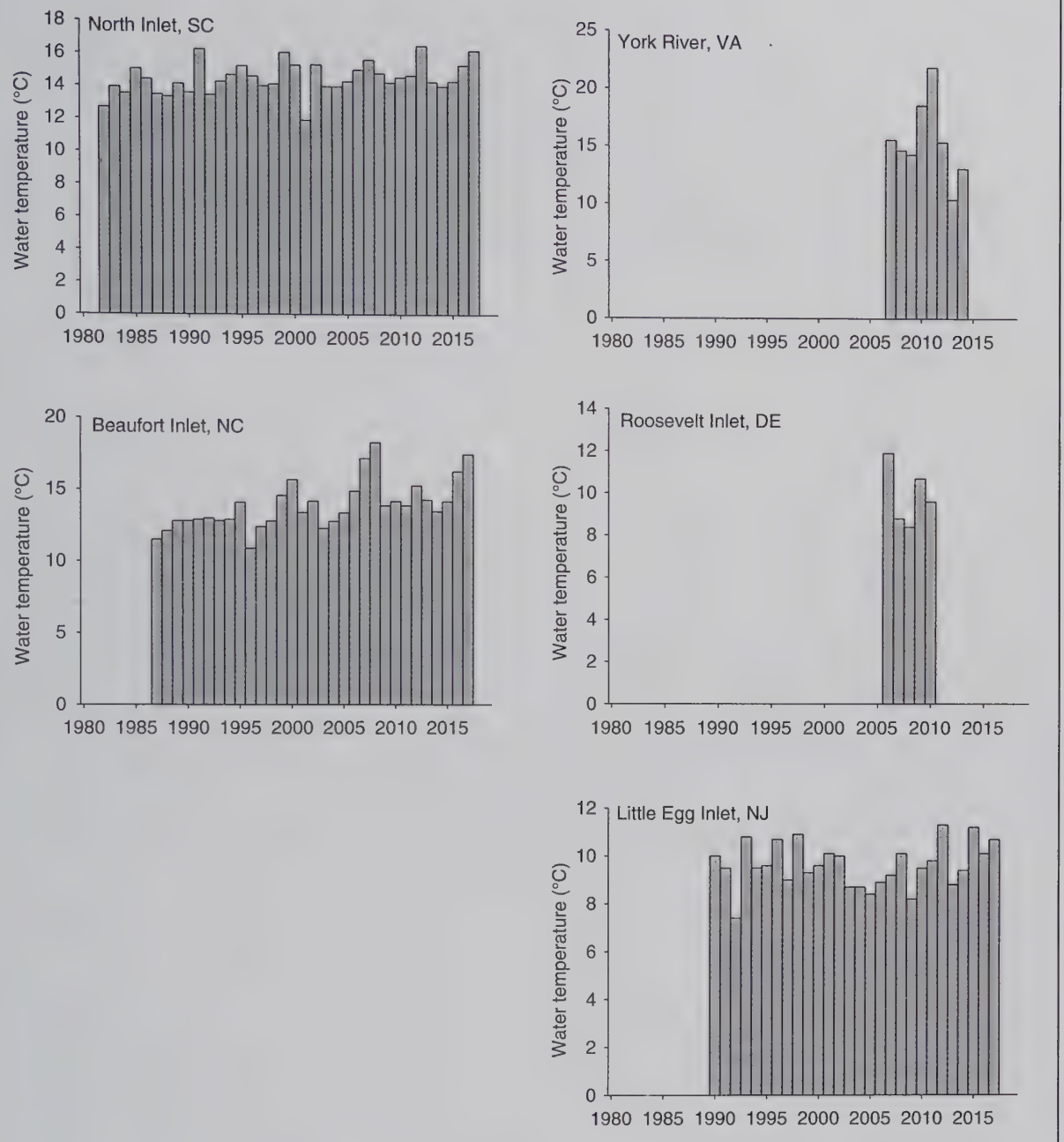

Figure 6

Average annual water temperatures for estuaries in South Carolina (SC), North Carolina (NC), Virginia (VA), Delaware (DE), and New Jersey (NJ) where larval and early juvenile (LEJ) spot (*Leiostomus xanthurus*) were collected during 1982–2017. Annual values are for a period of occurrence (POC) rather than a calendar year. The POCs used for comparisons of temperatures among years were as follows: 1 November–31 May in South Carolina and North Carolina and 1 January–30 June in Virginia, Delaware, and New Jersey. Values are means of temperatures measured at the time of all collections of LEJ spot in each estuary that year. Note that the scales on the *y*-axes vary among sites.

at 9–12 mm SL accounting for the largest proportion of the annual catches. The largest individual in New Jersey was 19 mm SL, whereas juveniles at 23–26 mm SL were collected at the other 4 estuaries. The smallest spot collected in the estuaries were 5–7 mm SL in North Carolina and New Jersey, and the smallest spot collected in South Carolina, Virginia, and Delaware were 8–9 mm SL (Fig. 7). Median lengths varied among years at all sites (Fig. 7). Long-term averages for median lengths were 14.4 mm SL in North Carolina, 15.3 mm SL in South Carolina, 11.4 mm SL in Virginia, 14.8 mm SL in Delaware, and 10.5 mm SL in New Jersey. Results of Mann–Whitney

Table 4

Phenology (timing of ingress) of larval and early juvenile (LEJ) spot (*Leiostomus xanthurus*) in estuaries in South Carolina (SC), North Carolina (NC), Virginia (VA), Delaware (DE), and New Jersey (NJ) during 1982–2017. Dates of ingress of LEJ spot for each year were determined by using the cumulative summation method with dates corresponding to 15% (early), 50% (middle), and 85% (late) of the sum of concentrations (number of spot per cubic meter) for all dates that year. Dates identifying the early, middle, and late occurrences are the averages for all years combined in each time series. Peak date is the average of the dates with the highest concentration. Duration is the average number of days between the early and late dates of occurrence. Range of duration is based on the years with the smallest and the largest number of days between the actual first and last occurrences of LEJ spot in each time series.

Metric	SC	NC	VA	DE	NJ
Early date	5 Feb.	29 Jan.	6 Mar.	8 Mar.	14 Mar.
Middle date	18 Feb.	22 Feb.	29 Mar.	13 Mar.	2 Apr.
Late date	17 Mar.	14 Mar.	28 Apr.	24 Apr.	12 May
Peak date	25 Feb.	22 Feb.	30 Mar.	17 Mar.	21 Apr.
Duration (d)	37	43	53	77	60
Range of duration (d)	13–104	10–84	5–136	10–104	14–106

Table 5

Results from Spearman's rank correlation analyses of relationships between phenological metrics, water temperature, and salinity for spot (*Leiostomus xanthurus*) sampled in estuaries in South Carolina (SC), North Carolina (NC), Virginia (VA), Delaware (DE), and New Jersey (NJ) over the time series from 1982 through 2017. Dates of ingress by LEJ spot each year were determined by using the cumulative summation method with dates corresponding to 15% (early), 50% (middle), and 85% (late) of the sum of concentrations (number of spot per cubic meter) for all dates that year. Peak date is the average of the dates with the highest concentration. Duration is the average number of days between the early and late dates of occurrence. Water temperature and salinity values were recorded on the phenological metric dates. Only Spearman's coefficients of multiple correlation with $P \leq 0.05$ are provided (cells with dashes had coefficients with $P > 0.05$. For North Carolina, correlation analyses with salinity were conducted with a number of samples (n) of 15.

	Spearman's coefficient of multiple correlation				
Variables	SC (n=33)	NC (n=31)	VA (n=7)	DE (n=5)	NJ (n=12)
Early vs. middle	+0.70, P<0.001	+0.44, P=0.015	–	–	+0.85, P<0.001
Late vs. middle	+0.54, P=0.001	+0.62, P<0.001	+0.89, P<0.001	–	+0.65, P=0.020
Early vs. late	–	–	–	–	+0.66, P=0.019
Early vs. peak	+0.44, P=0.010	–	–	–	+0.65, P=0.022
Middle vs. peak	+0.85, P<0.001	+0.54, P=0.002	+0.93, P<0.001	+0.98, P=0.017	+0.80, P<0.001
Late vs. peak	+0.66, P<0.001	+0.49, P=0.005	+0.93, P<0.001	–	+0.76, P=0.003
Early vs. duration	–	–	–	−1.0, P=0.017	–
Middle vs. duration	–	–	–	–	−0.60, P=0.036
Late vs. duration	+0.51, P=0.018	–	–	–	–
Early vs. temp.	+0.35, P=0.048	–	+0.75, P=0.038	–	+0.78, P=0.001
Middle vs. temp.	+0.67, P<0.001	–	+0.89, P<0.001	–	+0.84, P<0.001
Peak vs. temp.	+0.82, P<0.001	+0.52, P=0.004	+0.86, P<0.001	–	+0.88, P<0.001
Duration vs. temp.	−0.37, P=0.035	–	–	–	–
Early vs. salinity	+0.39, P=0.026	−0.63, P=0.011	–	–	–
Middle vs. salinity	–	−0.69, P=0.004	–	–	+0.84, P<0.001
Peak vs. salinity	–	–	–	–	–
Duration vs. salinity	–	–	–	–	–

rank sum tests indicate no differences between pairings of median lengths in South Carolina, North Carolina, Virginia, and Delaware or between lengths in Virginia and New Jersey over the years; however, median lengths in North Carolina and South Carolina were larger than those in New Jersey (n=11, P<0.001) for both paired comparisons.

Median lengths decreased over the time series for both South Carolina (n=34, r^2=−0.16, P=0.02) and North Carolina (n=16, r^2=−0.28, P=0.03) but not for New Jersey (Fig. 7).

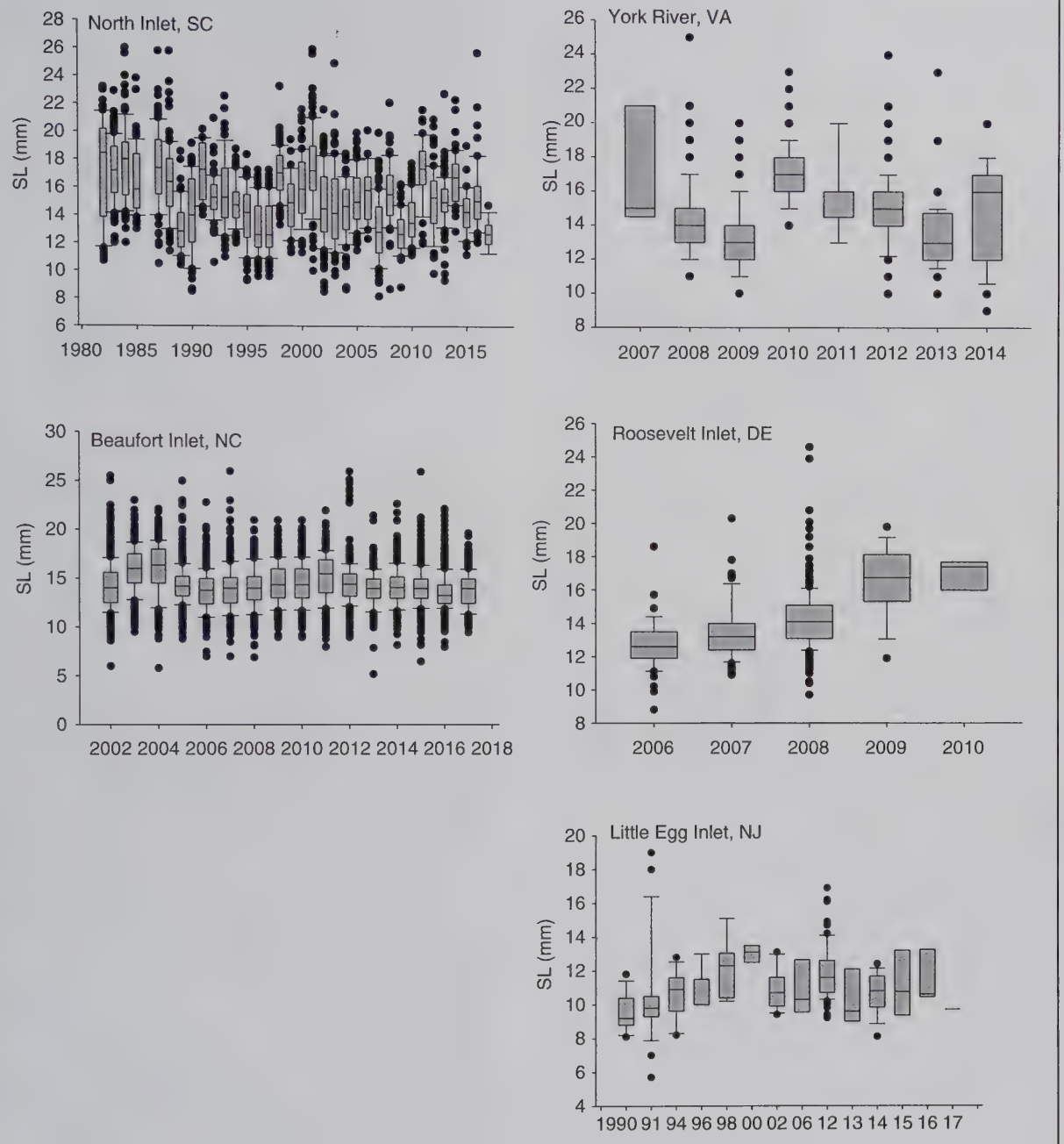

Figure 7

Standard lengths (SLs) by year for larval and early juvenile spot (*Leiostomus xanthurus*) collected in estuaries in South Carolina (SC), North Carolina (NC), Virginia (VA), Delaware (DE), and New Jersey (NJ) from 1982 through 2017. Box plots show the distributions of all length data for years (all months combined) in which data were available for at least 10 individuals. Note that scales on both axes vary among sites and that years are not continuous for Little Egg Inlet estuary. In each box plot, the black line in the middle is the median. The upper and lower parts of each box represent the first and third quartiles (the 25th and 75th percentiles). The whiskers extend above and below each box no more than 1.5 times the interquartile range. Data points beyond the end of the whiskers are outliers.

Interannual variation in lengths was observed in the shorter-term data sets for Virginia and Delaware; the general increase in median lengths in Delaware and decrease in Virginia over periods of 4–6 years were similar to the cyclical patterns for equivalent spans of time in the longer time series for South Carolina, North Carolina, and New Jersey. No long-term trends were found for minimum or maximum lengths in North Carolina, South Carolina, or New Jersey.

In South Carolina and North Carolina, median lengths of LEJ spot ingressing between November and January

were smaller than those for LEJ spot arriving in February and March when annual maximum median lengths occurred in both estuaries; however, median lengths in South Carolina and North Carolina decreased in April and May (Fig. 8). Some larvae <10 mm SL occurred during all months at the estuaries in South Carolina and North Carolina. Monthly length distributions were different in Virginia and Delaware, where median lengths increased from March to the end of the ingress period in June (Fig. 8). The distribution of lengths was more even across months

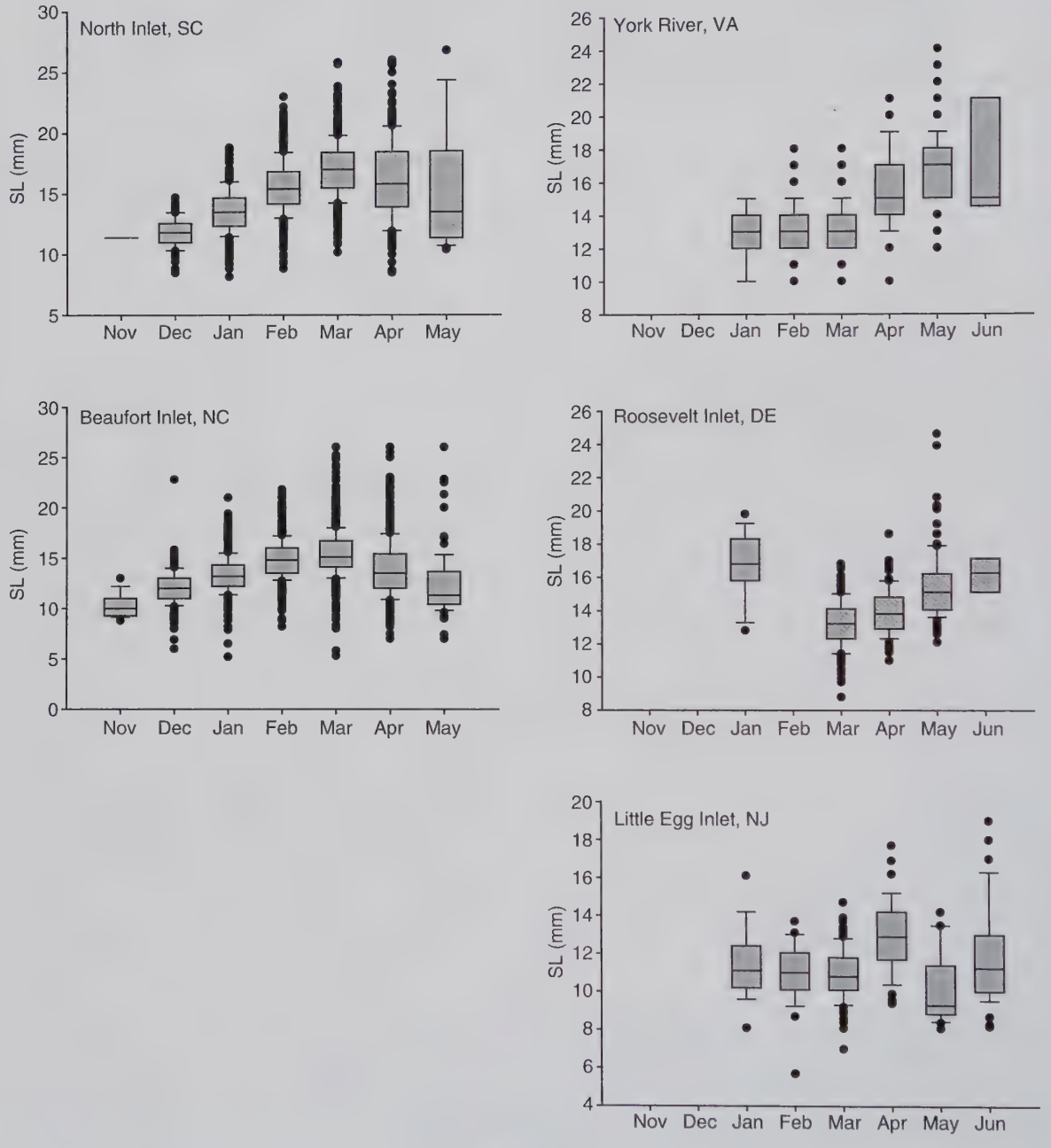

Figure 8

Standard lengths (SLs) by month for larval and early juvenile spot (*Leiostomus xanthurus*) collected in estuaries in South Carolina (SC), North Carolina (NC), Virginia (VA), Delaware (DE), and New Jersey (NJ) from 1982 through 2017. Box plots show distributions of all length data for months (all years combined) in which data were available for at least 10 individuals. Note that the scales on the *y*-axes vary among sites. In each box plot, the black line in the middle is the median. The upper and lower parts of each box represent the first and third quartiles (25th and 75th percentiles). The whiskers extend above and below each box no more than 1.5 times the interquartile range. Data points beyond the end of the whiskers are outliers.

in New Jersey, where LEJ spot were comparatively small throughout the ingress period (Fig. 8).

Median annual lengths of LEJ spot decreased with increasing annual mean water temperature in South Carolina (n=34, r=–0.37, P=0.03) and North Carolina (n=16, r=–0.67, P=0.005), but relationships between length and water temperature were not evident in Virginia, Delaware, or New Jersey. Median annual length and mean annual salinity did not appear to be related in any of the estuaries.

Discussion

Spawning locations along the East Coast

This first broadscale analysis of the early life history of spot on the East Coast by using novel data sets resulted in new information about the origins of larval spot on the continental shelf. Previous investigators focused on the outer shelf SoCH as a likely primary location of spot spawning, with most spawning found to occur in winter (Lewis and Judy, 1983; Warlen and Chester,1985; Flores-Coto and Warlen, 1993; Govoni et al., 2013). These previous studies were limited to that area. Our analysis of >31,000 ocean ichthyoplankton collections from Florida to Maine over several decades added spatial resolution to earlier findings that early-stage larvae were consistently found in greatest abundance near the edge of the continental shelf south of the latitude 35°15′ (Cape Hatteras) during winter. In the region SoCH, mean concentrations of LEJ spot were more than 100 times higher and frequencies of occurrence of LEJ spot in collections were more than 10 times higher than in the region NoCH.

Our observations of LEJ spot in multiple water masses with relatively high salinity NoCH indicate that some larvae spawned SoCH were entrained into the Gulf Stream and transported northward (Hare et al., 2002; Govoni et al., 2013). Results from previous studies on ocean currents and the distribution of larvae of other ocean-spawned species indicate that larvae produced SoCH can be transported onto the shelf NoCH (Grothues and Cowen, 1999; Hare et al., 2001; Grothues et al., 2002; Hare et al., 2002; Warlen et al., 2002). The species other than the spot that spawn in the ocean and enter estuaries NoCH as larvae and early juveniles include the Atlantic menhaden (*Brevoortia tyrannus*) (Warlen et al., 2002), Atlantic croaker (*Micropogonias undulatus*) (Norcross, 1991), summer flounder (*Paralichthys dentatus*) (Hoey et al., 2020), bluefish (*Pomatomus saltatrix*) (Hare and Cowen, 1996), and speckled worm eel (*Myrophis punctatus*) (Able et al., 2011).

We found evidence for a second source of larval spot NoCH. The occurrence of small larvae (≤4.9 mm SL) <40 km from shore NoCH from May through November indicates an origin other than outer continental shelf spawning SoCH. The highest concentrations of small larvae on the inner shelf NoCH occurred from July through October, when water temperatures were at annual highs. The greatest frequency of occurrence of small larvae NoCH was in September–October. The occurrence of small larval spot NoCH is best explained by adults spawning on the inner shelf or mid-shelf before spawning begins on the outer continental shelf SoCH in winter. Adult spot with developing ovaries have been found in lower Chesapeake Bay in September and October (Hildebrand and Schroeder, 1928). Whether adults that spawn on the inner shelf NoCH before November continue to migrate and spawn near the edge of the shelf in winter is unknown. Regardless, there are 2 sources of larvae for NoCH estuaries: 1) winter–spring spawning on the outer shelf from near or south of Cape Hatteras and 2) summer–fall spawning on the shelf NoCH. The absence of larvae SoCH from May through August and their near absence from September through November indicate that spawning in summer and early fall is not an important source of larvae for estuaries SoCH.

Ingress into estuaries

The timing of ingress of LEJ spot (January–June) in northern estuaries (Virginia, Delaware, and New Jersey) was similar in most years. Arrival of larvae and early juveniles of a wide range of sizes (8–18 mm SL) in all 3 estuaries NoCH from January through June indicates that they could have originated from both sources of larval production as described in the previous section. A comparison of the ingress of Atlantic menhaden between the estuaries in New Jersey and North Carolina revealed that larvae arriving in New Jersey early in the annual ingress period probably were spawned off New Jesrey by adults migrating toward primary winter spawning areas in deep waters and that larvae arriving later in winter were likely from spawning activity SoCH (Warlen et al., 2002). Norcross and Bodolus (1991) suggested that LEJ spot recruiting to Chesapeake Bay in winter and spring arrived 1–3 months after being produced at the edge of the continental shelf near Cape Hatteras, about 250 km to the south. How much winter spawning on the outer shelf SoCH contributed to LEJ spot in northern estuaries is unknown. However, because concentrations of all sizes of spot larvae in the ocean NoCH in winter were orders of magnitude less than those SoCH, it is likely that spawning NoCH from May through October was an important annual source of larvae for estuaries NoCH.

In New Jersey, LEJ spot arrived later and were smaller than those in Virginia and Delaware, indicating that delivery processes differed NoCH. Episodes of southerly winds in winter, and more frequently in spring, could facilitate the northward transport of larvae produced on the outer shelf around Cape Hatteras during winter (Norcross and Bodolus, 1991). Southerly winds could also affect the movement of larvae produced on the inner shelf NoCH in the fall. Wind events have been thought to be at least partly responsible for the high interannual variability in ingress observed in northern estuaries (Ribeiro et al., 2015). The ingress of smaller larvae in New Jersey could also be due to slow growth rates between fall spawning NoCH and ingress into this northernmost estuary. Larvae arriving in New Jersey during the winter and spring could

also be delivered more directly from the outer shelf by Gulf Stream eddies (Gangopadhyay et al., 2019, 2020) and other ocean processes that transport larvae to the coast more rapidly (Hare and Cowen, 1996).

The occurrence of LEJ spot in New Jersey during only 15 of the 28 years and at concentrations that were the lowest among the 5 estuaries indicates that Little Egg Inlet estuary in New Jersey is probably near the current northern limit of distribution of LEJ spot in estuaries on the East Coast. We were able to find records of spot in early life stages from only 2 estuaries north of New Jersey. Spot were rare in ichthyoplankton collections from Niantic Bay in Connecticut (eastern Long Island Sound) between 1976 and 2020, where a total of 12 larvae were collected on 11 dates from 1988 to 2019 (Millstone Environmental Laboratory[6]). They were also sparse in a survey conducted between 2002 and 2008 in Narragansett Bay in Rhode Island, with only 5 larvae collected on one date at a single station in 2007 (Schneider[7]). Studies of age and growth and chemical composition in otoliths of spot from the ocean and estuaries could further refine our understanding of the ocean origins and transport of LEJ spot to northern estuaries (Bath Martin et al., 2004; Bath Martin and Thorrold, 2005).

Spawning by spot on the outer shelf SoCH was almost certainly the source of LEJ spot entering estuaries in North Carolina and South Carolina. Larval and early juvenile spot in North Carolina were generally more abundant and smaller than those in South Carolina, and the timing of early, late, and peak occurrences was somewhat earlier. These findings indicate that Beaufort Inlet in North Carolina is more proximal to the main source of larvae in the ocean SoCH than North Inlet estuary in South Carolina. Consistently larger median lengths of spot arriving in South Carolina compared to those of spot arriving in North Carolina at the same time could result from longer transport across the shelf. Larval and early juvenile spot approaching the coast SoCH could be affected by the southward-directed coastal current (Blanton et al., 2003), possibly explaining the later timing and larger size of ingressing larvae and early juveniles in North Inlet estuary.

Early life stages of spot also arrive in estuaries in Georgia during winter and early spring (Rogers et al., 1984). Cross-shelf transport of larvae has been observed at least as far south as central Georgia (Marancik et al., 2005). The arrival of LEJ spot in estuaries in northern and central Florida could result from spawning on the outer shelf as far south as Cape Canaveral (Fahay, 1975). Larval and early juvenile spot occurred in the Guana-Tolomato-Matanzas estuary near St. Augustine, Florida, from December through April (Korsman et al., 2017); lengths of 8.5–12.5 mm SL and average concentrations around 0.3 individuals/m^3 were similar to those of LEJ spot collected in North Inlet estuary. Lower concentrations were reported for collections in the Indian River Lagoon near Melbourne, Florida, near the southernmost extent of estuarine ingress for LEJ spot (Reyier and Shenker, 2007). Spot in demersal (juvenile and adult) stages occur in Florida south of the Indian River Lagoon (Snyder and Burgess, 2016), but they do not appear to be as common as they are from central Florida to New Jersey. Spot are common in coastal waters and estuaries of the Gulf of Mexico, and spawning of spot there could contribute larvae and early juveniles to the east coast of Florida. Govoni et al. (2015) suggested that larvae of the chain pearlfish (*Echiodon dawsoni*) could be transported from the Gulf of Mexico to waters off the east coast of Florida and off states northward through the Loop Current and Gulf Stream; a similar pathway could be possible for spot as well.

The availability of records for many continuous years from South Carolina (36 years), North Carolina (31 years), and New Jersey (29 years) enabled comparisons of timing of ingress among and within the estuaries in these states. The timing of phenological events varied geographically; however, within each estuary, correlations between dates of early, middle, peak, and late occurrences were positive, indicating consistent relationships among these measures of timing among years. Strong relationships among phenological metrics within estuaries indicate largely symmetric patterns of ingress for each estuary over the years. However, these patterns varied among estuaries. Long-term trends with later dates of late arrival were identified for LEJ spot in South Carolina, North Carolina, and New Jersey. Peak ingress dates at all 3 of these sites were positively correlated with water temperature, indicating that peak ingress occurred later as water temperature increased. Positive correlations between water temperature and early and middle ingress dates in South Carolina, Virginia, and New Jersey also indicate responses by LEJ spot, with ingress delayed with increasing water temperatures. Thaxton et al. (2020) did not detect any long-term trends for phenological metrics for LEJ spot in Beaufort Inlet but found that ingress of many larval and early juvenile fish, including spot, occurred earlier during warm years. Differences in results between our study and the study by Thaxton et al. (2020), both of which used ichthyoplankton data from the same source in North Carolina, could be due to the use by Thaxton et al. (2020) of a shorter time series (1987–2013) and a different source of water temperature data (ocean-based sea-surface temperature). Results from analyses of sea-surface temperature off the Carolinas through 2015 do not indicate a warming of ocean waters (Shearman and Lentz, 2010; Morley et al., 2017); however, in a more recent analysis of temperatures in the region from North Carolina through the Florida Keys, an upward trend in sea-surface temperature beginning in 2014, particularly in winter and spring, was identified (Craig et al., 2021). High spatial and temporal variability within data sets for LEJ spot and water temperature present major challenges to understanding the relationships of water temperature and various aspects of LEJ spot in the ocean, but efforts to explore the influence of temperature on abundance, movements, and growth of LEJ spot in the ocean will be important for interpreting patterns of ingress into estuaries as environmental conditions change.

Warming temperatures could affect the size of larvae reaching the coast in several ways. For instance, if ocean water temperatures increase in the coming years, adults

migrating offshore could find suitable temperatures for spawning closer to the coast. If more spawning took place west of the long-recognized main spawning areas near the edge of the continental shelf, transport distances to estuaries would be shorter and smaller larvae might be expected to arrive at estuarine inlets. The occurrence of larval spot <4.9 mm SL within 40 km of the coast SoCH between December and April could indicate that some spawning occurs on the shelf, and that could be the source of small larvae collected in North Carolina and South Carolina in April and May. Warlen and Chester (1985) suggested that small LEJ spot collected toward the end of the ingress period might have originated from spawning at different locations than those arriving earlier in the year. The pattern that we observed for median lengths of LEJ spot in estuaries in South Carolina and North Carolina increasing between December and February and then decreasing in March and April had been previously reported for estuaries in North Carolina (Warlen and Burke, 1990; Flores-Coto and Warlen, 1993). Variations in the rates of transport across the shelf could also account for differences in the length of spot arriving in estuaries among years (Lewis and Judy, 1983) as well as within years.

The wide ranges of lengths of spot observed on most dates at all 5 sites of our study could be attributed to the presence of 2–10 birth-week cohorts throughout an ingress period of 4–5 months (Flores-Coto and Warlen, 1993). Beckman and Dean (1984) identified 3 primary cohorts of LEJ spot in North Inlet estuary, with length ranges of up to 10 mm SL within cohorts. It is not clear whether larvae collected in an estuary on a particular date were all or mostly new arrivals or if there was a mixture of new arrivals and LEJ spot that had already occupied the area for days or weeks. Wide ranges in lengths could also be related to differences in growth rates. Variation in growth can be expected within and between years as environmental factors, such as temperature, food supply, winds, and current velocities, vary during the months of cross-shelf transport (Govoni et al., 2010). Beckman and Dean (1984) determined that most 16-mm-SL spot entering North Inlet estuary were between 60 and 100 d old; therefore, it is possible that LEJ spot of the same length collected early in the ingress period (from January through March) had grown faster than those collected late in the period (in April and May).

Whether growth rates, rates of larval transport to the coast, or locations or timing of spawning for spot have changed is unknown. Clearly, more efforts are needed to understand many aspects of the early life history of spot in the ocean. The reestablishment of regular ichthyoplankton cruises SoCH (which currently take place NoCH) coupled with ongoing long-term collections of LEJ spot in estuaries would help answer many questions. Presently, long-term sampling programs are continuing in the estuaries in South Carolina, North Carolina, and New Jersey.

Variation of lengths, timing, and abundance of LEJ spot in estuarine collections could also be related by conditions close to shore. Upon arrival at inlets, passage of larvae into estuaries can be influenced by short- and long-term fluctuations in tide, sea-level pressure gradients, wind, or a combination as well as by other physical and biological factors (Pietrafesa and Janowitz, 1988; Hare et al., 2005; Hale and Targett, 2018; Whitfield et al., 2023a). Teodósio et al. (2016) suggested that ingress of larvae could not occur without behavioral responses to sensory cues, such as visual, sound, odor, and geomagnetic signals, that aid in navigation toward suitable estuarine nursery areas. Hettler and Hare (1998) determined that patterns in concentrations of larval spot outside of Beaufort Inlet were complex and probably were influenced by both the physical processes that supply larvae to inshore areas and the physical dynamics near the inlet. Certain conditions outside the inlet likely favor concentrating LEJ spot and influence ingress more than other conditions (Flores-Coto and Warlen, 1993). Several investigators have noted the importance of wind in the timing of estuarine ingress of LEJ spot and other species (Love et al., 2009; Schieler et al., 2014; Thaxton et al., 2020). Variations in the abundances, timing of occurrences, and lengths of LEJ spot between neighboring inlets in North Carolina (Hettler and Barker, 1993) and Florida (Korsman et al., 2017) were thought to be due to differences in local physical conditions controlling ingress.

The lack of significant relationships between salinity and the abundance and median lengths of LEJ spot in the 5 estuaries indicates that they were not very responsive to variable salinity conditions during winter. In addition, the almost total absence of correlations between early, middle, and late dates of occurrences in the estuaries with salinity indicates that ingressing spot did not have high sensitivity to variation in salinity. In laboratory studies of behavioral responses of larval spot (from 4 d to 4 weeks old) to rates of salinity change, De Vries et al. (1995) found that salinity gradients in the ocean were not likely to affect depth regulation, which could influence delivery to estuaries. As planktonic spot transform to juveniles and develop a demersal lifestyle, they occur across a wide range of salinities and, in river-driven estuaries, move toward tidal fresh water following ingress (Rogers et al., 1984).

Relationships between indices for NAO, AMO, or ENSO and the abundance and distribution of fishes in the North Atlantic Ocean have been reported by investigators interested in understanding how a changing climate affects fish and fisheries (Hare and Able, 2007; Thaxton et al., 2020; Gillanders et al., 2022; Whitfield et al., 2023b). In our study, very few correlations were found between LEJ spot and winter values for these broadscale indices. No relationships between the 3 indices and either abundance or the timing of ingress were found at any site; however, we found that the AMO index was positively correlated with water temperature in North Carolina between the mid-1980s and 2017, when water temperature increased in the estuary.

Although many environmental factors affect fish ecology, water temperature is most frequently identified as the most important in driving long-term changes in fish populations and their distribution. Several studies have produced evidence of latitudinal shifts in the distributions and timing of occurrence of some fish species in the North Atlantic

Ocean in recent decades with changes in temperature regimes (Perry et al., 2005; Nye et al., 2009; Walsh et al., 2015). Responses to changing temperature vary considerably among species and life stages of fish and zooplankton, even within the same assemblage (Allen et al., 2008; Morley et al., 2017; Morson et. al., 2019; Thaxton et al., 2020). In an analysis of long-term data sets for larval and trawl-caught fish in the shelf ecosystem of the northeastern United States, Walsh et al. (2015) found seasonal and spatial (latitudinal) shifts for many species but not for either larval or adult spot in the ocean. However, their analysis ended with collections made in 2008, prior to the increases in ocean water temperatures and marine heat wave events that started around 2010 (NEFSC[11]). For Little Egg Inlet estuary, Morson et al. (2019) reported an increasing presence of southern species and decreasing occurrence of northern species in association with warming temperatures.

A northerly shift in areas with temperatures around 20°C could result in a shift in the spawning of spot northward and westward away from the outer edge of the shelf SoCH. Such a shift could have major effects on the supply of spot larvae to estuaries both SoCH and NoCH. In addition, increasing winter water temperatures could provide expanded suitable habitats for juveniles and adults in northern estuaries. Our knowledge of the life history and ecology of spot is far from complete, but established relationships between water temperature and spawning and the observed long-term changes in lengths of early life stages and the timing of ingress in relation to changing temperature indicate that the occurrence and abundance of spot in estuaries of the East Coast will continue to be affected by the changing climate.

Conclusions

Our synthesis of data on LEJ spot from ichthyoplankton collections across the continental shelf north and south of Cape Hatteras and collections from 5 estuaries along the U.S. East Coast revealed new patterns of larval production, cross-shelf movement, and ingress into estuaries that could only be determined with data collected over multiple decades at multiple sites. Results of analyses of the oceanic data collected NoCH indicate for the first time that adult spot produce larvae on the inner shelf in summer and fall. Patterns of abundance, length, and timing of ingress in estuaries NoCH indicate that larvae spawned on the inner shelf supplemented those originating from the outer shelf. Ingressing spot in North Carolina and South Carolina originated from spawning near the edge of the shelf SoCH.

Over the decades, the lengths of LEJ spot arriving in the estuaries in North Carolina and South Carolina decreased. This change coincided with increasing water temperature over the same period. The timing of ingress became later over the decades, with the early, middle, and peak dates of ingress correlated with increasing water temperatures in South Carolina, North Carolina, and New Jersey. These relationships, which could be determined only from long-term data sets, indicate that the current trend for increasing ocean and estuarine water temperatures along the East Coast will lead to changes in the timing and locations of spawning, larval transport, and ingress of spot into estuaries. Given the important ecological and economic roles of spot, especially in estuaries, changes in their distribution and abundance could affect the structure of coastal food webs and both the recreational and commercial harvests of this species.

[11] NEFSC (Northeast Fisheries Science Center). 2021. 2021 state of the ecosystem: Mid-Atlantic, revised, 42 p. Report to the Mid-Atlantic Fishery Management Council. [Available from website.]

Resumen

Se examinaron de datos de ictioplancton colectados en estuarios de Carolina del Sur, Carolina del Norte, Virginia, Delaware y Nueva Jersey asi como de cruceros oceánicos frente a la costa este de EE.UU., para determinar los lugares de desove en el océano, la distribución de larvas entre plataformas y los movimientos de la croca (*Leiostomus xanthurus*) en los estuarios. La croca desova durante el otoño y el invierno cerca del borde de la plataforma continental, principalmente al sur del cabo Hatteras en Carolina del Norte. Documentamos desoves adicionales de la croca al norte del cabo Hatteras, cerca de la costa, en verano y otoño. Las larvas de esta especie entran en los estuarios de noviembre a mayo en Carolina del Sur y Carolina del Norte y de enero a junio en Virginia, Delaware y Nueva Jersey. El número de crocas por volumen de agua muestreada disminuyó de sur a norte entre los estuarios y en el océano. Las variaciones interanuales en la abundancia fueron elevadas y no se determinaron tendencias a largo plazo. Durante décadas, la mediana de la longitud anual de las larvas y juveniles de croca que ingresaban disminuyó al incrementarse la temperatura media anual del agua en Carolina del Sur y Carolina del Norte. El momento de la entrada se correlacionó positivamente con la temperatura del agua. Es probable que el aumento continuo de la temperatura del agua en la costa este provoque cambios adicionales en la distribución oceánica y en los patrones de entrada de la croca. Nuestros hallazgos indican el valor de sintetizar la información procedente de estudios a largo plazo realizados en escalas geográficas amplias.

Acknowledgments

We thank the many hundreds of individuals who collected samples, processed samples, managed data, and otherwise enabled us to create the data sets used in this analysis. Many federal agencies (especially the National Marine Fisheries Service, the NOAA National Estuarine Research Reserve Program, NOAA Sea Grant, and the National Science Foundation) and state agencies provided funding for the research programs over the decades.

Literature cited

Able, K. W., and M. P. Fahay.
2010. Ecology of estuarine fishes: temperate waters of the western North Atlantic, 566 p. Johns Hopkins Univ. Press, Baltimore, MD.

Able, K. W., D. M. Allen, G. Bath-Martin, J. A. Hare, D. E. Hoss, K. E. Marancik, P. M. Powles, D. E. Richardson, J. C. Taylor, H. J. Walsh, et al.
2011. Life history and habitat use of the speckled worm eel, *Myrophis punctatus*, along the east coast of the United States. Environ. Biol. Fishes 92:237–259.

Allen, D. M., and D. L. Barker.
1990. Interannual variations in larval fish recruitment to estuarine epibenthic habitats. Mar. Ecol. Prog. Ser. 63:113–125.

Allen, D. M., V. Ogburn-Matthews, T. Buck, and E. M. Smith.
2008. Mesozooplankton responses to climate change and variability in a southeastern U.S. estuary (1981–2003). J. Coast. Res. 2008(10055):95–110.

Bath Martin, G., and S. R. Thorrold.
2005. Temperature and salinity effects on magnesium, manganese, and barium incorporation in otoliths of larval and early juvenile spot *Leiostomus xanthurus*. Mar. Ecol. Prog. Ser. 293:223–232.

Bath Martin, G., S. R. Thorrold, and C. M. Jones.
2004. Temperature and salinity effects on strontium incorporation in otoliths of larval spot (*Leiostomus xanthurus*). Can. J. Fish. Aquat. Sci. 61:34–42.

Beckman, D. W., and J. M. Dean.
1984. The age and growth of young-of-the-year spot, *Leiostomus xanthurus* Lacépède, in South Carolina. Estuaries 7:487–496.

Bernal, M., Y. Stratoudakis, S. Coombs, M. M. Angelico, A. Lago de Lanzós, C. Porteiro, Y. Sagarminaga, M. Santos, A. Uriarte, E. Cunha, et al.
2007. Sardine spawning off the European Atlantic coast: characterization of and spatio-temporal variability in spawning habitat. Prog. Oceanogr. 74:210–227.

Blanton, B. O., A. Aretxabaleta, F. E. Werner, and H. E. Seim.
2003. Monthly climatology of the continental shelf waters of the South Atlantic Bight. J. Geophys. Res. 108(C8):3264.

Bourne, D. W., and J. J. Govoni.
1988. Distribution of fish eggs and larvae and patterns of water circulation in Narragansett Bay, 1972–1973. Am. Fish. Soc. Symp. 3:132–148.

Chant, R. J., M. C. Curran, K. W. Able, and S. M. Glenn.
2000. Delivery of winter flounder (*Pseudopleuronectes americanus*) larvae to settlement habitats in coves near inlets. Estuar. Coast. Shelf Sci. 51:529–541.

Checkley, D. M., Jr., P. B. Ortner, F. E. Werner, L. R. Settle, and S. R. Cummings.
1999. Spawning habitat of the Atlantic menhaden in Onslow Bay, North Carolina. Fish. Oceanogr. 8(s2):22–36.

Collins, M. R., and B. W. Stender.
1989. Larval striped mullet (*Mugil cephalus*) and white mullet (*Mugil curema*) off the southeastern United States. Bull. Mar. Sci. 45:580–589.

Craig, J. K., G. T. Kellison, S. M. Binion-Rock, S. D. Regan, M. Karnauskas, S.-K. Lee, R. He, D. M. Allen, N. M. Bacheler, H. Blondin, et al.
2021. Ecosystem status report for the U.S. South Atlantic region. NOAA Tech. Memo. NMFS-SEFSC-753, 145 p.

De Vries, M. C., R. B. Forward Jr., and W. F. Hettler.
1995. Behavioral response of larval Atlantic menhaden *Brevoortia tyrannus* (Latrobe) and spot *Leiostomus xanthurus* (Lacépède) to rates of salinity change. J. Exp. Mar. Biol. Ecol. 185:93–108.

Ejsymont, L., and K. Sherman.
2000. Poland and the United States' cooperation in fisheries ecology: a multidecadal retrospective. Bull. Sea Fish. Inst. Gdynia 3:3–10.

Enfield, D. B., A. M. Mestas-Nunez, and P. J. Trimble.
2001. The Atlantic Multidecadal Oscillation and its relationship to rainfall and river flows in the continental U.S. Geophys. Res. Lett. 28:2077–2080.

Fahay, M. P.
1975. An annotated list of larval and juvenile fishes captured with surface-towed meter net in the South Atlantic Bight during four RV *Dolphin* cruises between May 1967 and February 1968. NOAA Tech. Rep. NMFS SSRF-685, 37 p.

Flores-Coto, C., and S. M. Warlen.
1993. Spawning time, growth, and recruitment of larval spot *Leiostomus xanthurus* into a North Carolina estuary. Fish. Bull. 91:8–22.

Gangopadhyay, A., G. Gawarkiewicz, E. N. S. Silva, M. Monim, and J. Clark.
2019. An observed regime shift in the formation of warm core rings from the Gulf Stream. Sci. Rep. 9:12319.

Gangopadhyay, A., G. Gawarkiewicz, E. N. S. Silva, A. M. Silver, M. Monim, and J. Clark.
2020. A census of the warm-core rings of the Gulf Stream: 1980–2017. J. Geophys. Res., Oceans 125:e2019JC016033.

Gillanders, B. M., M. N. McMillan, P. Reis-Santos, L. J. Baumgartner, L. R. Brown, J. Conallin, F. V. Feyrer, S. Hernriques, N. C. James, A. J. Jaureguizar, et al.
2022. Climate change and fishes in estuaries. *In* Fish and fisheries in estuaries: a global perspective (A. K. Whitfield, K. W. Able, S. J. M. Blaber, and M. Elliott, eds.), p. 380–457. John Wiley and Sons, Chichster, UK.

Govoni, J. J., and L. J. Pietrafesa.
1994. Eulerian views of layered water currents, vertical distribution of some larval fishes, and inferred advective transport over the continental shelf off North Carolina, USA, in winter. Fish. Oceanogr. 3:120–132.

Govoni, J. J., and H. L. Spach.
1999. Exchange and flux of larval fishes across the western Gulf Stream front south of Cape Hatteras, USA, in winter. Fish. Oceanogr. 8(Suppl. 2):77–92.

Govoni, J. J., J. A. Hare, E. D. Davenport, M. H. Chen, and K. E. Marancik.
2010. Mesoscale, cyclonic eddies as larval fish habitat along the southeast United States shelf: a Lagrangian description of the zooplankton community. ICES J. Mar. Sci. 67:403–411.

Govoni, J. J., J. A. Hare, and E. D. Davenport.
2013. The distribution of larval fishes of the Charleston Gyre region off the southeastern United States in winter shaped by mesoscale, cyclonic eddies. Mar. Coast. Fish. 5:246–259.

Govoni, J. J., M. Terwilliger, and D. F. Markle.
2015. Age, growth, and long-distance dispersal in the western North Atlantic of vexillifer larvae of the pearlfish, *Echiodon dawsoni*, with notes on *Carapus bermudensis* (Ophidiiformes: Carapidae). Ichthyol. Res. 62:409–419.

Greve, W., S. Prinage, H. Zidowitz, J. Nast, and F. Reiners.
2005. On the phenology of North Sea ichthyoplankton. ICES J. Mar. Sci. 62:1216–1223.

Grothues, T. M., and R. K. Cowen.
1999. Larval fish assemblages and water mass history in a major faunal transition zone. Cont. Shelf Res. 19:1171–1198.

Grothues, T. M., R. K. Cowen, L. J. Pietrafesa, F. Bignami, G. L. Weatherly, and C. N. Flagg.
2002. Flux of larval fish around Cape Hatteras. Limnol. Oceanogr. 47:165–175.

Hale, E. A., and T. E. Targett.
2018. Vertical distribution of larval Atlantic menhaden (*Brevoortia tyrannus*) and Atlantic croaker (*Micropogonias undulatus*): implications for vertical migratory behaviour and transport. Fish. Oceanogr. 27:222–231.

Hare, J. A., and R. K. Cowen.
1996. Transport mechanisms of larval and pelagic juvenile bluefish (*Pomatomus saltatrix*) from South Atlantic Bight spawning grounds to Middle Atlantic Bight nursery habitats. Limnol. Oceanogr. 41:1264–1280.

Hare, J. A., and J. J. Govoni.
2005. Comparison of average larval fish vertical distributions among species exhibiting different transport pathways on the southeast United States continental shelf. Fish. Bull. 103:728–736.

Hare, J. A., and K. W. Able.
2007. Mechanistic links between climate and fisheries along the east coast of the United States: explaining population outbursts of Atlantic croaker (*Micropogonias undulatus*). Fish. Oceanogr. 16:31–45.

Hare, J. A., J. A. Quinlan, F. E. Werner, B. O. Blanton, J. J. Govoni, R. B. Forward, L. R. Settle, and D. E. Hoss.
1999. Larval transport during winter in the SABRE study area: results of a coupled vertical larval behaviour–three-dimensional circulation model. Fish. Oceanogr. 8(Suppl. 2):57–76.

Hare, J. A., M. P. Fahay, and R. K. Cowen.
2001. Springtime ichthyoplankton of the slope region off the north-eastern United States of America: larval assemblages, relation to hydrography and implications for larval transport. Fish. Oceanogr. 10:164–192.

Hare, J. A., J. H. Churchill, R. K. Cowen, T. J. Berger, P. C. Cornillon, P. Dragos, S. M. Glenn, J. J. Govoni, and T. N. Lee.
2002. Routes and rates of larval fish transport from the southeast to the northeast United States continental shelf. Limnol. Oceanogr. 47:1774–1789.

Hare, J. A., S. Thorrold, H. Walsh, C. Reiss, A. Valle-Levinson, and C. Jones.
2005. Biophysical mechanisms of larval fish ingress into Chesapeake Bay. Mar. Ecol. Prog. Ser. 303:295–310.

Herman, S. S.
1963. Planktonic fish eggs and larvae of Narragansett Bay. Limnol. Oceanogr. 8:103–109.

Hettler, W. F., and A. B. Powell.
1981. Egg and larval fish production at the NMFS Beaufort Laboratory, Beaufort, N.C., U.S.A. Rapp. P.-v. Reun. Cons. Int. Explor. Mer 178:501–503.

Hettler, W. F., Jr., and A. J. Chester.
1990. Temporal distribution of ichthyoplankton near Beaufort Inlet, North Carolina. Mar. Ecol. Prog. Ser. 68:157–168.

Hettler, W. F., Jr., and D. L. Barker.
1993. Distribution and abundance of larval fishes at two North Carolina inlets. Estuar. Coast. Shelf Sci. 37:161–179.

Hettler, W. F., Jr., and J. A. Hare.
1998. Abundance and size of larval fishes outside the entrance to Beaufort Inlet, North Carolina. Estuaries 21:476–499.

Hettler, W. F., Jr., D. S. Peters, D. R. Colby, and E. H. Laban.
1997. Daily variability in abundance of larval fishes inside Beaufort Inlet. Fish. Bull. 95:477–493.

Hildebrand, S. F., and W. C. Schroeder.
1928. The fishes of Chesapeake Bay. Fish. Bull. 43:1–388.

Hildebrand, S. F., and L. E. Cable.
1930. Development and life history of fourteen teleostean fishes at Beaufort, N.C. Fish. Bull. 46:383–488.

Hodson, R. G., J. O. Hackman, and C. R. Burnett.
1981. Food habits of young spots in nursery areas of the Cape Fear River estuary, North Carolina. Trans. Am. Fish. Soc. 110:495–501.

Hoey, J. A., F. J. Fodrie, Q. A. Walker, E. J. Hilton, G. T. Kellison, T. E. Targett, J. C. Taylor, K. W. Able, and M. L. Pinsky.
2020. Using multiple natural tags provides evidence for extensive larval dispersal across space and through time in summer flounder. Mol. Ecol. 29:1421–1435.

Hurrell, J. W., Y. Kushnir, G. Ottersen, and M. Visbeck (eds.).
2003. The North Atlantic Oscillation: climatic significance and environmental impact. Geophys. Monograph 134, 279 p. Am. Geophys. Union, Washington, DC.

Johnson, D. L., and W. W. Morse.
1994. Net extrusion of larval fish: correction factors for 0.333 mm versus 0.505 mm mesh bongo nets. NAFO Sci. Council Studies 20:85–92.

Jossi, J. W., and R. R. Marak.
1983. MARMAP plankton survey manual. NOAA Tech. Memo. NMFS-F/NEC-21, 153 p.

Joyeux, J.-C.
1999. The abundance of fish larvae in estuaries: within-tide variability at inlet and immigration. Estuaries 22:889–904.

Kennish, M. J. (ed.).
2003. Estuarine research, monitoring, and resource protection, 320 p. CRC Press, Boca Raton, FL.

Korsman, B. M., M. E. Kimball, and F. J. Hernandez Jr.
2017. Spatial and temporal variability in ichthyoplankton communities ingressing through two adjacent inlets along the southeastern U.S. Atlantic coast. Hydrobiologia 795:219–237.

Lewis, R. M, and M. H. Judy.
1983. The occurrence of spot, *Leiostomus xanthurus*, and Atlantic croaker, *Micropogonias undulatus*, larvae in Onslow Bay and Newport River estuary, North Carolina. Fish. Bull. 81:405–412.

Love, J. W., D. F. Luers, and B. D. Williams.
2009. Spatio-temporal patterns of larval fish ingress to Chincoteague Bay, Maryland, USA during winter and spring 2004 to 2007. Mar. Ecol. Prog. Ser. 377:203–212.

Marancik, K. E., L. M. Clough, and J. A. Hare.
2005. Cross-shelf and seasonal in variation larval fish assemblages on the southeast United States continental shelf off the coast of Georgia. Fish. Bull. 103:108–129.

Morley, J. W., R. D. Batt, and M. L. Pinsky.
2017. Marine assemblages respond rapidly to winter climate variability. Global Change Biol. 23:2590–2601.

Morson, J. M., T. Grothues, and K. W. Able.
2019. Change in larval fish assemblage in a USA east coast estuary estimated from twenty-six years of fixed weekly sampling. PLoS ONE 14(10):e0224157.

Norcross, B. L.
1991. Estuarine recruitment mechanisms of larval Atlantic croakers. Trans. Am. Fish. Soc. 120:673–683.

Norcross, B. L., and D. A. Bodolus.
1991. Hypothetical northern spawning limit and larval transport of spot. *In* Larval fish recruitment and research in the Americas: proceedings of the thirteenth annual fish conference; Mérida, 21–26 May 1989 (R. D. Hoyt, ed.), p. 77–88. NOAA Tech. Rep. NMFS 95.

Nye, J. A., J. S. Link, J. A. Hare, and W. J. Overholtz.
2009. Changing spatial distribution of fish stocks in relation to climate and population size on the Northeast United States continental shelf. Mar. Ecol. Prog. Ser. 393:111–129.

Olney, J. E., and G. W. Boehlert.
1988. Nearshore ichthyoplankton associated with seagrass beds in lower Chesapeake Bay. Mar. Ecol. Prog. Ser. 45:33–43.

Perry, A. L., P. J. Low, J. R. Ellis, and J. D. Reynolds.
2005. Climate change and distribution shifts in marine fishes. Science 308:1912–1915.

Pietrafesa, L. J., and G. S. Janowitz.
1988. Physical oceanographic processes affecting larval transport around and through North Carolina inlets. Am. Fish. Soc. Symp. 3:34–50.

Powell, A. B., and H. R. Gordy.
1980. Egg and larval development of the spot, *Leiostomus xanthurus* (Sciaenidae). Fish. Bull. 78:701–714.

Powell, A. B., and R. E. Robbins.
1994. Abundance and distribution of ichthyoplankton along an inshore-offshore transect in Onslow Bay, North Carolina. NOAA Tech. Rep. NMFS 120, 28 p.

Powell, A. B., D. G. Lindquist, and J. A. Hare.
2000. Larval and pelagic juvenile fishes collected with three types of gear in Gulf Stream and shelf waters in Onslow Bay, North Carolina, and comments on ichthyoplankton distribution and hydrography. Fish. Bull. 98:427–438.

Quattrini, A. M., D. G. Lindquist, F. M. Bingham, T. E. Lankford, and J. J. Govoni.
2005. Distribution of larval fishes among water masses in Onslow Bay, North Carolina: implications for cross-shelf exchange. Fish. Oceanogr. 14:413–431.

Reyier, E. A., and J. M. Shenker.
2007. Ichthyoplankton community structure in a shallow subtropical estuary of the Florida Atlantic coast. Bull. Mar. Sci. 80:267–293.

Ribeiro, F., E. Hale, E. J. Hilton, T. R. Clardy, A. L. Deary, T. E. Targett, and J. E. Olney.
2015. Composition and temporal patterns of larval fish communities in Chesapeake and Delaware Bays, USA. Mar. Ecol. Prog. Ser. 527:167–180.

Rogers, S. G., T. E. Targett, and S. B. Van Sant.
1984. Fish-nursery use in Georgia salt-marsh estuaries: the influence of springtime freshwater conditions. Trans. Am. Fish. Soc. 113:595–606.

Ross, S. W.
2003. The relative value of different estuarine nursery areas in North Carolina for transient juvenile fishes. Fish. Bull. 101:384–404.

Schieler, B. M., E. A. Hale, and T. E. Targett.
2014. Daily variation in ingress of fall-spawned larval fishes into Delaware Bay in relation to alongshore and along-estuary wind components. Estuar. Coast. Shelf Sci. 151:141–147.

Shearman, R. K., and S. J. Lentz.
2010. Long-term sea surface temperature variability along the U.S. East Coast. J. Phys. Oceanogr. 40:1004–1017.

Snyder, D. B., and G. H. Burgess.
2016. Marine fishes of Florida, 392 p. Johns Hopkins Univ. Press, Baltimore, MD.

Stegmann, P. M., and Y. A. Yoder.
1996. Variability of sea-surface temperature in the South Atlantic Bight as observed from satellite: implications for offshore-spawning fish. Cont. Shelf Res. 16:843–861.

Stegmann, P. M., J. A. Quinlan, F. E. Werner, B. O. Blanton, and P. Berrien.
1999. Atlantic menhaden recruitment to a southern estuary: defining potential spawning regions. Fish. Oceanogr. 8(Suppl. 2):111–123.

Summers, J. K., T. T. Polgar, J. A. Tarr, K. A. Rose, D. G. Heimbuch, J. McCurley, R. A. Cummins, G. F. Johnson, K. T. Yetman, and G. T. DiNardo.
1985. Reconstruction of long-term time series for commercial fisheries abundance and estuarine pollution loadings. Estuaries 8:114–124.

Teodósio, M. A., C. B. Paris, E. Wolanski, and P. Morais.
2016. Biophysical processes leading to the ingress of temperate fish larvae into estuarine nursery areas: a review. Estuar. Coast. Shelf Sci. 183:187–202.

Thaxton, W. C., J. C. Taylor, and R. G. Asch.
2020. Climate-associated trends and variability in ichthyoplankton phenology from the longest continuous larval fish time series on the east coast of the United States. Mar. Ecol. Prog. Ser. 650:269–287.

van der Lingen, C. D., L. Hutchings, D. Merkle, J. J. van der Westhuizen, and J. Nelson.
2001. Comparative spawning habitats of anchovy (*Engraulis capensis*) and sardine (*Sardinops sagax*) in the Southern Benguela upwelling ecosystem. *In* Spatial processes and management of marine populations. Alsk. Sea Grant Rep. AK-SG-01-02 (G. H. Kruse, N. Bez, A. Booth, M. W. Dorn, S. Hills, R. N. Lipcius, D. Pelletier, C. Roy, S. J. Smith, and D. Witherell, eds.), p. 185–209. Univ. Alsk. Sea Grant Coll. Program, Fairbanks, AK.

Walsh, H. J.
2007. Distribution of fall/winter-spawned larval fish in relation to hydrographic fronts on the North Carolina shelf: implications for larval transport mechanisms. M.S. thesis, 73 p. N.C. State Univ., Raleigh, NC. [Available from website.]

Walsh, H. J., D. E. Richardson, K. E. Marancik, and J. A. Hare.
2015. Long-term changes in the distributions of larval and adult fish in the Northeast U.S. shelf ecosystem. PLoS ONE 10(9):e0137382.

Warlen, S. M., and J. S. Burke.
1990. Immigration of larvae of fall/winter spawning marine fishes into a North Carolina estuary. Estuaries 13:453–461.

Warlen, S. M., and A. J. Chester.
1985. Age, growth, and distribution of larval spot, *Leiostomus xanthurus*, off North Carolina. Fish. Bull. 83:587–599.

Warlen, S. M., K. W. Able, and E. H. Laban.
2002. Recruitment of larval Atlantic menhaden (*Brevoortia tyrannus*) to North Carolina and New Jersey estuaries: evidence for larval transport northward along the east coast of the United States. Fish. Bull. 100:609–623.

Werner, F. E., B. O. Blanton, J. A. Quinlan, and R. A. Luettich Jr.
1999. Physical oceanography of the North Carolina continental shelf during the fall and winter seasons: implications for the transport of larval menhaden. Fish. Oceanogr. 8(Suppl. 2):7–21.

Whitfield, A. K., I. C. Potter, F. J. Neira, and E. D. Houde.
2023a. Modes of ingress by larvae and juveniles of marine fishes into estuaries: from microtidal to macrotidal systems. Fish Fish. 24:488–503.

Whitfield, A. K., B. M. Gillanders, and K. W. Able.
2023b. Climate change effects on fish populations. *In* Climate change and estuaries (M. J. Kennish, H. W. Paerl, and J. R. Crosswell, eds.), p. 475–506. CRC Press, Boca Raton, FL.

National Marine
Fisheries Service
NOAA

Fishery Bulletin
established in 1881

Spencer F. Baird
First U.S. Commissioner
of Fisheries and founder
of *Fishery Bulletin*

Descriptions of post-settlement juveniles of 3 greeneye species, *Chlorophthalmus nigromarginatus*, *C. acutifrons*, and *C. albatrossis* (Teleostei: Chlorophthalmidae), from Japan, with notes on their rapid metamorphosis after settlement

Katsuya Kimura (contact author)[1,3]
Ryo Misawa[2]
Fumihito Tashiro[3]

Email address for contact author: kmrkty1973@gmail.com

[1] Faculty of Fisheries Sciences
Hokkaido University
3-1-1 Minato-cho
Hakodate, Hokkaido 041-8611, Japan

[2] Demersal Fish Resources Division
Fisheries Stock Assessment Center
Fisheries Resources Institute
Japan Fisheries Research and Education Agency
25-259 Shimomekurakubo
Same, Hachinohe, Aomori 031-0841, Japan

[3] Fisheries Science Center
The Hokkaido University Museum
3-1-1 Minato-cho
Hakodate, Hokkaido 041-8611, Japan

Abstract—Post-settlement juveniles of 3 greeneye species in the family Chlorophthalmidae, the blackedge greeneye (*Chlorophthalmus nigromarginatus*), humpback greeneye (*C. acutifrons*), and bigeyed greeneye (*C. albatrossis*), are described for the first time on the basis of 5, 2, and 9 specimens, respectively, collected from northern Japan. These identifications were well supported by an analysis of mitochondrial cytochrome *c* oxidase subunit I gene sequences of juveniles and adults of the 3 species and congeners. Among the 3 species, post-settlement juveniles of *C. albatrossis* are readily distinguishable by the following characters: inner pelvic-fin rays heavily pigmented (versus lightly pigmented or unpigmented), grayish blotches on body variegated and form a transverse band from the posterior end of the dorsal-fin base to the pelvic-fin origin (versus round or elliptical, not forming transverse bands), and 13–14 upper and 12–13 lower procurrent caudal-fin rays (versus 10–12 and 9–10). Although post-settlement juveniles of *C. nigromarginatus* and *C. acutifrons* are superficially very similar to each other, they are separable by the shape of grayish blotches and several proportional and meristic characters. On the basis of examination of post-settlement specimens, juveniles of the genus *Chlorophthalmus* appear to undergo a very rapid metamorphosis after settlement on the seafloor when they change from pelagic to benthic lifestyles.

Manuscript submitted 6 March 2024.
Manuscript accepted 21 August 2024.
Fish. Bull. 122:186–202 (2024).
Online publication date: 13 September 2024.
doi: 10.7755/FB.122.4.4

The views and opinions expressed or implied in this article are those of the author (or authors) and do not necessarily reflect the position of the National Marine Fisheries Service, NOAA.

Greeneye species of the genus *Chlorophthalmus* Bonaparte, 1840, are demersal fish species distributed on the continental shelf and upper slope in tropical to temperate waters of all major oceans (Fricke and Durville, 2020). This group currently comprises 20 valid species (Fricke and Durville, 2020; Prokofiev, 2020) and several others that remain undescribed (Gomon et al., 2014). Although some species of this genus are rare and known from only a few type specimens (e.g., Fujiwara et al., 2019; Fricke and Durville, 2020), substantial amounts of other species are caught by bottom trawling and are important fishery resources (e.g., Honda et al., 2001; Yoshida, 2003; D'Onghia et al., 2006; Bineesh et al., 2014). Especially in Japan, the bigeyed greeneye (*Chlorophthalmus albatrossis* Jordan and Starks, 1904) (Teleostei: Chlorophthalmidae) is important as a food fish caught in offshore bottom-trawl fisheries, and it recently has been designated as a target species for stock assessment in Japan (Hirakawa et al., 2007; Inoue and Horie, 2024). Chlorophthalmids, as well as other members of the suborder Alepisauroidei, are known to be simultaneous hermaphrodites (Davis and Fielitz, 2010), and the intricate reproductive biology of the shortnose greeneye (*Chlorophthalmus agassizi* Bonaparte, 1840) has been well investigated (e.g., D'Onghia et al., 2006; Parenti et al., 2015).

In contrast to the rich diversity of species and their large biomass, knowledge of the morphology of larvae and juveniles of members of *Chlorophthalmus* is scarce (Okiyama, 1984). To date, a complete developmental series from larvae to juveniles has been well documented only for *C. agassizi*, with descriptions based on specimens from

the Mediterranean Sea and Atlantic Ocean (Sanzo, 1915; Tåning, 1918; Ditty, 2006). Only brief morphological descriptions of a species common in the western Pacific Ocean, *C. albatrossis*, from larvae to juveniles, were reported by Saruwatari et al. (2005) and Saruwatari (2008). Other fragmentary accounts of the morphology of early life stages of this genus have been limited to larvae of the Brazilian greeneye (*Chlorophthalmus brasiliensis* Mead, 1958), robust greeneye (*Chlorophthalmus mento* Garman, 1899), blackedge greeneye (*Chlorophthalmus nigromarginatus* Kamohara, 1953), and Hawaiian greeneye (*Chlorophthalmus proridens* Gilbert and Cramer, 1897) and unidentified species (Ahlstrom, 1971; Pertseva-Ostroumova and Rass, 1973; Miller et al., 1979; Okiyama, 1984, 1988; Chiu, 1999; Ditty, 2006; Okiyama, 2014).

Except for in the work by Saruwatari et al. (2005) and Saruwatari (2008), who identified larvae and juveniles using molecular techniques, the basis for species identification has been ambiguous because morphological characters adequate for distinguishing the species of *Chlorophthalmus* from congeners have not been provided from previous studies. Furthermore, because most previously reported larvae and juveniles were collected from pelagic waters with mid-water trawl nets or plankton nets, little is known about post-settlement juveniles. Settlement is an important event in the early life stages of demersal fishes. Fish of these species change lifestyles from pelagic to demersal during settlement, and metamorphosis occurs at or around the time of this shift, bringing changes to their morphology and pigmentation (McCormick et al., 2002). It is crucial, therefore, for exploration of the early life history and recruitment of greeneye species to accumulate fundamental information about post-settlement juvenile morphology and to enable accurate species identification.

Recently, 16 post-settlement juvenile specimens of *Chlorophthalmus* were collected during bottom-trawl surveys conducted off the Pacific coast of Tohoku District in northern Japan. Morphological examinations and an analysis of mitochondrial cytochrome *c* oxidase subunit I (COI) gene sequences revealed that these juveniles represent 3 species, *C. nigromarginatus*, the humpback greeneye (*Chlorophthalmus acutifrons* Hiyama, 1940), and *C. albatrossis*. Herein, we provide the first detailed morphological descriptions of post-settlement juveniles of these 3 species. In addition, we discuss the rapid metamorphosis after settlement of these species inferred from the specimens.

Materials and methods

All post-settlement juveniles described in this study were collected during bottom-trawl surveys conducted off the Pacific coast of Tohoku District, in northern Japan, from late September through late November of 2022 and 2023 (for details on sampling stations, see Misawa et al., 2020). Bottom otter trawl nets were deployed from the R/V *Wakataka-maru* belonging to the Japan Fisheries Research and Education Agency. Developmental stages of the specimens were defined as follows: early metamorphosing, individuals with grayish blotches on body weakly developed but indistinct; late metamorphosing, individuals with grayish blotches moderately developed; and metamorphosed, individuals with grayish blotches well developed. Methods for counts and measurements followed Fujiwara et al. (2019). Pectoral-fin rays were counted on both sides. Gill rakers were counted on the right side of the first arch. A full morphological description is provided only for *C. nigromarginatus*, for which specimens of various developmental stages were obtained and little information about its early life stages exists; characters shared by the 3 species are omitted from descriptions of *C. albatrossis* and *C. acutifrons*. Standard length is abbreviated as SL. Measurements were made to the nearest 0.1 mm with a digital caliper. Stereomicroscopes with a camera lucida were used for making line drawings of the specimens. Institutional codes follow Sabaj (2020).

The following adult specimens (maturation not investigated) were used as comparative material for morphological examinations: *Chlorophthalmus acutifrons*: HUMZ 39774, 140 mm SL, Mimase fish market, Kochi, Japan, 29 February 1974; HUMZ 48685, 170 mm SL, Mimase fish market, Kochi, Japan, 6 October 1972; HUMZ 146581, 146597, 146609, 129–138 mm SL, Okinawa Trough, 2 August 1994; HUMZ 177868, 176 mm SL, Mimase fish market, Kochi, Japan, 15 January 2001; HUMZ 191229, 148 mm SL, off Java, Indonesia, 6 September 2004; HUMZ 193614–193616, 108–127 mm SL, off Java, Indonesia, 4 May 2005; HUMZ 193999, 139 mm SL, off Java, Indonesia, 11 May 2005; HUMZ 201365, 117 mm SL, Mimase fish market, Kochi, Japan, 11 February 2008; HUMZ 208026, 178 mm SL, off Katsurahama, Kochi, Japan, 1 March 2010. *Chlorophthalmus albatrossis*: HUMZ 207252, 207255, 101–142 mm SL, Numazu fish market, Shizuoka, Japan, 12 February 2010. *Chlorophthalmus nigromarginatus*: FAKU 148097, 114 mm SL, off Omaezaki, Shizuoka, Japan, 27 November 2020; HUMZ 39044, 39056, 39060, 39076, 39759, 119–184 mm SL, Mimase fish market, Kochi, Japan, 2 March 1974; HUMZ 48298, 48489, 48497, 128–180 mm SL, Mimase fish market, Kochi, Japan, 29 March 1974; HUMZ 48517, 127 mm SL, Mimase fish market, Kochi, Japan, 26 March 1974; HUMZ 148174, 100 mm SL, Okinawa Trough, 2 August 1994; HUMZ 177760, 124 mm SL, Saga fishing port, Kochi, Japan, 22 January 2001; HUMZ 199981, 213 mm SL, East China Sea, 4 June 2007. *Chlorophthalmus vityazi* Kobyliansky, 2013: HUMZ 190747, 195 mm SL, off Sumatra, Indonesia, 3 October 2004. *Chlorophthalmus* sp.: HUMZ 190745, 67 mm SL, off Sumatra, Indonesia, 3 October 2004.

Specimens from Indonesia were collected during 2004 and 2005 in the Japan–Indonesia Deep Sea Fisheries Resources Joint Exploration Project conducted by the Overseas Fishery Cooperation Foundation of Japan and the Agency for Marine and Fisheries Research, Indonesia Ministry of Marine Affairs and Fisheries.

In addition to the 16 post-settlement juvenile specimens described herein, 6 adult specimens (maturation

not investigated) from 5 species of *Chlorophthalmus* and 1 specimen of *Paraulopus filamentosus* Okamura, 1982, were used for DNA barcoding (Table 1). Total DNA was extracted from an eye or muscle tissue stored in 99% ethanol by using a Wizard Genomic DNA Purification Kit[1] (Promega Corp., Madison, WI). The partial COI gene sequence was amplified by using polymerase chain reaction (PCR) with the primers Fish F1 (5′TCAACCAACCACAAAGACATTGGCAC-3′) and Fish R1 (5′-TAGACTTCTGGGTGGCCAAAGAATCA3′) (Ward et al., 2005). Amplification through PCR was done with a single reaction volume of 10 µL containing 1.0 µL of a template DNA solution, 5.0 µL of KAPA2G Robust HotStart ReadyMix with dye (Roche CustomBiotech, Penzberg, Germany), 1.0 µL of forward and reverse primers (5 µM), and 2.0 µL of dissolved water. The following protocol was performed for PCR: predenaturation at 94°C for 5 min, 30 cycles of denaturation at 94°C for 15 s, annealing at 54°C for 15 s, extension at 72°C for 30 s, and final extension at 72°C for 7 min. The PCR products were purified by using Applied Biosystems ExoSAP-IT Express reagent (Thermo Fisher Scientific, Waltham, MA) and sequenced by the DNA sequencing service Eurofins Genomics (Tokyo, Japan) with primers used in PCR.

All sequences in this study were deposited in the DNA Data Bank of Japan, which is part of the International Nucleotide Sequence Database Collaboration, under accession numbers LC799382–LC799404. Sequences

[1] Mention of trade names or commercial companies is for identification purposes only and does not imply endorsement by the National Marine Fisheries Service, NOAA.

Table 1

Details about the specimens of *Chlorophthalmus* and *Paraulopus* for which gene sequences were analyzed in this study. Juveniles were collected during bottom-trawl surveys from late September through late November in 2022 and 2023 in northern Japan. Adults used as comparative material were collected from Japan and Emperor Seamounts during 2016–2022 or from waters of Indonesia in 2004. Asterisks (*) indicate sequences previously published in databases of the International Nucleotide Sequence Database Collaboration (INSDC).

Species	INSDC accession no.	Voucher specimen	Stage	Locality
Chlorophthalmus nigromarginatus	LC799382	HUMZ 233382	Juvenile	Off Ibaraki Prefecture, Japan
	LC799383	HUMZ 234649	Juvenile	Off Miyagi Prefecture, Japan
	LC799384	HUMZ 234783	Juvenile	Off Ibaraki Prefecture, Japan
	LC799385	HUMZ 234792	Juvenile	Off Fukushima Prefecture, Japan
	LC799386	HUMZ 234796	Juvenile	Off Miyagi Prefecture, Japan
	LC799387	FAKU 148097	Adult	Off Omaezaki, Japan
	LC799388	FAKU 149265	Adult	Sea of Japan off Yamaguchi Prefecture, Japan
	KF714739*	NMV A 29713-007	Unknown	Western Australia
	KJ190053*	FMNH 120838	Unknown	Yilan County, Taiwan
Chlorophthalmus acutifrons	LC799389	HUMZ 234650	Juvenile	Off Miyagi Prefecture, Japan
	LC799390	HUMZ 234793	Juvenile	Off Fukushima Prefecture, Japan
	LC799391	FAKU 147423	Adult	Off Fukushima Prefecture, Japan
	KF714716*	NMV A 29672-020	Unknown	Western Australia
Chlorophthalmus albatrossis	LC799392	HUMZ 234534	Juvenile	Off Iwate Prefecture, Japan
	LC799393	HUMZ 234780	Juvenile	Off Fukushima Prefecture, Japan
	LC799394	HUMZ 234787	Juvenile	Off Fukushima Prefecture, Japan
	LC799395	HUMZ 234788	Juvenile	Off Fukushima Prefecture, Japan
	LC799396	HUMZ 234789	Juvenile	Off Fukushima Prefecture, Japan
	LC799397	HUMZ 234803	Juvenile	Off Fukushima Prefecture, Japan
	LC799398	HUMZ 234804	Juvenile	Off Fukushima Prefecture, Japan
	LC799399	HUMZ 234805	Juvenile	Off Fukushima Prefecture, Japan
	LC799400	HUMZ 234806	Juvenile	Off Fukushima Prefecture, Japan
	LC799401	FAKU 148899	Adult	Off Iwate Prefecture, Japan
	KF714717*	NMV A 26661-003	Unknown	Taiwan
Chlorophthalmus borealis	KF714735*	NSMT-P 66506	Adult	Off Ibaraki Prefecture, Japan
Chlorophthalmus pectoralis	KF714741*	AMS I.36455-016	Unknown	Philippines
Chlorophthalmus vityazi	LC799402	HUMZ 190747	Adult	Off Sumatra, Indonesia
Chlorophthalmus sp. 2 sensu Okamura (1984c)	LC799403	FAKU 141991	Adult	Off Nii-jima Island, Japan
Paraulopus filamentosus	LC799404	FAKU 146791	Adult	Emperor Seamounts

determined in this study and those previously published in databases of the International Nucleotide Sequence Database Collaboration (Table 1) were aligned by using the program Clustal W, vers. 2.1 (Thompson et al., 1994). *Paraulopus filamentosus* was used as an outgroup of the phylogenetic analysis because the family Paraulopidae has been placed more basally in Aulopiformes than Chlorophthalmidae (e.g., Davis, 2010). The phylogenetic tree was constructed by using the neighbor-joining method as implemented in MEGA11 (vers. 11.0.13; Tamura et al., 2021), with the Kimura 2-parameter model (Kimura, 1980) being selected to calculate genetic distances. The robustness of each node was tested by using the bootstrap method with 1000 replications.

Results

DNA barcoding

On the basis of the phylogenetic analysis of COI gene sequences (Fig. 1), we placed the juvenile specimens in 3 clades, in which sequences of *C. nigromarginatus*, *C. acutifrons*, or C. *albatrossis* and *C. borealis* Kuronuma and Yamaguchi, 1941, are included. Within the 3 clades, distances calculated with the Kimura 2-parameter model were 0.00–1.02%, 0.00–0.51%, and 0.00–0.67%, values that are lower than or within intraspecific genetic distances of the genus (0.10–1.56%) reported by Gomon et al. (2014). Although *C. borealis* was recently treated as a

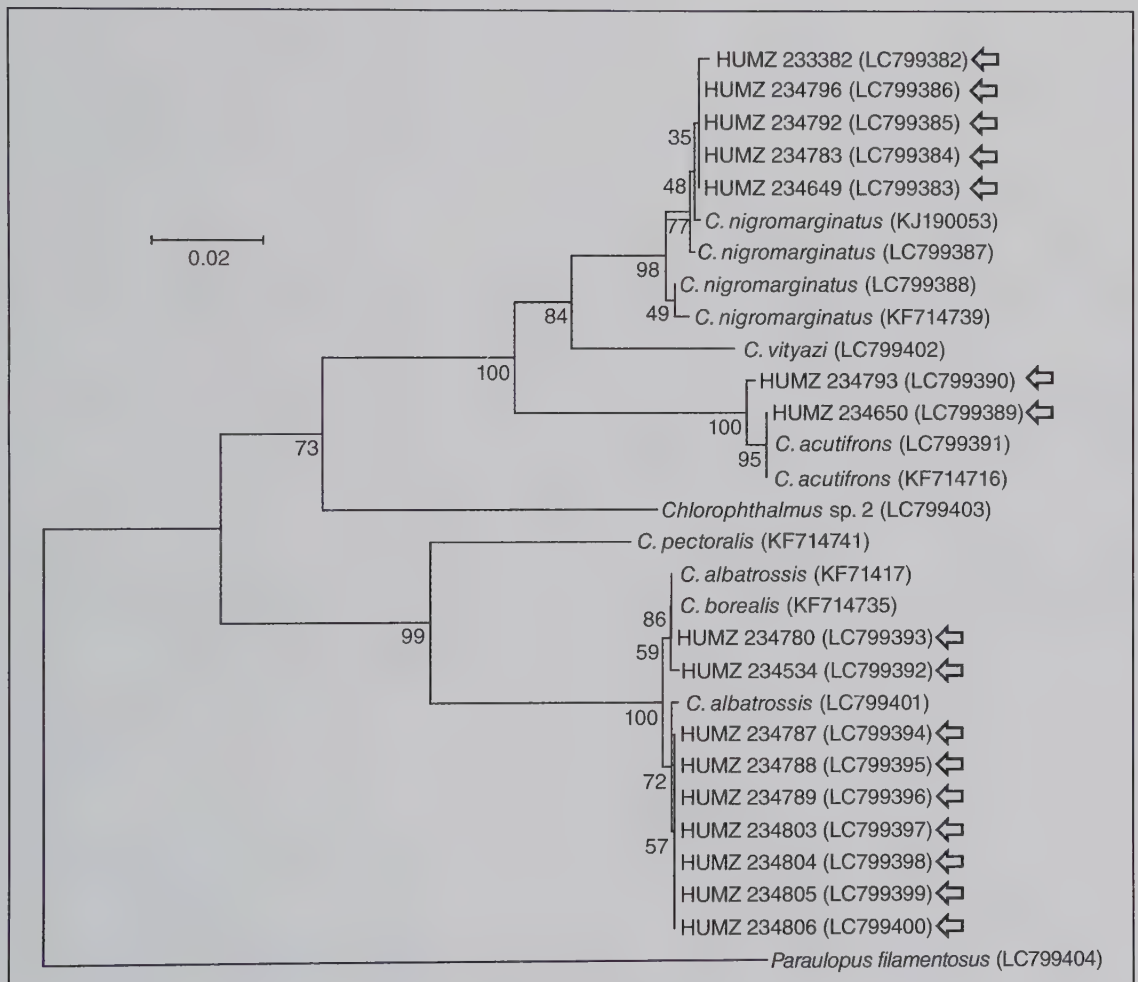

Figure 1

Neighbor-joining tree based on mitochondrial cytochrome *c* oxidase subunit I gene sequences of specimens of species of *Chlorophthalmus*, with *Paraulopus filamentosus* as an outgroup. Juvenile specimens were collected during bottom-trawl surveys from late September through late November in 2022 and 2023. Adults used as comparative material were collected from waters of Japan and Emperor Seamounts during 2016–2022 or from waters of Indonesia in 2004. International Nucleotide Sequence Database Collaboration accession numbers are provided in parentheses. Arrows indicate sequences of the post-settlement juveniles of *Chlorophthalmus* reported in this study. Numbers below branches indicate bootstrap values from testing with 1000 replications.

valid species in many studies (e.g., Nakabo and Kai, 2013; Gomon et al., 2014; Fricke and Durville, 2020), its possible synonymy under *C. albatrossis* has long been pointed out because of its morphological similarity with that species (e.g., Okamura, 1984a; Nakabo and Kai, 2013; Prokofiev, 2020). Results of molecular studies also indicate that these 2 species are not distinguishable on the basis of 16S rRNA (Saruwatari et al., 2005; Saruwatari, 2008) and COI gene sequences (Gomon et al., 2014; this study). Although the validity of *C. borealis* should be carefully assessed through a further taxonomic study with adequate materials, we identified all 9 juveniles included in the third clade, the one for *C. albatrossis* and *C. borealis*, as the former species because the juveniles were not separable morphologically. Consequently, in this study, 5 post-settlement juveniles were identified as *C. nigromarginatus*, 2 specimens were identified as *C. acutifrons*, and 9 specimens were identified as *C. albatrossis*.

The COI gene sequence of *C. vityazi* determined in this study (accession number: LC799402; voucher specimen: HUMZ 190747) differed from the previously registered sequence of the same specimen (accession number: KF714725) and completely matched the registered sequence of another specimen (accession number: KF714718; voucher specimen: HUMZ 190745); these specimens were identified by Gomon et al. (2014) as "*C. alb-like* IO" and *C. vityazi*, respectively. On the basis of examinations of voucher specimens of these sequences and a personal communication with the author (Gomon[2]), it is likely that the catalog numbers of vouchers (HUMZ 190745 and HUMZ 190747) of the 2 previously published sequences were mistakenly swapped.

Descriptions of post-settlement juveniles

Chlorophthalmus nigromarginatus Kamohara, 1953
Blackedge greeneye
Standard Japanese name: Tsumaguro-aome-eso
Figures 2A and 3, Tables 2 and 3

Materials examined

Early metamorphosing: HUMZ 233382, 38.3 mm SL, off Hitachi, Ibaraki Prefecture, 36°31′19″N, 140°58′8″E–36°29′49″N, 140°56′58″E, 154 m depth, bottom temperature 13.2°C, station (stn.) H150, 28 October 2022; HUMZ 234796, 38.8 mm SL, off Minamisanriku, Miyagi Prefecture, 38°39′8″N, 142°0′53″E–38°39′24″N, 142°0′57″E, 344–346 m depth, bottom temperature 5.0°C, stn. DE350, 16 November 2023.

[2] Gomon, M. F. 2023. Personal commun. Museums Victoria, GPO Box 666, Melbourne, Victoria 3001, Australia.

Figure 2

Line drawings of preserved specimens of post-settlement juveniles caught off the Pacific coast of northern Japan: (**A**) blackedge greeneye (*Chlorophthalmus nigromarginatus*), HUMZ 233382, 38.3 mm in standard length (SL), off Hitachi, Ibaraki Prefecture, 28 October 2022, and (**B**) bigeyed greeneye (*C. albatrossis*), HUMZ 234803, 41.2 mm SL, off Soma, Fukushima Prefecture, 15 November 2023, mirror image of right side. The scale bar in each panel indicates a length of 5 mm.

Table 2

Measurements and counts of post-settlement juveniles of blackedge greeneye (*Chlorophthalmus nigromarginatus*), humpback greeneye (*C. acutifrons*), and bigeyed greeneye (*C. albatrossis*) caught off the Pacific coast of northern Japan from late September through late November in 2022 and 2023. Measurements are given in percentage of standard length (SL). All specimens of each species were examined for each measurement, unless the number of specimens examined is given in parentheses after a measurement range for a species. Asterisks (*) indicate that values are approximate because of the badly damaged condition of a single specimen (HUMZ 234650). *n*=number of specimens.

Characteristic	*C. nigromarginatus* *n*=5	*C. acutifrons* *n*=2	*C. albatrossis* *n*=9
SL (mm)	38.3–44.3	42.8*–43.9	41.2–49.5
Measurements (% SL)			
Head length	28.2–30.7	28.2–31.3*	27.4–31.1
Head depth	13.5–15.2 (4)	13.9–14.7*	14.3–16.0
Post-orbital length	11.7–12.6	11.6–12.9*	10.6–12.2
Body depth at dorsal-fin origin	13.5–19.6	13.1*–16.4	14.0–18.6
Body depth at anal-fin origin	10.5–13.1	9.3*–10.9	9.6–11.8
Body width	12.4–13.2	11.2–11.7*	11.7–13.4
Snout length	8.1–9.4	8.2–9.1*	7.3–8.7
Upper-jaw length	9.7–11.3	10.5–12.6*	10.0–12.9
Maxillary depth	2.3–2.6	2.3–2.6*	2.0–2.9
Horizontal orbit diameter	8.4–9.6	8.2–10.0*	9.2–11.3
Vertical orbit diameter	7.7–8.2	7.3–9.3*	7.7–9.8 (8)
Horizontal pupil diameter	3.4–4.2	3.2–4.4*	3.3–5.1
Anterior interorbital width	9.3–10.1	8.7–9.3*	9.5–11.1
Posterior interorbital width	12.4–13.8	11.6–12.9*	13.3–14.6
Least interorbital width	4.0–7.6	3.3*–5.5	3.1–8.3 (8)
Caudal-peduncle length	17.0–19.1	17.3*–19.8	16.0–19.5
Caudal-peduncle depth	7.7–8.5 (4)	7.5*–8.0	6.8–7.9
Anus-to-anal-fin-origin length	26.4–29.1	27.3–27.8*	26.0–29.0
Pre-adipose-fin length	77.3–79.8	77.4–81.1*	75.0–78.3
Dorsal-to-adipose-fin length	40.5–44.2	43.3–45.3*	37.1–42.5
Pre-dorsal-fin length	36.3–39.2	34.6–37.9*	36.7–38.8
Dorsal-caudal length	63.4–65.9	63.8*–66.1	63.1–66.3
Dorsal-fin base length	11.9–13.6	11.9*–12.1	11.5–13.4
Longest dorsal-fin ray length	17.5–19.3 (3)	17.8–20.8*	17.2–20.9 (7)
Pre-anal-fin length	74.4–75.4	74.0–75.9*	74.7–77.3
Anal-caudal length	24.2–26.7	25.7*–27.1	24.5–27.3
Anal-fin base length	7.5–7.9	8.4–8.9*	7.5–9.0
Longest anal-fin ray length	9.5–11.1 (4)	9.8–11.4*	12.0–14.2
Pre-pectoral-fin length	27.5–30.0	27.6–30.1*	27.4–30.9
Pectoral-fin length	18.0–21.9 (4)	19.8 (1)	21.1–26.4
Pre-pelvic-fin length	37.4–39.2	37.8–39.3*	38.4–41.8
Pelvic-fin length	17.0–18.8	17.3 (1)	18.7–22.2 (6)
Pelvic-fin base length	3.6–4.2	3.7*–3.9	3.5–4.2
Pectoral-to-pelvic-fin length	11.9–13.5	11.0*–11.8	12.6–14.1
Pelvic-to-anal-fin length	34.5–38.9	36.7*–36.9	35.0–38.4
Counts			
Dorsal-fin rays	11	11	10–11
Anal-fin rays	9	9	8–10
Pectoral-fin rays	14–16	15–16	15–16
Pelvic-fin rays	9	9	9
Principal caudal-fin rays	19	19	19
Upper caudal procurrent rays	10–11 (4)	10–12	13–14
Lower caudal procurrent rays	9–10 (4)	9–10	12–13
Gill rakers	3 + 16–17 =19–20	2–3 + 15–16 =17–19	2–3 + 16–18 =18–21

Table 3

Frequency distributions for the number of pectoral-fin rays and gill rakers on juvenile and adult specimens of blackedge greeneye (*Chlorophthalmus nigromarginatus*) and humpback greeneye (*C. acutifrons*) examined in this study. Juveniles were collected during bottom-trawl surveys off the Pacific coast of northern Japan from late September through late November in 2022 and 2023. Adults were collected from waters of Kochi and Shizuoka, Japan, or the Okinawa Trough during 1972–2020 or from waters of Indonesia in 2005. *n*=number of specimens.

		Pectoral-fin rays				Upper gill rakers			Lower gill rakers						Total gill rakers					
Species	*n*	14	15	16	17	2	3	4	14	15	16	17	18	19	17	18	19	20	21	22
C. nigromarginatus	18	1	29	5	1	1	12	5	0	0	4	8	5	1	0	1	3	5	6	3
C. acutifrons	15	0	6	24	0	1	14	0	2	6	7	0	0	0	3	5	7	0	0	0

Late metamorphosing: HUMZ 234792, 44.3 mm SL, off Tomioka, Fukushima Prefecture, 37°21′7″N, 141°37′30″E–37°22′17″N, 141°37′18″E, 250–255 m depth, bottom temperature 7.2°C, stn. FG250, 20 November 2023.

Metamorphosed: HUMZ 234649, 43.0 mm SL, off Soma, Fukushima Prefecture, 37°35′43″N, 141°35′33″E–37°37′34″N, 141°35′58″E, 210–213 m depth, bottom temperature 8.3°C, stn. F210, 23 October 2023; HUMZ 234783, 42.5 mm SL, off Hitachi, Ibaraki Prefecture, 36°30′55″N, 140°58′55″E–36°29′36″N, 140°58′3.6″E, 210–213 m depth, bottom temperature 13.1°C, stn. H210, 11 November 2023.

Description

Proportional measurements and counts presented in Table 2. Body slender and cylindrical (Figs. 2A and 3); depth largest between pectoral-fin base and dorsal-fin origin. Tip of snout pointed. Anterior and posterior nostrils located near midway between snout tip and anterior margin of orbit. Eye large; horizontal orbit diameter almost equal to or slightly greater than snout length. Aphakic space on anterior portion of pupil weakly developed in metamorphosed specimens.

Mouth subterminal; tip of lower jaw slightly protruding anteriorly. Posterior margin of maxilla reaching beyond vertical through anterior margin of orbit and not reaching vertical through anterior margin of pupil. In early metamorphosing specimen (HUMZ 234796), several small, conical teeth on premaxilla (damaged on right side), and slender, curved, conical teeth in single row on dentary, with 1 tooth on anterior portion of dentary; in another early metamorphosing specimen (HUMZ 233382) and in late metamorphosing specimens, jaws edentate or with several small, conical teeth; in metamorphosed specimens, premaxilla almost edentate with several small, conical teeth, and dentary with small, conical teeth arranged in single row. Vomer with 1 tooth on each side of anterolateral margin, except for metamorphosed specimen (HUMZ 234649) with 2–3 teeth on each side. Palatine edentate or with 1 conical tooth on anterior portion, except for metamorphosed specimen (HUMZ 234649) with several conical teeth arranged in single row. Basihyal with 3 large, posteriorly curved, fang-like teeth on each side of anterior margin in early metamorphosing specimen (HUMZ 234796); 2 fang-like teeth on right side in other early metamorphosing specimen (HUMZ 233382), 1 fang-like tooth on left side in late metamorphosing specimen, and 1 small, conical tooth on each side (HUMZ 234783) or left side (HUMZ 234649) of anterior portion of basihyal in metamorphosed specimens.

Posterior and lower margins of opercular bones smooth. Gill rakers moderately developed. Pseudobranch present. Anus located slightly posterior to pelvic-fin base. Perianal light organ present. Scales on body developed but mostly lost; few scales remaining around anus and pectoral-fin base. Dorsal fin on anterior half of body; its origin slightly anterior to vertical through pelvic-fin origin; 3rd ray longest; 1st and 2nd rays unbranched, other rays branched. Anal fin on posterior half of body; 3rd or 4th ray longest; anterior 3 or 4 rays unbranched, other rays branched. Adipose fin small; its origin above base of 3rd, 4th, 5th, or 6th anal-fin ray. Pectoral fin long; its tip hardly reaching or reaching slightly beyond vertical through posterior end of dorsal-fin base. Pelvic fin long and pointed; its origin below base of 2nd or 3rd dorsal-fin ray. Caudal fin deeply forked.

Coloration

When fresh (Fig. 3), head and body white; posterior part of head to pectoral-fin base with orange tinge. In metamorphosed specimens, silver coloration appears on opercular region, belly, and mid-lateral portion of trunk (Fig. 3, D and E). Sparse pigment on lachrymal, anterior portion of lower jaw and on occipital region in early metamorphosing specimen, becoming more concentrated with growth in late metamorphosing and metamorphosed specimens. Pigment on opercular region and dorsal surface of head appears in late metamorphosing specimen and becomes more concentrated in metamorphosed specimens. Black dots arranged in slanting rows on almost entire body except lateral line. Grayish blotches composed of fine melanophores weakly developed on dorsal and lateral surfaces of body in early

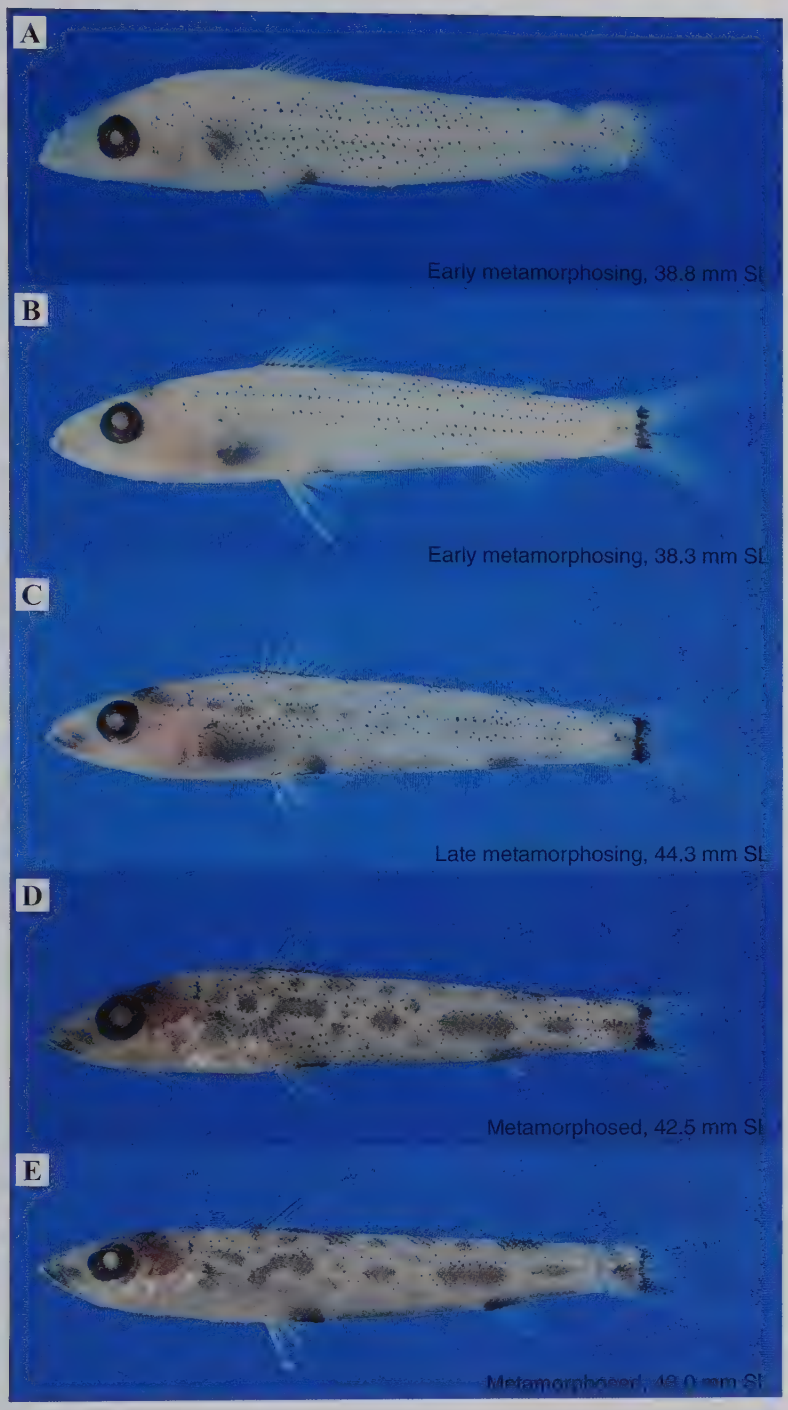

Figure 3

Fresh specimens of post-settlement juvenile blackedge greeneye (*Chlorophthalmus nigromarginatus*) from northern Japan: (**A**) HUMZ 234796, 38.8 mm in standard length (SL), off Minamisanriku, Miyagi Prefecture, 16 November 2023; (**B**) HUMZ 233382, 38.3 mm SL, off Hitachi, Ibaraki Prefecture, 28 October 2022; (**C**) HUMZ 234792, 44.3 mm SL, off Tomioka, Fukushima Prefecture, 20 November 2023; (**D**) HUMZ 234783, 42.5 mm SL, off Hitachi, Ibaraki Prefecture, 11 November 2023, mirror image of right side; and (**E**) HUMZ 234649, 43.0 mm SL, off Soma, Fukushima Prefecture, 23 October 2023. The developmental stage of each specimen—early metamorphosing, late metamorphosing, or metamorphosed—is provided.

metamorphosing specimens (Fig. 3, A and B), more distinct in late metamorphosing specimens (Fig. 3C), and well developed in fully metamorphosed specimens (Fig. 3, D and E); shape of blotches mostly round or elliptical, without transverse bands; single large blotch below middle of dorsal-fin base oblong and merged with anteroventral blotch.

Single peritoneal pigment section near pectoral-fin base visible externally in metamorphosing specimens (Fig. 3, A–C) but not in metamorphosed specimens. Perianal light organ black. Iris black; dorsal portion of iris with yellowish tinge in metamorphosed specimen (HUMZ 234649; Fig. 3E). Single black blotch on caudal-fin base (Fig. 3, B–E) except for early metamorphosing specimen (HUMZ 234796; Fig. 3A). Dorsal, pectoral, pelvic, and caudal fins sparsely pigmented. Anal and adipose fins almost completely unpigmented. In preservation, head and body white or yellowish white; orangish, yellowish, and silver coloration lost. Other coloration almost same as when fresh.

Remarks

Although Chiu (1999) described larvae and juveniles of the genus collected around Taiwan as *C. nigromarginatus*, including illustrations of a 7.4-mm larva and 30.7-mm juvenile, descriptions fail to clearly identify the specimens. The illustrated juvenile, at least, is unlikely to be *C. nigromarginatus* and more closely resembles *C. albatrossis* because it has approximately 13 upper and 12 lower procurrent caudal-fin rays (see the "Morphological comparisons" section in the "Discussion" section). Fricke et al. (2019) reported a single small specimen (50.5 mm in total length) of *C. nigromarginatus* from New Ireland of Papua New Guinea, but they provided neither a morphological description nor a figure of the specimen. Adults or young of the species have been previously reported from southern Japan, Taiwan, the South China Sea, Indonesia, New Ireland, the Northern Territory in Australia, and Western Australia (Randall and Lim, 2000; Hutchins, 2001; Larson et al., 2013; Nakabo and Kai, 2013; Fricke et al., 2019; Teramura et al., 2019; Koeda, 2020; Ho et al., 2021). Because the previous northernmost record of the species was a

specimen from Suruga Bay in Japan (Teramura et al., 2019), the juvenile specimens recently collected off the Pacific coast of Tohoku District extend the northern distributional limit of the species, with a single specimen (HUMZ 234796) from off Minamisanriku, Miyagi Prefecture, representing the northernmost record of the species.

Chlorophthalmus acutifrons Hiyama, 1940
Humpback greeneye
Standard Japanese name: Tomo-mehikari
Figure 4, Tables 2 and 3

Materials examined

Late metamorphosing: HUMZ 234793, 43.9 mm SL, off Tomioka, Fukushima Prefecture, 37°21′7″N, 141°37′30″E–37°22′17″N, 141°37′18″E, 250–255 m depth, bottom temperature 7.2°C, stn. FG250, 20 November 2023.

Metamorphosed: HUMZ 234650, ca. 42.8 mm SL (fractured in front of anal-fin origin), off Soma, Fukushima Prefecture, 37°35′43″N, 141°35′33″E–37°37′34″N, 141°35′58″E, 210–213 m depth, bottom temperature 8.3°C, stn. F210, 23 October 2023.

Description

Proportional measurements and counts presented in Table 2. Body depth largest at pectoral-fin base (Fig. 4). Horizontal orbit diameter equal to or slightly greater than snout length. Aphakic space on anterior portion of pupil weakly developed. Posterior margin of maxilla reaching beyond vertical through anterior margin of orbit and not reaching vertical through anterior margin of pupil. In late metamorphosing specimen, jaws almost edentate, with 1 small, conical tooth on anterior portion of premaxilla and dentary; in metamorphosed specimen, conical teeth arranged in 1–2 rows on premaxilla and dentary, with 3 teeth on anterior portion of dentary. Vomer with 1 tooth (in late metamorphosing) or 2–3 teeth (in metamorphosed) on each side of anterolateral margin. Palatine edentate in late metamorphosing specimen; conical teeth arranged in single row in metamorphosed specimen. Basihyal with 1 large, posteriorly curved, fang-like tooth on right side in late metamorphosing specimen; 1 small, conical tooth on each side in metamorphosed specimen. Third anal-fin ray longest; anterior 4 anal-fin rays unbranched, other rays branched. Adipose-fin origin above base of 5th or 6th anal-fin ray. Tip of pectoral fin reaching slightly beyond vertical through posterior end of dorsal-fin base. Pelvic-fin origin below base of 3rd dorsal-fin ray.

Coloration

When fresh (Fig. 4), head and body white. In metamorphosed specimen, silver coloration present on opercular region, belly, and mid-lateral portion of trunk (Fig. 4B). Grayish blotches on body mostly round or elliptical, without transverse bands; single large blotch below middle of dorsal-fin base round and not merged with other blotches. Single peritoneal pigment section near pectoral-fin base visible externally in late metamorphosing specimen (Fig. 4A) and invisible in metamorphosed specimen (Fig. 4B). Dorsal portion of iris with yellowish tinge in metamorphosed specimen (Fig. 4B). Single black blotch on caudal-fin base. Dorsal, pectoral, pelvic, and caudal fins sparsely pigmented. Anal and adipose fins almost completely unpigmented.

Figure 4

Fresh specimens of post-settlement juvenile humpback greeneye (*Chlorophthalmus acutifrons*) from northern Japan: (**A**) HUMZ 234793, 43.9 mm in standard length (SL), off Tomioka, Fukushima Prefecture, 20 November 2023, and (**B**) HUMZ 234650, ca. 42.8 mm SL, off Soma, Fukushima Prefecture, 23 October 2023. The developmental stage of each specimen—late metamorphosing or metamorphosed—is provided.

Remarks

Saruwatari et al. (2006) reported a larva (9.9 mm SL) of *C. acutifrons* from eastern water off Taiwan on the basis of molecular identification using a 16S rRNA sequence, but they provided no morphological description of the specimen. Shinohara et al. (1996) reported 4 small specimens (50–54 mm SL) of the species, collected during bottom-trawl surveys off Fukushima Prefecture in Japan, without any descriptions and figures. Therefore, the juvenile morphology

of the species is described for the first time herein on the basis of the results of our study.

Chlorophthalmus albatrossis Jordan and Starks, 1904
Bigeyed greeneye
Standard Japanese name: Aome-eso
Figures 2B, 5, and 6; Table 2

Materials examined

Early metamorphosing: HUMZ 234803, 41.2 mm SL, off Soma, Fukushima Prefecture, 37°49′35″N, 141°58′22″E–37°48′4″N, 141°58′37″E, 481–484 m depth, bottom temperature 4.3°C, stn. F490, 15 November 2023; HUMZ 234806, 42.4 mm SL, off Soma, Fukushima Prefecture, 37°44′56″N, 141°53′32″E–37°43′50″N, 141°53′47″E, 409–410 m depth, bottom temperature 4.8°C, stn. F410, 15 November 2023.

Late metamorphosing: HUMZ 234780, 45.2 mm SL, off Iwaki, Fukushima Prefecture, 36°57′55″N, 141°31′28″E–36°56′7″N, 141°30′49″E, 354–372 m depth, bottom temperature 6.3°C, stn. G350, 12 November 2023.

Metamorphosed: HUMZ 234534, 49.2 mm SL, off Rikuzentakata, Iwate Prefecture, 38°54′28″N, 142°5′30″E–38°56′15″N, 142°5′41″E, 354–348 m depth, bottom temperature 3.1°C, stn. D350, 28 September 2023; HUMZ 234787–234789, 3 specimens, 42.7–45.1 mm SL, off Iwaki, Fukushima Prefecture, 36°54′53″N, 141°26′34″E–36°56′15″N, 141°26′55″E, 299–311 m depth, bottom temperature 6.3°C, stn. G310, 8 November 2023; HUMZ 234804–234805, 2 specimens, 45.0–49.5 mm SL, off Soma, Fukushima Prefecture, 37°49′35″N, 141°58′22″E–37°48′4″N, 141°58′37″E, 481–484 m depth, bottom temperature 4.3°C, stn. F490, 15 November 2023.

Description

Proportional measurements and counts presented in Table 2. Body depth largest between pectoral-fin base and dorsal-fin origin (Figs. 2B and 5). Horizontal orbit diameter slightly greater than snout

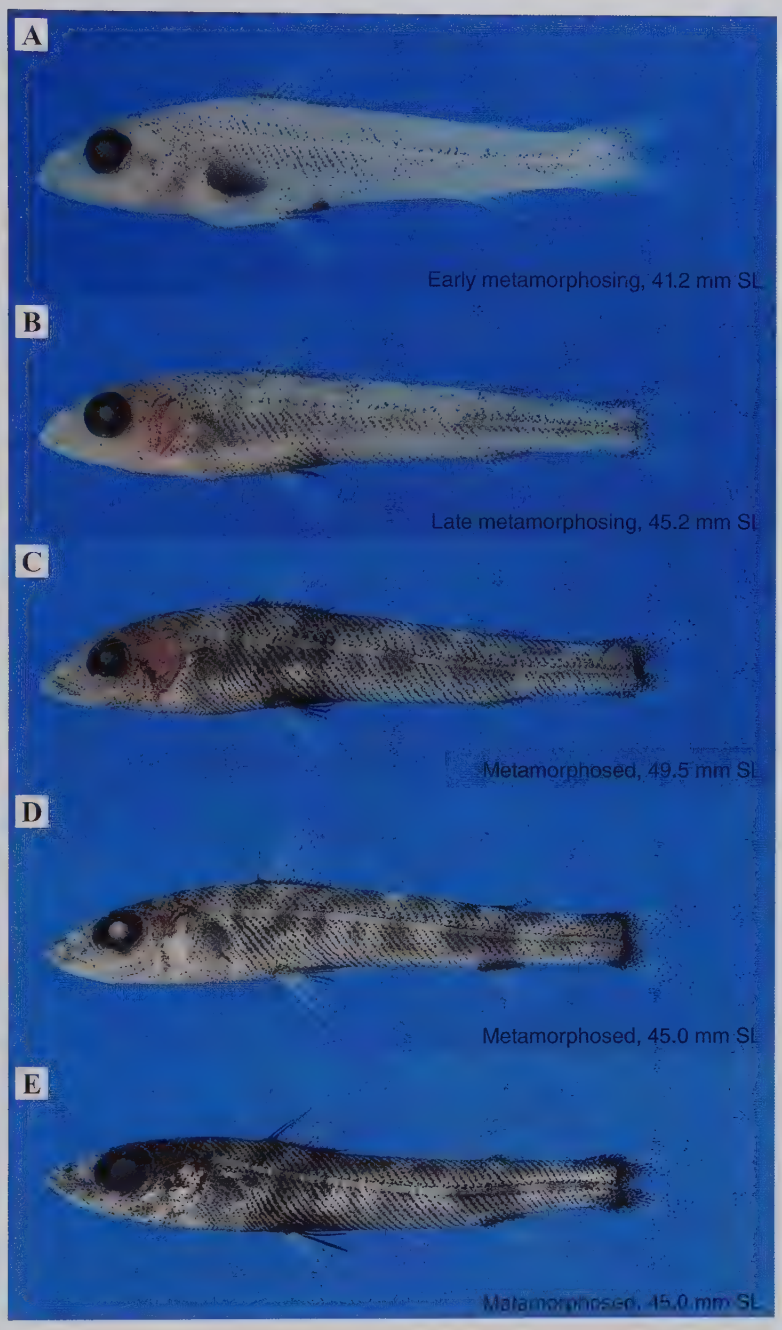

Figure 5

Fresh specimens of post-settlement juvenile bigeyed greeneye (*Chlorophthalmus albatrossis*) from northern Japan: (**A**) HUMZ 234803, 41.2 mm in standard length (SL), off Soma, Fukushima Prefecture, 15 November 2023, mirror image of right side; (**B**) HUMZ 234780, 45.2 mm SL, off Iwaki, Fukushima Prefecture, 12 November 2023; (**C**) HUMZ 234804, 49.5 mm SL, off Soma, Fukushima Prefecture, 15 November 2023; (**D**) HUMZ 234788, 45.0 mm SL, off Iwaki, Fukushima Prefecture, 8 November 2023; and (**E**) HUMZ 234805, 45.0 mm SL, off Soma, Fukushima Prefecture, 15 November 2023. The developmental stage of each specimen—early metamorphosing, late metamorphosing, or metamorphosed—is provided.

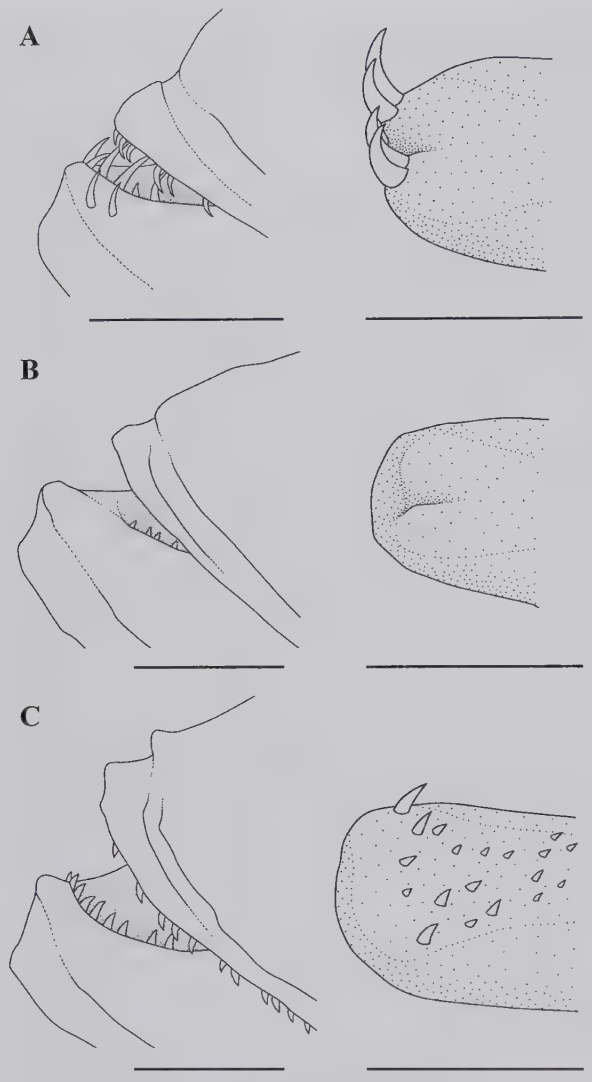

Figure 6

Line drawings of teeth on the jaws (left) and basihyal (right) of 3 post-settlement juvenile bigeyed greeneye (*Chlorophthalmus albatrossis*) from northern Japan: (**A**) HUMZ 234803, 41.2 mm in standard length (SL), off Soma, Fukushima Prefecture, 15 November 2023, illustration of jaw teeth is mirror image of right side; (**B**) HUMZ 234788, 45.0 mm SL, off Iwaki, Fukushima Prefecture, 8 November 2023; and (**C**) HUMZ 234805, 45.0 mm SL, off Soma, Fukushima Prefecture, 15 November 2023. The scale bar in each panel indicates a length of 1 mm.

length. Aphakic space on anterior portion of pupil weakly developed in metamorphosed specimens except for HUMZ 234804. Posterior margin of maxilla reaching beyond vertical through anterior margin of orbit and not reaching vertical through anterior margin of pupil; in single metamorphosed specimen (HUMZ 234805), it reaches slightly beyond vertical through anterior margin of pupil. In single early metamorphosing specimen (HUMZ 234803), curved, conical teeth in single row on anterior part of premaxilla, and slender, curved, conical teeth in single row on dentary, with 1–2 teeth on anterior portion of dentary (Fig. 6A); in other early metamorphosing (HUMZ 234806), late metamorphosing, and single metamorphosed (HUMZ 234804) specimens, jaws edentate or with few small, conical teeth; in 4 metamorphosed specimens (HUMZ 234534, HUMZ 234787–234789), premaxilla edentate or with few small, conical teeth, and dentary with small, conical teeth arranged in 1–2 rows (Fig. 6B); in single metamorphosed specimen (HUMZ 234805), premaxilla with small, conical teeth arranged in single row, and dentary with small, conical teeth arranged in 1–2 rows (Fig. 6C).

Vomer with slightly slender, curved, conical teeth arranged on anterior margin in early metamorphosing specimens; 1–2 small, conical teeth on each side of anterolateral margin in late metamorphosing and metamorphosed specimens, except for HUMZ 234534 with 3–4 small, conical teeth on each side of anterolateral margin and for HUMZ 234805 with small, conical teeth arranged on anterior margin. Palatine with slightly slender, conical teeth in single row in single early metamorphosing specimen (HUMZ 234803); edentate or with 1–2 small, conical teeth in other early metamorphosing (HUMZ 234806), late metamorphosing, and metamorphosed specimens, except for 2 specimens (HUMZ 234534 and HUMZ 234805) with about 5 small, conical teeth in single row. Basihyal with 2 large, posteriorly curved, fang-like teeth on each side of anterior margin in early metamorphosing specimens (Fig. 6A); 1 fang-like tooth on right side in late metamorphosing specimen; edentate in 2 metamorphosed specimens (HUMZ 234804 and HUMZ 234788) (Fig. 6B); small, conical teeth scattered on anterior portion of basihyal in other metamorphosed specimens (Fig. 6C). Third or 4th anal-fin ray longest; 4 anterior anal-fin rays unbranched, other rays branched. Adipose-fin origin above base of 2nd, 3rd, or 4th anal-fin ray. Tip of pectoral fin reaching slightly or well beyond vertical through posterior end of dorsal-fin base. Pelvic-fin origin below base of 3rd or 4th dorsal-fin ray.

Coloration

When fresh (Fig. 5), head and body white in metamorphosing specimens and pale gray in metamorphosed specimens. In late metamorphosing and metamorphosed specimens, silver coloration appears on opercular region, belly, and mid-lateral portion of trunk (Fig. 5, B–E). Grayish blotches on body variegated and form transverse band from posterior end of dorsal-fin base to pelvic-fin origin. Single peritoneal pigment section near pectoral-fin base visible externally in early metamorphosing specimen (Fig. 5A) and invisible in late metamorphosing and metamorphosed specimens (Fig. 5, B–E). Dorsal portion of iris with yellowish tinge in metamorphosed specimen (HUMZ 234805) (Fig. 5E). Single black blotch on caudal-fin base absent in metamorphosing specimens (Fig. 5, A and B) and present in metamorphosed specimens (Fig. 5, C–E). Each fin sparsely pigmented; inner pelvic-fin rays heavily pigmented (Figs. 2B and 5).

Remarks

Although Fricke et al. (2019) reported 6 small specimens (37.6–65.9 mm SL) from Papua New Guinea as *C. albatrossis* without a morphological description or figure, the identification should be reassessed because no adults of the species are known from waters of Papua New Guinean and several undescribed species similar to *C. albatrossis* have been reported to occur in tropical waters of the Indo-Pacific (Gomon et al., 2014). Saruwatari et al. (2005) and Saruwatari (2008) briefly reported the morphology of pelagic larvae and juveniles (from 7.3 mm in notochord length to 33.5 mm SL) of *C. albatrossis* collected from the East China Sea, basing their identification on molecular evidence based on 16S rRNA.

Although occurrences of small post-settlement juveniles (ca. 40–60 mm SL) of the species from Japan have been documented in several fishery and life history studies (Yoshida, 2003; Sakaji et al., 2006; Hirakawa et al., 2007; Inoue and Horie, 2024), the morphology of post-settlement juveniles is provided herein for the first time. Hirakawa et al. (2007) examined otolith increments of *C. albatrossis* and estimated that the settlement season of the species in northern Japan (off Fukushima Prefecture) is winter (from October through March), whereas those in central and southern Japan are autumn and summer, respectively. The dates of the recent collection of post-settlement juveniles of the species from northern Japan (i.e., from late September through early November) mostly agree with the estimation by Hirakawa et al. (2007). On the other hand, trawl surveys conducted in Tosa Bay, in southern Japan, revealed that individuals of *C. albatrossis* measuring 40–50 mm SL (smallest individual: 31.6 mm SL) settle in the depth zone of 150–200 m from August through February and gradually migrate to greater depths with growth (Sakaji et al., 2006). Because specimens described in our study were collected at much greater depths (299–484 m), settlement depths of the species may differ between regions.

Discussion

Morphological comparisons

Among the post-settlement juveniles of the 3 species examined in this study, the specimens of *C. albatrossis* are readily distinguishable from those of *C. nigromarginatus* and *C. acutifrons* by the following characters: inner pelvic-fin rays heavily pigmented (Figs. 5 and 7E) (versus lightly pigmented or unpigmented; Figs. 3, 4, and 7, A and C); grayish blotches on body variegated and form transverse band from posterior end of dorsal-fin base to pelvic-fin origin (Figs. 5 and 7E) (versus round or elliptical, without transverse bands; Figs. 3, 4, and 7, A and C); 13–14 upper and 12–13 lower procurrent caudal-fin rays (Fig. 7F) (versus 10–12 and 9–10; Fig. 7, B and D). In addition, differences between *C. albatrossis* and the other species are evident in several proportional measurements, such as the longest anal-fin ray, pectoral-fin, and pelvic-fin lengths (Fig. 8, A–C; Table 2). Although most pigmentation on the body is not developed in pelagic juveniles of the species (Saruwatari, 2008), the number of procurrent caudal-fin rays may be a useful character in their identification.

Similar patterns in post-settlement juvenile *C. albatrossis* have been observed not only in adults of the species (Okamura, 1982, 1984b; this study) but also in some

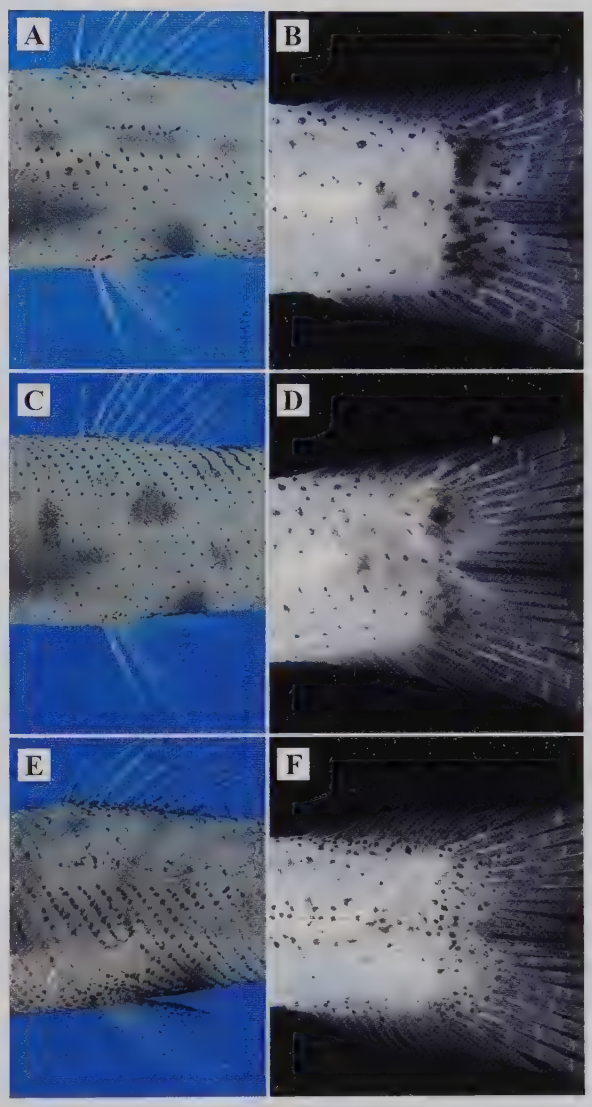

Figure 7

Body (left panels) and caudal fin (right panels) of post-settlement juveniles of 3 species of *Chlorophthalmus* collected in northern Japan: (**A** and **B**) blackedge greeneye (*C. nigromarginatus*), HUMZ 234792, 44.3 mm in standard length (SL), off Tomioka, Fukushima Prefecture, 20 November 2023; (**C** and **D**) humpback greeneye (*C. acutifrons*), HUMZ 234793, 43.9 mm SL, off Tomioka, Fukushima Prefecture, 20 November 2023; and (**E** and **F**) bigeyed greeneye (*C. albatrossis*), HUMZ 234780, 45.2 mm SL, off Iwaki, Fukushima Prefecture, 12 November 2023.

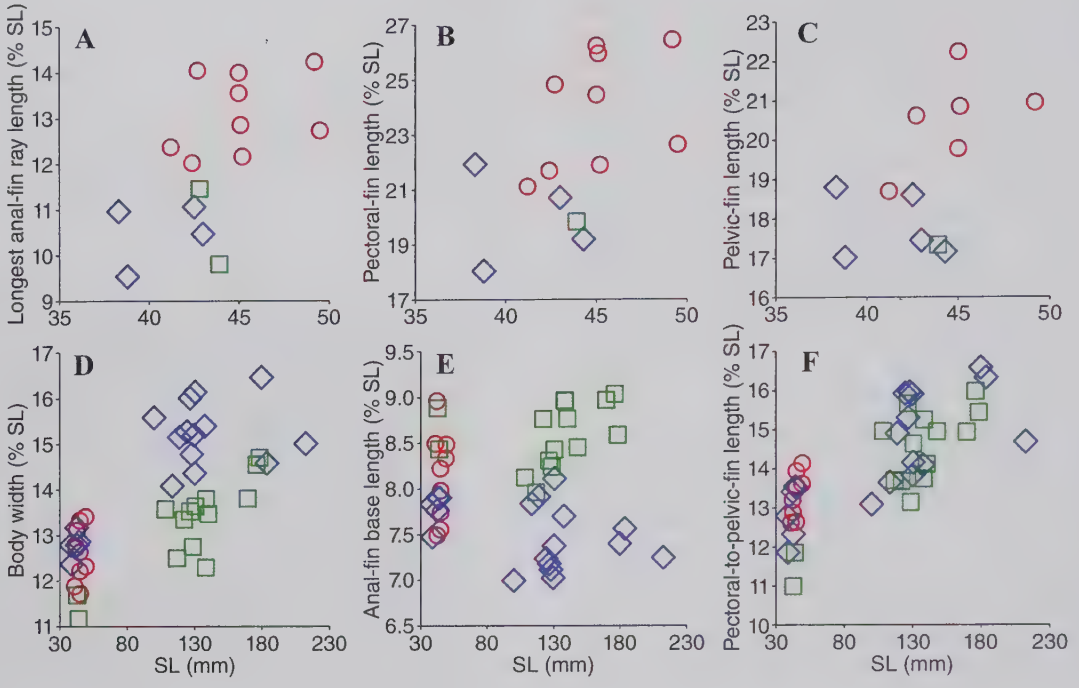

Figure 8

Relationships between standard length (SL) and (**A**) longest anal-fin ray length, (**B**) pectoral-fin length, (**C**) pelvic-fin length, (**D**) body width, (**E**) anal-fin base length, and (**F**) length between the pectoral and pelvic fins in post-settlement juvenile blackedge greeneye (*Chlorophthalmus nigromarginatus*) (diamonds), humpback greeneye (*C. acutifrons*) (squares), and bigeyed greeneye (*C. albatrossis*) (circles) caught off the Pacific coast of Tohoku District, in northern Japan, from late September through late November in 2022 and 2023. Plots in the bottom panels also include data for adults collected from waters of Kochi and Shizuoka, Japan, or the Okinawa Trough during 1972–2020 or from waters of Indonesia in 2005.

congeners, including *C. pectoralis* Okamura and Doi, 1984, *C. mascarensis* Kobyliansky, 2013, and *C. imperator* Fujiwara et al., 2019 (Okamura and Doi, 1984; Kobyliansky, 2013; Fujiwara et al., 2019), indicating that the pigmentation characters may not be diagnostic for post-settlement juveniles of *C. albatrossis*. Nevertheless, the aforementioned pigmentation characters are at least valid to distinguish post-settlement juveniles of *C. albatrossis* from the other 2 species described herein.

Post-settlement juveniles of *C. nigromarginatus* and *C. acutifrons* are superficially very similar to each other. Although the number of specimens of each species examined in our study was limited, we determined that post-settlement juveniles of the 2 species are separable by the following features: shape of a single large, grayish blotch below the middle of the dorsal-fin base (oblong and merged with an anteroventral blotch in *C. nigromarginatus* [Figs. 3 and 7A] versus round and not merged with other blotches in *C. acutifrons* [Figs. 4 and 7C]); body width (12.4–13.2% SL versus 11.2–11.7% SL); anal-fin base length (7.5–7.9% SL versus 8.4–8.9% SL); length between the pectoral and pelvic fins (11.9–13.5% SL versus 11.0–11.8% SL) (Fig. 8, D–F; Table 2). Adult specimens of the 2 species were examined to complement the scarcity of juvenile specimens and to evaluate interspecific differences mentioned previously herein. As a result, a similar proportional relationship was found in the body width (14.1–16.5% SL in *C. nigromarginatus* versus 12.3–14.7% SL in *C. acutifrons*) and anal-fin base length (7.0–8.1% SL versus 8.0–9.0% SL) but not in the length between the pectoral and pelvic fins (13.1–16.6% SL versus 13.1–16.0% SL) (Fig. 8, D–F). Examinations of the adult specimens also revealed slight differences in the number of pectoral-fin rays (14–17, modally 15 in *C. nigromarginatus* versus 15–16, modally 16 in *C. acutifrons*) and lower gill rakers (16–19, modally 17 versus 14–16, modally 16) (Table 3), and these differences may help to distinguish juveniles of the 2 species with diagnostic characters that are not yet sufficiently developed.

Metamorphosis after settlement

Among post-settlement juveniles of the 3 species of *Chlorophthalmus* described herein, remarkable ontogenetic variations were observed, especially in pigmentation, tooth morphology, and eye direction. Post-settlement ontogenetic changes of these characters inferred from the specimens are discussed later in this "Discussion" section.

Pigmentation Pelagic larvae and juveniles of the genus reported in previous studies completely lack body

pigmentation, except for a single peritoneal pigment section and pigment over the hypural complex (e.g., Tåning, 1918; Ditty, 2006, Okiyama, 2014). Because other pigmentation in the recently collected post-settlement juveniles is considered to appear after settlement, for all 3 species, we inferred that the less pigmented individuals observed in our study had shorter post-settlement periods than individuals with more developed pigmentation. In post-settlement juveniles of the 3 species, body pigmentation is primally composed of black dots arranged in slanting rows and grayish blotches. A common developmental process of body pigmentation, with black dots developing first and grayish markings appearing subsequently, was recognized in the 3 species. The peritoneal pigment section, which is characteristic of pelagic larvae and juveniles, is still clearly visible externally in early and late metamorphosing individuals of *C. nigromarginatus* (Fig. 3, A–C) and *C. acutifrons* (Fig. 4A), but it is clearly visible only in early metamorphosing individuals of *C. albatrossis* (Fig. 5A) and indistinct or invisible in subsequent stages. Marked changes were also observed in the pigmentation of the caudal-fin base, with a single black blotch appearing in early or late metamorphosing individuals of *C. nigromarginatus* (Fig. 3, B–E) and *C. acutifrons* (Fig. 4) and in only fully metamorphosed *C. albatrossis* (Fig. 5, C–E).

Tooth morphology Okiyama (2014) examined flexion (6.7–7.5 mm) and post-flexion (7.0–17.0 mm) larvae of *Chlorophthalmus* sp. and reported that these specimens had small, conical teeth arranged on margins of both jaws, with 3 strongly curved canine teeth on the anterolateral portion of the lower jaw. Teeth on the basihyal were illustrated by Rosen (1971, fig. 7B), and Hartel and Stiassny (1986, fig. 3C) on the basis of larvae or small juveniles (20–22 mm SL) of *Chlorophthalmus* spp. described 2 or 3 recurved, fang-like teeth arranged on each side of the anterior margin of the basihyal. Among the post-settlement juveniles examined in our study, only a single early metamorphosing specimen each of *C. nigromarginatus* (HUMZ 234796) and *C. albatrossis* (HUMZ 234803) retained this form of larval dentition (Fig. 6A); these specimens appear to have the shortest post-settlement period, judging from the poorly developed pigmentation in specimens of both species. On the other hand, the other early metamorphosing specimen of *C. albatrossis* (HUMZ 234806) has a basihyal with larval dentition and almost edentate jaws. In the other early metamorphosing specimen of *C. nigromarginatus* (HUMZ 233382) and late metamorphosing specimens of all 3 species, jaws, vomer, palatine, and basihyal were almost edentate or bearing only a few teeth. In these specimens, remaining fang-like teeth on the basihyal, if present, were loosely or barely attached to the bone. In metamorphosed specimens, these bones were still edentate or had small, conical teeth developed in various degrees (Fig. 6B); relatively well-developed dentition was observed in specimens of *C. acutifrons* (HUMZ 234650) and *C. albatrossis* (HUMZ 234805) (Fig. 6C). On the basis of the tooth configurations observed, we assume juveniles of the genus lose larval dentition after settlement, with adult dentition developed subsequently. A similar ontogenetic loss of larval teeth in metamorphosing juveniles has also been reported for *Parasudis* Regan, 1911, the other genus of the family (Hartel and Stiassny, 1986).

Eye direction Sanzo (1915) examined larvae and juveniles (4.5–47 mm) of *C. agassizi* and noted that eyes directed sideways and slightly downwards in small larvae change direction with growth to look to the side and upwards. He suggested this metamorphosis is related to the transition from a pelagic lifestyle to a benthic lifestyle. Tåning (1918) also noted the direction of eyes in larval and juvenile *C. agassizi* and considered the movement of eyes to take place at lengths between 25 and 44 mm SL. Although the direction of eyes in the recently collected post-settlement juveniles was already dorsolateral, we observed the transition in eye direction and that it coincides with changes of the least interorbital width during developmental stages (Fig. 9). The relatively wide interorbital space in early metamorphosing specimens gradually became narrower in late metamorphosing and metamorphosed individuals, as the eye redirected more dorsally.

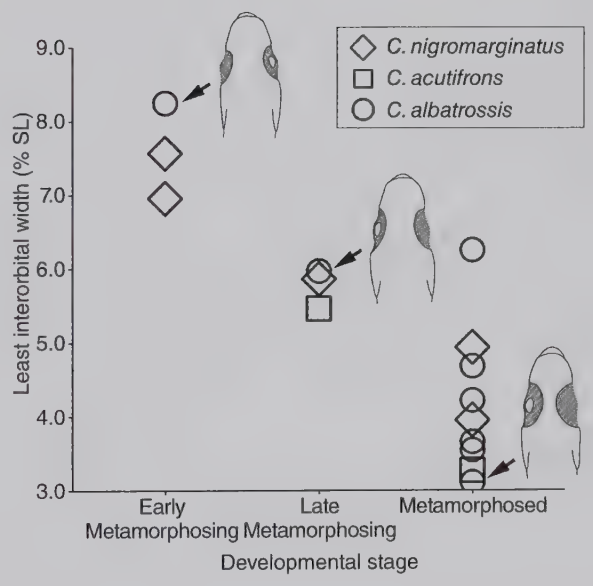

Figure 9

Relationships between least interorbital width and the 3 developmental stages in blackedge greeneye (*Chlorophthalmus nigromarginatus*), humpback greeneye (*C. acutifrons*), and bigeyed greeneye (*C. albatrossis*) collected off the Pacific coast of northern Japan from late September through late November in 2022 and 2023. Drawings of the dorsal view of the heads of specimens of *C. albatrossis* in early metamorphosing (HUMZ 234803), late metamorphosing (HUMZ 234780), and metamorphosed (HUMZ 234805) stages are provided (each arrow indicates the symbol for the specimen in that stage).

Conclusions

The remarkable morphological changes discussed herein were observed in specimens with relatively small differences in body size: 38.3–44.3 mm SL in *C. nigromarginatus*, 42.8–43.9 mm SL in *C. acutifrons*, and 41.2–49.5 mm SL in *C. albatrossis*. In addition, the degree of development for each character did not necessarily correspond to body size. In fact, individuals with the most developed characteristics for each species (Figs. 3E, 4B, and 5E) were not the largest specimens. These data indicate that juveniles of the genus undergo a very rapid metamorphosis triggered by settlement on the seafloor when the individual's lifestyle changes from pelagic to benthic. In further studies, including an analysis of otolith increments, this hypothesis will be evaluated, and more information on the process of the settlement and metamorphosis of these 3 species will be provided. Because knowledge of post-settlement juveniles of *Chlorophthalmus*, as well as pelagic larvae and juveniles, remains scarce, further sampling of larvae and juveniles and improvement in the accuracy of their identifications are essential to reveal more about the processes during the early life stages of these species.

Resumen

Se describen por primera vez el post-asentamiento de juveniles de 3 especies de ojiverdes de la familia Chlorophthalmidae, *Chlorophthalmus nigromarginatus*, *C. acutifrons* y *C. albatrossis*, a partir de 5, 2 y 9 ejemplares, respectivamente, colectados en el norte de Japón. Estas identificaciones fueron corroboradas por un análisis de las secuencias del gen mitocondrial citocromo c oxidasa I de juveniles y adultos de las 3 especies y congéneres. Entre las 3 especies, los juveniles post-asentamiento de *C. albatrossis* se distinguen fácilmente por los siguientes caracteres: radios internos de la aleta pélvica claramente pigmentados (contra ligeramente pigmentados o no pigmentados), manchas grisáceas en el cuerpo abigarradas y que forman una banda transversal desde el extremo posterior de la base de la aleta dorsal hasta el origen de la aleta pélvica (contra redondas o elípticas, que no forman bandas transversales), y 13–14 radios superiores y 12–13 inferiores de la aleta caudal (contra 10–12 y 9–10). Aunque los juveniles post-asentamiento de *C. nigromarginatus* y *C. acutifrons* son superficialmente muy similares entre sí, se pueden separar por la forma de las manchas grisáceas y varios caracteres en sus proporciones y merísticos. Al examinar los especímenes ya asentados, los juveniles del género Chlorophthalmus parecen sufrir una rápida metamorfosis al asentarse en el fondo marino, cuando cambian del estilo de vida pelágico a bentónico.

Acknowledgments

We are deeply grateful to the captain and crew of R/V *Wakataka-maru*, Y. Narimatsu, K. Fujiwara, Y. Suzuki, E. Morikawa, S. Tokioka, and J. Nagao (Japan Fisheries Research and Education Agency) and M. Furusho (Hokkaido University) for collecting the specimens, T. Senda (Kyoto University) for providing literature, Y. Kai (Kyoto University) for providing comparative materials, and M. Gomon (Museums Victoria) for valuable comments on and corrections to English usage and grammar in an early draft. This research was financially supported by the Japan Fisheries Research and Education Agency and by the Fisheries Agency, Ministry of Agriculture, Forestry and Fisheries of Japan.

Literature cited

Ahlstrom, E. H.
1971. Kinds and abundance of fish larvae in the eastern tropical Pacific, based on collections made on EASTROPAC I. Fish. Bull. 69:3–77.

Bineesh, K. K., K. V. Akhilesh, M. F. Gomon, E. M. Abdussamad, N. G. K. Pillai, and A. Gopalakrishnan.
2014. Redescription of *Chlorophthalmus corniger*, a senior synonym of *Chlorophthalmus bicornis* (Family: Chlorophthalmidae). J. Fish Biol. 84:513–522.

Bonaparte, C. L.
1840. Iconografia della fauna italica per le quattro classi degli animali vertebrati. Tomo 3. Pesci. Fasc. 27–29, puntata 136–154, 10 plates. Tipogr. Salviucci, Rome.

Chiu, T. S.
1999. Fish larvae of Taiwan, 296 p. Natl. Mus. Mar. Biol. Aquar., Kaohsiung, Taiwan. [In Chinese.]

Davis, M. P.
2010. Evolutionary relationships of the Aulopiformes (Euteleostei: Cyclosquamata): a molecular and total evidence approach. *In* Origin and phylogenetic interrelationships of teleosts (J. S. Nelson, H.-P. Schultze, and M. V. H. Wilson, eds.), p. 431–470. Verlag Dr. Friedrich Pfeil, München, Germany.

Davis, M. P., and C. Fielitz.
2010. Estimating divergence times of lizardfishes and their allies (Euteleostei: Aulopiformes) and the timing of deep-sea adaptations. Mol. Phylogenetics Evol. 57:1194–1208.

Ditty, J. G.
2006. Suborder Chlorophthalmoidei: Chlorophthalmidae and Ipnopidae. *In* Early stages of Atlantic fishes: an identification guide for the western central north Atlantic (W. J. Richards, ed.), p. 325–345. CRC Press, Boca Raton, FL.

D'Onghia, G., L. Sion, P. Maiorano, Ch. Mytilineou, S. Dalessandro, R. Carlucci, and S. Desantis.
2006. Population biology and life strategies of *Chlorophthalmus agassizii* Bonaparte, 1840 (Pisces: Osteichthyes) in the Mediterranean Sea. Mar. Biol. 149:435–446.

Fricke, R., and P. Durville.
2020. *Chlorophthalmus vulcanus*, a new species of greeneye from La Réunion, southwestern Indian Ocean (Teleostei: Chlorophthalmidae). FishTaxa 17:1–11.

Fricke, R., G. R. Allen, D. Amon, S. Andréfouët, W.-J. Chen, J. Kinch, R. Mana, B. C. Russell, D. Tully, and W. T. White.
2019. Checklist of the marine and estuarine fishes of New Ireland Province, Papua New Guinea, western Pacific Ocean, with 810 new records. Zootaxa 4588:1–360.

Fujiwara, K., H. Wada, and H. Motomura.
2019. A new species of the greeneye genus *Chlorophthalmus* (Teleostei: Chlorophthalmidae) from the central North Pacific. Zootaxa 4555:396–406.

Garman, S.
1899. Reports on an exploration off the west coasts of Mexico, Central and South America, and off the Galapagos Islands, in charge of Alexander Agassiz, by the U. S. Fish Commission steamer "Albatross," during 1891, Lieut. Commander Z. L. Tanner, U. S. N., commanding. XXVI. The fishes. Mem. Mus. Comp. Zool., Harvard Coll., vol. 24, 431 p.

Gilbert, C. H., and F. Cramer.
1897. Report on the fishes dredged in deep water near the Hawaiian Islands, with descriptions and figures of twenty-three new species. Proc. U.S. Natl. Mus. 19:403–435, plates 36–48.

Gomon, M. F., R. D. Ward, S. Chapple, and J. M. Hale.
2014. The use of DNA barcode evidence for inferring species of *Chlorophthalmus* (Aulopiformes, Chlorophthalmidae) in the Indo-West Pacific. Mar. Freshw. Res. 65:1027–1034.

Hartel, K. E., and M. L. J. Stiassny.
1986. The identification of larval *Parasudis* (Teleostei, Chlorophthalmidae); with notes on the anatomy and relationships of aulopiform fishes. Breviora 487:1–23.

Hirakawa, N., N. Suzuki, Y. Narimatsu, T. Saruwatari, and A. Ohno.
2007. The spawning and settlement season of *Chlorophthalmus albatrossis* along the Pacific coast of Japan. Raffles Bull. Zool. Suppl. 14:167–170.

Hiyama, Y.
1940. Descriptions of two new species of fish, *Raja tobitukai* and *Chlorophthalmus acutifrons*. Jpn. J. Zool. 9(1):169–173.

Ho, H.-C., S. Oktaviyani, T. Peristiwady, M.-Y. Lee, Z. Jaafar, K. Lim, and T. H. Hui.
2021. Preliminary checklist of fishes obtained from South Java Deep-Sea (SJADES) Biodiversity Expedition 2018. Raffles Bull. Zool. Suppl. 36:496–526.

Honda, H., H. Sakaji, and K. Nashida.
2001. Seasonal changes in biomass of demersal fish and benthos inhabiting the continental shelf and the upper continental slope area of Tosa Bay, southwestern Japan. Natl. Sci. Mus. Monogr. 20:345–362.

Hutchins, J. B.
2001. Checklist of the fishes of Western Australia. Rec. West. Aust. Mus. Suppl. 63:9–50.

Inoue, T., and T. Horie.
2024. Characteristics of the *Chlorophthalmus albatrossis* group caught with bottom trawl in Suruga Bay I. Appearance analysis by standard length composition. Rep. Mar. Ecol. Res. Inst. 30:18–26. [In Japanese with English abstract.]

Jordan, D. S., and E. C. Starks.
1904. List of fishes dredged by the steamer *Albatross* off the coast of Japan in the summer of 1900, with descriptions of new species and a review of the Japanese Macrouridae. Bull. U.S. Fish Comm. 22(1902):577–630, plates 1–8.

Kamohara, T.
1953. A review of the fishes of the family Chlorophthalmidae found in the waters of Japan. Jpn. J. Ichthyol. 3:1–6.

Kimura, M.
1980. A simple method for estimating evolutionary rates of base substitutions through comparative studies of nucleotide sequences. J. Mol. Evol. 16:111–120.

Kobyliansky, S. G.
2013. Two new species of green eyes of the genus *Chlorophthalmus* (Chlorophthalmidae, Aulopiformes) from the continental slope and submarine rises of the western tropical part of the Indian Ocean. J. Ichthyol. 53:373–379.

Koeda, K.
2020. *Chlorophthalmus nigromarginatus* Kamohara, 1953. *In* Fishes of southern Taiwan, vols. 1–2, 2nd ed. (K. Koeda and H.-C. Ho, eds.), p. 303. Natl. Mus. Mar. Biol. Aquar., Pingtung, Taiwan.

Kuronuma, K., and M. Yamaguchi.
1941. Description of a new iniomid fish from Chosi, Japan. Zool. Mag. Tokyo 53(5):272–274.

Larson, H. K., R. S. Williams, and M. P. Hammer.
2013. An annotated checklist of the fishes of the Northern Territory, Australia. Zootaxa 3696:1–293.

McCormick, M. I., L. Makey, and V. Dufour.
2002. Comparative study of metamorphosis in tropical reef fishes. Mar. Biol. 141:841–853.

Mead, G. W.
1958. Three new species of archibenthic iniomous fishes from the western North Atlantic. J. Wash. Acad. Sci. 48:362–372.

Miller, J. M., W. Watson, and J. M. Leis.
1979. An atlas of common nearshore marine fish larvae of the Hawaiian Islands. Univ. Hawaii Sea Grant Misc. Rep. 80-02, 179 p. Univ. Hawaii Sea Grant College Program, Honolulu, HI.

Misawa, R., K. Kimura, K. Mizumachi, T. Hattori, Y. Narimatsu, Y. Suzuki, E. Morikawa, S. Tokioka, J. Nagao, Y. Shibata, et al.
2020. New distributional records of trawled fishes off the Pacific coasts of Tohoku District, northern Japan. Jpn. J. Ichthyol. 67:265–286. [In Japanese with English abstract.]

Nakabo, T., and Y. Kai.
2013. Chlorophthalmidae. *In* Fishes of Japan with pictorial keys to the species, 3rd ed. (T. Nakabo, ed.), p. 429–430, 1853–1854. Tokai Univ. Press, Hadano, Japan. [In Japanese.]

Okamura, O.
1982. *Chlorophthalmus albatrossis* Jordan et Starks. *In* Fishes of the Kyushu-Palau Ridge and Tosa Bay. The intensive research of unexploited fishery resources on continental slopes (O. Okamura, K. Amaoka, and F. Mitani, eds.), p. 97, 334. Jpn. Fish. Resource Conserv. Assoc., Tokyo, Japan.
1984a. *Chlorophthalmus borealis* Kuronuma et Yamaguchi. *In* The fishes of the Japanese Archipelago (H. Masuda, K. Amaoka, C. Araga, T. Ueno, and T. Yoshino, eds.), p. 62–63, plate 63-I. Tokai Univ. Press, Tokyo, Japan. [In Japanese.]
1984b. *Chlorophthalmus albatrossis* Jordan et Starks. *In* The fishes of the Japanese Archipelago (H. Masuda, K. Amaoka, C. Araga, T. Ueno, and T. Yoshino, eds.), p. 62, plate 63-H. Tokai Univ. Press, Tokyo, Japan. [In Japanese.]
1984c. *Chlorophthalmus* sp. 2. *In* The fishes of the Japanese Archipelago (H. Masuda, K. Amaoka, C. Araga, T. Ueno, and T. Yoshino, eds.), p. 62, plate 63-G. Tokai Univ. Press, Tokyo, Japan. [In Japanese.]

Okamura, O., and M. Doi.
1984. *Chlorophthalmus pectoralis* Okamura et Doi, sp. nov. *In* Fishes of the Okinawa Trough and the adjacent waters. Vol. 1. The intensive research of unexploited fishery resources on continental slopes (O. Okamura and T. Kitajima, eds.), p. 173–175. Jpn. Fish. Resource Conserv. Assoc., Tokyo, Japan.

Okiyama, M.
1984. Myctophiformes: development. *In* Ontogeny and systematics of fishes. Based on an international symposium dedicated to the memory of Elbert Halvor Ahlstrom; La Jolla, 15–18 August 1983 (H. G. Moser, W. J. Richards, D. M. Cohen, M. P. Fahay, A. W. Kendall, Jr., and S. L. Richardson, eds.), p. 206–218. Am. Soc. Ichthyol. Herpetol., Spec. Publ. 1.
1988. *Chlorophthalmus* sp. *In* An atlas of the early stage fishes in Japan (M. Okiyama, ed.), p. 178–179. Tokai Univ. Press, Tokyo, Japan. [In Japanese.]
2014. *Chlorophthalmus* sp. *In* An atlas of early stage fishes in Japan, 2nd ed. (M. Okiyama, ed.), p. 286–287. Tokai Univ. Press, Hadano, Japan. [In Japanese.]

Parenti, L. R., H. J. Grier, and M. Uribe.
2015. Reproductive biology of *Chlorophthalmus agassizi* Bonaparte, 1840 (Teleostei: Aulopiformes: Chlorophthalmidae) as revealed through histology of archival museum specimens. Copeia 103:821–837.

Pertseva-Ostroumova, T. A., and T. S. Rass.
1973. Ichthyoplankton of the southeastern Pacific Ocean. Tr. Inst. Okeanol. Akad. Nauk SSSR 94:7–70. [In Russian. English translation in Fish. Mar. Serv. Transl. Ser. 4097:1–117.]

Prokofiev, A. M.
2020. A new species of greeneye (Chlorophthalmidae) from the waters of Vietnam. J. Ichthyol. 60:938–942.

Randall, J. E., and K. K. P. Lim.
2000. A checklist of the fishes of the South China Sea. Raffles Bull. Zool. Suppl. 8:569–667.

Regan, C. T.
1911. The anatomy and classification of the teleostean fishes of the order Iniomi. Ann. Mag. Nat. Hist. 7(37):120–133.

Rosen, D. E.
1971. The Macristiidae, a ctenothrissiform family based on juvenile and larval scopelomorph fishes. Am. Mus. Novit. 2452:1–22.

Sabaj, M. H.
2020. Codes for natural history collections in ichthyology and herpetology. Copeia 108:593–669.

Sakaji, H., H. Honda, and K. Nashida.
2006. Growth and ontogenetic migration of greeneye *Chlorophthalmus albatrossis* in Tosa Bay, Pacific coast of southwestern Japan. Fish. Sci. 72:1250–1255.

Sanzo, L.
1915. Contributo alla conoscenza dello sviluppo negli Scopelini Müller (*Saurus griseus* Lowe, *Chlorophthalmus agassizii* Bp. ed *Aulopus filamentosus* Cuv.). R Comitato Talassografico Italiano, Memoria 49:1–21.

Saruwatari, T.
2008. Larvae and juveniles of Mehikari, *Chlorophthalmus* spp. Vast oceanic migration inferred from their small body. Aquabiology 30:733–739. [In Japanese with English abstract.]

Saruwatari, T., T. Masaoka, T. Kobayashi, K. Hoshino, N. Hirakawa, A. Ohno, and S. Yamauchi.
2005. Species identification of *Chlorophthalmus* larvae and juveniles using DNA sequence data. DNA Polymorph. 13:135–139.

Saruwatari, T., N. Hirakawa, M. Motegi, A. Ohno, T. Masaoka, and N. Cho.
2006. Life history of Tomomehikari, *Chlorophthalmus acutifrons*, inferred from molecular data. DNA Polymorph. 14:215–221.

Shinohara, G., H. Endo, and K. Matsuura.
1996. Deep-water fishes collected from the Pacific coast of northern Honshu, Japan. Mem. Natl. Sci. Mus. Tokyo 29:153–185.

Tamura, K., G. Stecher, and S. Kumar.
2021. MEGA11: molecular evolutionary genetics analysis version 11. Mol. Biol. Evol. 38:3022–3027.

Tåning, A. V.
1918. Mediterranean Scopelidae (*Saurus*, *Aulopus*, *Chlorophthalmus* and *Myctophum*). *In* Report on the Danish oceanographical expeditions 1908–1910 to the Mediterranean and adjacent seas. Vol. 2: biology (A.7), p. 1–154. A. F. Høst and Son, Copenhagen.

Teramura, A., M. Yasuda, Y. Amano, S. Mitsui, F. Sakurai, S. Hirase, and H. Senou.
2019. Northernmost records of three fish species from Suruga Bay, Japan, with notes on distributional implications for these species. Bull. Kanagawa Prefect. Mus., Nat. Sci. 48:13–20. [In Japanese with English abstract.]

Thompson, J. D., D. G. Higgins, and T. J. Gibson.
1994. CLUSTAL W: improving the sensitivity of progressive multiple sequence alignment through sequence weighting, position-specific gap penalties and weight matrix choice. Nucleic Acids Res. 22:4673–4680.

Ward, R. D., T. S. Zemlak, B. H. Innes, P. R. Last, and P. D. N. Hebert.
2005. DNA barcoding Australia's fish species. Philos. Trans. R. Soc., B 360:1847–1857.

Yoshida, T.
2003. Catch fluctuation of the genus *Chlorophthalmus* in Fukushima Prefecture. Bull. Fukushima Prefect. Fish. Exp. Stn. 11:11–26. [In Japanese.]

Acknowledgment of reviewers

The editorial staff of *Fishery Bulletin* would like to acknowledge the scientists who reviewed manuscripts in 2023–2024. Their contributions have helped ensure the publication of quality science. An asterisk (*) after a name indicates a scientist that reviewed 2–4 manuscripts.

Joel Anderson

Christine Barry
Henry Bart Jr.
Daniel Beckman
Andrea Bellodi
Katherine Bemis
Anthony Booth

Matthew Campbell
Jeffrey Carrier
Víctor Cruz-Escalona

Kyle Dettloff
Kevin Dillon
William Driggers III*

Brian Gallagher
Jeffrey Gearhart
Matthew Girard
Gretchen Grammer

Eric Hoffmayer*

Stephen Kajiura*
Gen Kume

Richard Langton
Karin Limburg
Pedro Lino
Timothy Loher
Gustavo Lovrich

Hongguang Ma
Erin Markin
J. Fernando Márquez-Farías
Rene Martin
Mark Maunder
Richard McBride
M. Conor McManus
Richard Merrick
Richard Methot
Anthony Miskiewicz

Lisa Natanson

Martin O'Connell

Lynne Parenti
Michelle Passerotti
Juan Pérez Jiménez
Mark Peterson
Adam Pollack
Gregg Poulakis
André Punt*

Joseph Quattro

Claire Rosemond
Stacy Rowe

David Schneider
George Sedberry
Kenneth Severin

Susanne Tanner

John Walter III
Nicholas Whitney
Caroline Wiernicki

Special thanks to

William Driggers III

for reviewing 40 manuscripts

over the last 7 years

Fishery Bulletin

Guidelines for authors

Contributions published in *Fishery Bulletin* describe original research in marine fishery science, fishery engineering and economics, and marine environmental and ecological sciences (including modeling). Preference will be given to manuscripts that examine processes and underlying patterns. Descriptive reports, surveys, and observational papers may occasionally be published but should appeal to an audience outside the locale in which the study was conducted.

Although all contributions are subject to peer review, responsibility for the contents of papers rests upon the authors and not on the editor or publisher. *Submission of an article implies that the article is original and is not being considered for publication elsewhere.*

All submissions are subject to a double-blind review to remove the identity of author and reviewer during the review process.

Plagiarism and double publication are considered serious breaches of publication ethics. To verify the originality of the research in papers and to identify possible previous publication, manuscripts may be screened with plagiarism-detection software.

Manuscripts must be written in English; authors whose native language is not English are strongly advised to have their manuscripts checked by English-speaking colleagues before submission.

Artificial intelligence (AI), machine learning, or similar algorithmic tools should not be used to write or generate scientific content, including text, tables, and figures, for manuscripts submitted to *Fishery Bulletin*. Although some authors may use such tools to improve the readability or syntax of their manuscript, it must be done with extreme caution, and authors must review and edit the result. If such a tool is used, authors must declare the name of the tool, where it was used, and the purpose for which it was used in an "Artificial intelligence declaration" section after the "Acknowledgments" section. Authors remain accountable for all elements of their manuscript and should state that they take full responsibility for the content of their manuscript in the AI declaration.

Once a paper has been accepted for publication, online publication takes approximately 2 weeks.

There is no cost for publication in *Fishery Bulletin*.

Types of manuscripts accepted by the journal

Articles generally range from 20 to 30 double-spaced typed pages (12-point font) and describe an original contribution to fisheries science, engineering, or economics. Tables and figures are not included in this page count, but the number of figures should not exceed 1 figure for every 4 pages of text. Articles contain the following divisions: abstract, introduction, methods, results, discussion, and conclusions.

Notes are generally less than 10 double-spaced typed pages (12-point font), including the Literature cited section. Like articles, notes describe an original contribution to fisheries science. They follow a format similar to that for articles: abstract, introduction, methods, results, and discussion, but the results and discussion sections may be combined and a conclusions section should not be included. They should include no more than 2 figures or tables (2 of each would be too many). They are distinguished from full articles in that they report a noteworthy new observation or discovery—such as the first report of a new species, a unique finding, condition, or event that expands our knowledge of fisheries science, engineering, or economics—and do not require a lengthy discussion. Manuscripts on range extensions will not be considered.

Companion articles should be submitted together and are published together as a scientific contribution. Both articles should address a closely related topic and may be articles that result from a workshop or conference.

Review articles published under the banner "A Marine Fisheries Review" are papers of exceptional quality that continue the traditions of our sister journal *Marine Fisheries Review* inside the pages of *Fishery Bulletin* (*Marine Fisheries Review* will suspend publication in fall 2024). Review articles should address a timely topic that is relevant to aspects of fisheries science and marine biology. They should include an abstract, but the format of an article, per se, will be up to its author. Please contact the scientific editor to discuss your ideas regarding a potential review article before embarking on such a project.

Perspective essays generally are less than 5 double-spaced typed pages (12-point font) and provide clarification of misused terms or misunderstood topics in fisheries science. Essays are accepted at the discretion of the scientific editor. Opinion pieces on policy will not be considered. They should include an abstract and a list of the literature cited, but no other sections should divide the article. Please contact the scientific editor to discuss your idea before making a submission.

Preparation of manuscript

Title page should include authors' full names, affiliations, mailing addresses, and the senior author's email address.

Abstract should be limited to 200 words (one-half typed page), state the main scope of the research, and emphasize the authors' conclusions and relevant findings. Do not review the methods of the study or list the contents of the paper. Because abstracts are circulated by abstracting agencies, it is important that they represent the research clearly and concisely.

General text must be typed in 12-point Times New Roman font throughout. A brief introduction should convey the

broad significance of the paper; the remainder of the paper should be divided into the following sections: Materials and methods, Results, Discussion, Conclusions, and Acknowledgments. Headings within each section must be short, reflect a logical sequence, and follow the rules of subdivision (i.e., there can be no subdivision without at least 2 subheadings). The entire text should be intelligible to interdisciplinary readers; therefore, all acronyms, abbreviations, and technical terms should be written out in full and defined the first time they are mentioned. Abbreviations should be used sparingly because they are not carried over to indexing databases and slow readability for those readers outside a discipline. They should never be used for the main subject (e.g., species or method) of a paper.

For general style, follow the U.S. Government Publishing Office *Style Manual* (2016, available at website) and *Scientific Style and Format: the CSE Manual for Authors, Editors, and Publishers* (2014, 8th ed.) published by the Council of Science Editors. For scientific nomenclature, use the current edition of the American Fisheries Society's (AFS) *Common and Scientific Names of Fishes from the United States, Canada, and Mexico* and its companion volumes (*Crustaceans, Mollusks, Cnidaria and Ctenophora*, and *World Fishes Important to North Americans*). For species not found in the previously mentioned AFS publications and for more recent changes in nomenclature, use the Integrated Taxonomic Information System (ITIS, available at website), or, secondarily, the California Academy of Sciences *Catalog of Fishes* (available at website) for species names not included in ITIS. Common (vernacular) names of species should be lowercase. Citations must be given for the identification of specimens. For example, "Fish species were identified according to Collette and Klein-MacPhee (2002); sponges were identified according to Stone et al. (2011)."

Dates should be written as follows: 11 November 2018. Measurements should be expressed in metric units, for example, "58 metric tons (t);" if other units of measurement are used, please make this fact explicit to the reader. Use numerals, not words, to express whole and decimal numbers in the general text, tables, and figure captions (except at the beginning of a sentence). For example, "We considered 3 hypotheses. We collected 7 samples in this location." Use American spelling. Refrain from using the shorthand slash (/), an ambiguous symbol, in the general text.

Cite all software, special equipment, and chemical solutions used in the study within parentheses in the general text, including the version number, company name, and the city and state (or nation) of the company headquarters, for example, "SAS, vers. 9.4 (SAS Institute Inc., Cary, NC)."

Word usage and grammar that may be useful are the following:

- *Aging*
  For our journal, the word *aging* is used to mean both age determination and the aging process (senescence). Authors should make clear which meaning is intended where ambiguity may arise.

- *Fish and fishes*
  The plural of the word *fish* (a collective noun that implies individuals without regard to species) is *fish*.
  Example: The *fish* were collected by trawl net.
  Example: The numbers of *fish* collected that season were less than the numbers from previous years.

  The plural for *fish species* is *fishes* (a contrived plural used by taxonomists to mean several or more *fish species*) or one can use *fish species* (which is preferred in this journal for clarity across disciplines).
  Example: The *fishes* of Puget Sound [biodiversity is implied] or
  Example: The *fish species* of Puget Sound [preferred plural for clarity across disciplines].

- *Crab and crabs, squid and squids, etc.*
  The plural of the word *crab* (i.e., many individuals without regard to species) is *crab*.
  Example: The crab were sorted by weight.
  Example: Many red king *crab* were dying [Many individuals of one species of crab.]

  The plural of *crab species* is *crabs* (a word used by taxonomists) or *crab species* (the latter is preferred in this journal for clarity).
  Example: These *crabs* were selected for treatment. [Different crab species are implied.]
  Example: These *crab species* were selected for treatment. [Preferred word choice for clarity.]
  Example: Snow *crabs* are found throughout the North Pacific Ocean and Bering Sea. [There are 2 species of snow crab; therefore the word *crabs* can be used here.]
  Example: *Two species* of snow *crab* are found throughout the North Pacific Ocean and Bering Sea. [Preferred usage for clarity.]
  Example: Three crabs were selected for treatment. [3 species of crab are implied.]
  Example: Three crab species were selected for treatment. [Preferred word choice for clarity.]

- We use *fisherman* and *fishermen*, not *fisher* and *fishers*, in this journal. One can always use crew member, vessel operator, and angler (the latter for recreational fishing).

- *The definite article with common names of species*
  When the singular common name of a species represents the entire class or group to which it belongs, use the definite article.
  Example: Only one species of the genus *Salmo* is found in the Atlantic Ocean—*the* Atlantic salmon (*Salmo salar*).
  Example: The sonic emissions of *the* bottlenose dolphin are complex.

  For plural common names, this rule does not apply.
  Example: Chinook salmon are found throughout the Pacific Ocean.
  Example: Bottlenose dolphins are found in temperate and tropical waters.

- *Sex*
  For the meaning of male and female, use the word *sex*, not *gender*. Do not write, "fish were sexed." Write, "sex was determined."

- *Participles*
  As adjectives, participles must modify a specific noun or pronoun.
  Example: Using mark-recapture methods, these scientists determined the size of the population. [Correct. The participle *using* modifies the word *scientists*.]
  Example: These scientists, based on the collected data, concluded that the mortality rate of these fish had increased. [Incorrect. The scientists were not based on the collected data.]
  Example: These scientists concluded, on the basis of collected data, that the mortality rate of these fish had increased. [Correct. The offending participle has been eliminated and an adverbial phrase modifies the verb *concluded*.]

Equations and mathematical symbols should be set from a standard mathematical program (MathType or Equation Editor). Equations formatted in LaTex are not acceptable. For mathematical symbols in the general text (α, χ^2, π, $\pm$, etc.), use the symbols provided by the MS Word program and italicize all variables, except those variables represented by Greek letters and the superscript and subscript parts of variables and expressions. Do not use photo mode when creating these symbols in the general text, and do not cut and paste equations, letters, or symbols from a different software program.

Number equations (if there are more than one) for future reference by scientists; place the number within parentheses at the end of the first line of the equation.

Literature cited section comprises published works and those accepted for publication (in press) in peer-reviewed journals. Follow the name and year system for citation format in this section (i.e., citations should be listed alphabetically by the authors' last names, and then by year if there is more than one citation by the same author. A list of abbreviations for citing journal titles can be found on our website.

Authors are responsible for the accuracy and completeness of all citations. Avoid the use of multiple citations when a single citation sufficiently supports a statement; cite the work that first reported the information that supports a statement, not all of the subsequent works. Literature citation format: Authors (last name, followed by initials for first name and, if given, middle name of first author; then list names of additional authors with initials before last names). Year. Title of article. Abbreviated title of the journal in which it was published. Always include either the range of page numbers (for a journal article) or a total number of pages (for a book or other type of publication). List a sequence of citations in the general text chronologically, for example, "(Smith, 1932; Green, 1998; Smith and Jones, 2015)."

Acknowledgments should be no more than 6 lines of text. Only those who have contributed in an outstanding way should be acknowledged by name. For recognition of other persons or groups, use a general term, such as *crew*, *observers*, or *research coordinators*, and do not include names with these terms.

Digital object identifier (doi) code ensures that a publication has a permanent location online. A doi link (which may include a doi code) should be included at the end of citations of published literature. Authors are responsible for submitting accurate doi links. Faulty links will be deleted at the page-proof stage.

Footnotes are used for all documents that have not been formally peer reviewed and for observations and personal communications, but these types of references should be cited sparingly in manuscripts submitted to the journal.

All reference documents, administrative reports, internal reports, progress reports, project reports, contract reports, personal observations, personal communications, unpublished data, manuscripts in review, and council meeting notes are footnoted in 10-point font and placed at the bottom of the page on which they are first cited. Footnote format is the same as that for formal literature citations. A link to the online source (e.g., [Available from http://www..., accessed July 2017.]), or the mailing address of the agency or organization holding the document, should be provided so that readers may obtain a copy of the document.

Tables are often overused in scientific papers; it is seldom necessary to present all the data associated with a study. Tables should not be excessive in size and must be cited in numerical order in the text. Headings should be short but ample enough to allow the table to be intelligible on its own.

All abbreviations and unusual symbols must be explained in the table legend. Other incidental comments may be footnoted with numeral footnote markers. Use asterisks only to indicate significance in statistical data. Do not put a table legend on a page separate from the table; place the legend above the table. *Do not submit tables in photo mode.*

- Note probability with a capital, italic *P*.
- Provide a zero before all decimal points for values less than one (e.g., 0.07).
- Round all values to 2 decimal points.
- Use a comma in numbers of 5 digits or more (e.g., 13,000 but 3000).

Figures must be cited in numerical order in the text. Graphics should aid in the comprehension of the text, but they should be limited to presenting patterns rather than raw data. The number of figures should not exceed 1 figure for every 4 pages of text.

Figure legends should explain all symbols and abbreviations seen in the figure and should be double spaced on a separate page at the end of the manuscript.

Line art and halftone figures should be saved at resolutions >600 dots per inch (dpi) and >300 dpi, respectively. Color is allowed in figures to show morphological differences among species (for species identification), to show stain reactions, to show gradations (such as those of temperature and salinity within maps), and to distinguish between numerous lines and symbols in graphs. Figures approved for color should be saved in CMYK format.

All figures must be submitted as PDF, TIFF, or EPS files.

- Capitalize only the first letter of the first word and proper nouns in all labels within figures.
- Do not use overly large font sizes for labels in maps and for axis labels in graphs.
- Use the same point size for all labels, except for panel labels (e.g., **A**), which should be slightly larger than other labels (e.g., 11 point versus 8 point).
- Use a sans serif font for all labels. Panel labels (e.g., **A**), however, should be in Times New Roman font.
- Do not use bold fonts or bold lines in figures. Do not use italic fonts. Exceptions include use of italic fonts for labels of bodies of water in maps and a bold font for panel labels (e.g., **A**).
- Do not place outline rules around graphs.
- Do not include vertical and horizontal lines in the background of graphs. Ticks for values on the *x*-axis and *y*-axis will suffice.
- Place a north arrow and label degrees latitude and longitude (e.g., 170°E) in all maps. If scale of map requires more than degrees, use degrees minutes, not decimal degrees.
- Place panel labels (e.g., **A**, **B**, and **C**) within the upper-left area of each graph or photo in a multi-panel figure, from left to right, then top to bottom. If the letter is not visible against a dark background, put a white box behind it. Do not use white labels.
- Avoid placing labels vertically or diagonally. *Y*-axis labels can be vertical. Words in horizontal labels can be stacked vertically to fit.
- Use symbols, shading, or patterns (not clip art) in maps and graphs.
- For scale bars in maps, use kilometers. Use the label *km* or *kilometers* (lowercased).

Supplementary materials that are considered essential, but are too large or impractical for inclusion in a paper (e.g., metadata, figures, tables, videos, and websites), may be provided with an article. These materials are subject to the editorial standards of the journal. A URL to the supplementary material and a brief explanation for including such material should be sent at the time of initial submission of the paper to the journal.

- **Metadata, figures, and tables** should be submitted in standard digital format (MS Word or PDF file) and should be cited in the general text, for example, as "... was determined (Suppl. Table 3, Suppl. Fig. 1)."
- **Websites** should be cited with a URL in the general text.
- **Videos** must not be larger than 30 MB to allow a swift technical response for viewing the video. Authors should consider whether a short video uniquely captures what text alone cannot capture for the understanding of a process or behavior under examination in the article. Supply an online link to the location of the video.

Copyright law does not apply to *Fishery Bulletin*, which falls within the public domain. However, if an author reproduces any part of an article from *Fishery Bulletin*, reference to source is considered correct form (e.g., Source: Fish. Bull. 117:105).

Failure to follow these guidelines and failure to correspond with editors in a timely manner will delay publication of a manuscript.

Submission of manuscript

Submit a manuscript online at the ScholarOne Manuscripts website for *Fishery Bulletin*. Commerce Department authors must provide proof of internal clearance of their manuscripts with either a completed and signed NOAA Form 25-700 or a copy of the clearance email from the Research Publication Tracking System. For further details on electronic submission, please contact the associate editor, Cara Mayo, at

cara.mayo@noaa.gov.

When requested, the text and tables should be submitted in MS Word format. Each figure should be sent as a separate PDF, TIFF, or EPS file. Send a copy of a figure in the original software if conversion to any of these formats yields a degraded version of the figure.

Questions? If you have questions regarding these guidelines, please contact the managing editor, Kathryn Dennis, at

kathryn.dennis@noaa.gov.

Questions regarding manuscripts under review should be addressed to Associate Editor Cara Mayo.

Fishery Bulletin

Subscription form

Superintendent of Documents **Publications** Order Form

*5178

☐ YES, please send me the following publications:

____ Subscriptions to *Fishery Bulletin*
for $32.00 per year ($44.80 foreign)

The total cost of my order is $ _____ . Prices include regular domestic postage and handling and are subject to change.

_____
(Company or Personal Name) (Please type or print)

_____
(Additional address/attention line)

_____
(Street address)

_____
(City, State, ZIP Code)

_____
(Daytime phone including area code)

_____
(Purchase Order No.)

Charge your order. IT'S EASY!

VISA

MasterCard

Please Choose Method of Payment:

☐ Check payable to the Superintendent of Documents
☐ GPO Deposit Account ☐☐☐☐☐☐☐–☐
☐ VISA or MasterCard Account
☐☐☐☐☐☐☐☐☐☐☐☐☐☐☐☐
☐☐☐☐ (Credit card expiration date)

To fax your orders (202) 512-2104

_____
(Authorizing Signature)

Mail to: Superintendent of Documents
P.O. Box 979050, St. Louis, Missouri 63197
Tel. no. (U.S. callers): 866-512-1800
Tel. no. (International callers): 1-202-512-1800

Thank you for your order!

Also available online at
https://bookstore.gpo.gov/products/fishery-bulletin
email: ContactCenter@gpo.gov